Acta Universitatis Szegediensis

Acta Biologica Szegediensis

Volume 51, Number 1, 2007

University of Szeged, Szeged, Hungary

Acta Biologica Szegediensis

Acta Biologica Szegediensis (ISSN 1588-385X print form; ISSN 1588-4082 online form), a member of the Acta Universitatis Szegediensis family of scientific journals (ISSN 0563-0592), is published yearly by the University of Szeged. Acta Biologica Szegediensis covers the growth areas of modern biology and publishes original research articles and reviews, involving, but not restricted to, the fields of anatomy, embryology and histology, anthropology, biochemistry, biophysics, biotechnology, botany and plant physiology, all areas of clinical sciences, conservation biology, ecology, genetics, microbiology, molecular biology, neurosciences, paleontology, pharmacology, physiology and pathophysiology, and zoology. Occasionally, Acta Biologica Szegediensis will publish symposium materials. Acta Biologica Szegediensis particularly encourages young investigators and clinicians to submit novel results of interest.

Submission of manuscripts

Manuscripts should be prepared in accordance with the Instructions to Authors published in each issue, also available at http://www.sci.u-szeged.hu/ABS, and submitted to:

Károly Gulya
Acta Biologica Szegediensis, Editorial Office
Department of Cell Biology and Molecular Medicine
University of Szeged
4 Somogyi u., H-6720 Szeged, Hungary
Phone: 36 (62) 544-570, fax: 36 (62) 544-569
E-mail: gulyak@bio.u-szeged.hu

Correspondence relating to the status of the manuscripts, proofs, publication, reprints and advertising should be sent to:

Tamás Mikola
Acta Biologica Szegediensis, Editorial Office
Department of Cell Biology and Molecular Medicine
University of Szeged
4 Somogyi u., H-6720 Szeged, Hungary
Phone: 36 (62) 544-569, fax: 36 (62) 544-569
E-mail: mikolat@molmed.szote.u-szeged.hu

Subscriptions

Acta Biologica Szegediensis is published yearly in two issues per volume. All subscriptions relate to the calendar year and must be pre-paid. The annual subscription rate is currently 50 USD and includes air mail delivery and handling.

Acta Biologica Szegediensis is indexed in BIOSIS Database, EMBASE, Excerpta Medica, Elsevier BIOBASE (Current Awareness in Biological Sciences) and Zoological Record.

The Table of Contents for the current issue and those for previous issues can be found at http://www.sci.u-szeged.hu/ABS.

ACTA BIOLOGICA SZEGEDIENSIS

VOLUME 51(1), 2007

Table of Contents

Milestones

Articles

On the cover: Vegetation at the Lake Qarun in the Fayoum, Western Desert, Egypt (Photo: Dr. László Erdei)

Volume 51(1):1-5, 2007
Acta Biologica Szegediensis
http://www.sci.u-szeged.hu/ABS

MILESTONES

From acetylcholinesterase of motor end plates to the chemoanatomy of the thalamic reticular nucleus: celebrating the 80th birthday of Professor Bertalan Csillik

András Mihály

Department of Anatomy, Faculty of Medicine, University of Szeged, Szeged, Hungary

It was 86 years ago, when the Szeged Department of Anatomy was established in the building at Kossuth Lajos Avenue No. 40. First director-professors of the Department were: Dr. Leo Davida, Dr. Jenő Davida, Dr. Ferenc Kiss, Dr. Albert Gellért. The fifth professor of the Szeged Department of Anatomy, Bertalan Csillik celebrated his 80th birthday in November 2007. We organized a scientific meeting in the Faculty of Medicine, to celebrate him. Previously, when he was 75, we also greeted him with scientific lectures. The past 5 years brought development in the Department of Anatomy, and this development (new colleagues, PhD achievements) has been witnessed by Professor Csillik. He was really glad, seeing that neurohistochemistry (nowadays mainly immunohistochemistry) is still a decisive field in the Department, and the scientific results based on this methodology are excellent, and publishable in good international journals, all over the world. One of his famous mottos was: "publish or perish". He was living according to this motto, and always stimulated his colleagues to publish the scientific results. The number of his publications is almost 300, amongst them 5 books, and 15 university handouts (all of them very popular amongst the students). He stimulated a number of talented young scientists (e.g.: Ferenc Joó, Péter Kása, Elizabeth Knyihár, Lajos Tóth and the author of this paper), who grew up in the Szeged Anatomy Department and became internationally acknowledged researchers and university teachers. He was chairman of the Department for 25 years, and during this quarter of a century he reshaped the Anatomy Institute, reshaped the way of anatomy teaching and renewed the research conducted there. His main scientific discoveries were as follows:

The exact description of acetylcholinesterase activity and localization in motor endplates – including the developmental aspects.

The detailed neuroanatomical description of the localization of fluoride-resistant acid phosphatase (FRAP) in the dorsal horn of the spinal cord and the spinal trigeminal nucleus.

Accepted Oct 12, 2007
*Corresponding author. E-mail: mihaly@anatomy.szote.u-szeged.hu

The plasticity of the primary nociceptive neuron following peripheral nerve transection: transganglionic degenerative atrophy (TDA), which is a transient disconnection of the synapses in the dorsal horn, followed by complete structural and functional restitution, *i.e.* regeneration in the central nervous system (CNS). The TDA and the following CNS regeneration are entirely new discoveries, listed in the Encyclopedia of Neuroscience.

The exact chemoanatomy and morphology of large calyciform nerve endings in the thalamic reticular nucleus – this is a discovery of the past ten years, as indicated in the publication list.

We tried to summarize (it was not easy) the decisive events of the 58 years' long scientific carrier of Professor Csillik

January 2, 1949. Enters the Anatomy Department as a student instructor (demonstrator). Preparation of human anatomy specimens for the Anatomy Museum. First steps in histotechnique and histochemistry.

1951. Sabbatical at Prof. J. Szentágothai's Department of Anatomy; learning histotechnique of silver impregnation of the nervous system and the methods for detection of axon degeneration.

1954. Diploma (MD), becomes a general practitioner and gets a position (teaching and research assistant) in the Department of Anatomy of the Szeged Medical University.

1954. First paper on the acetylcholinesterase reaction of motor end plates (presented on the Annual Meeting of the Hungarian Physiological Society).

1957: Sabbatical at Prof. G. Romhányi's Department of Pathology (Pécs): learning the basics of polarization microscopical analysis.Assistant Professor at the Szeged Department of Anatomy.

1958. First paper on degeneration and regeneration of the acetylcholinesterase-active subneural apparatus of the motor end plate, together with simultaneous protargol (silver) impregnation of nerve fibers (Acta Neurovegetativa).

1959. First papers on the submicroscopic organization of

The staff of the Department of Anatomy in 1969, one year after the promotion of Professor Csillik, as the chairman of the Institute.

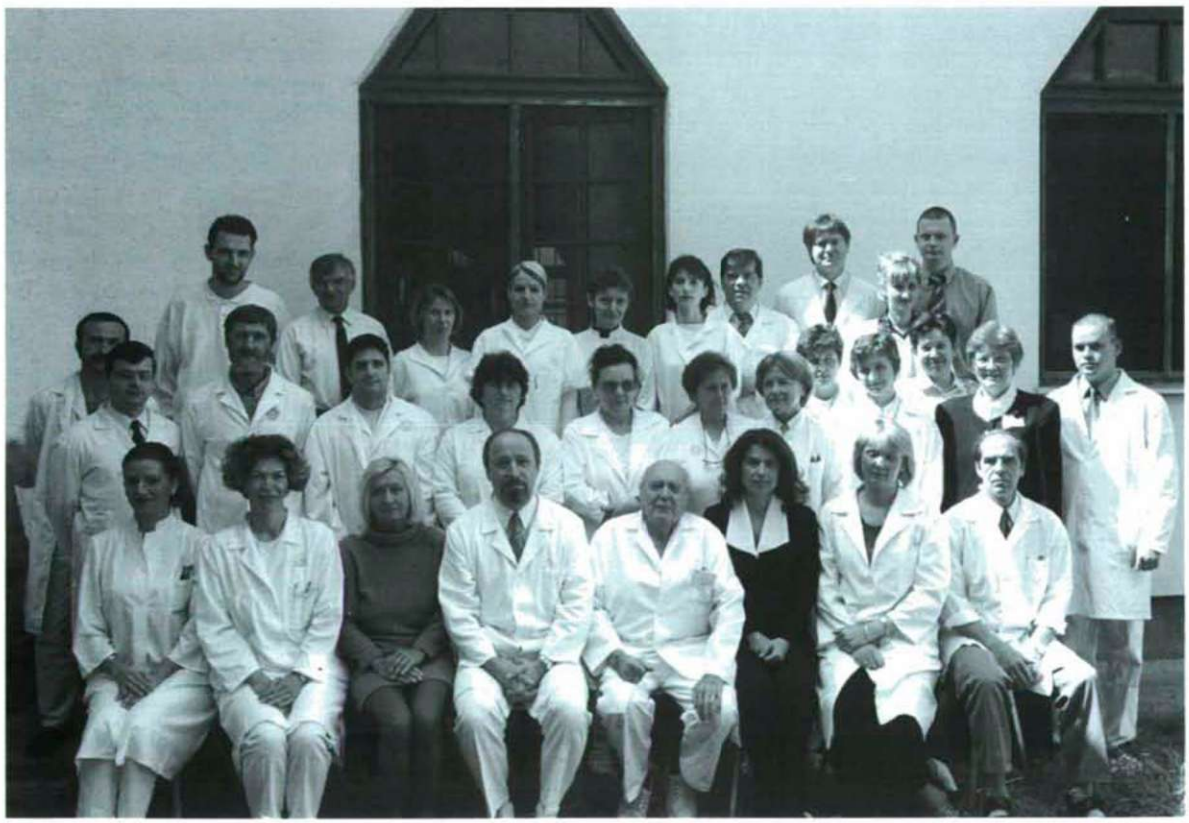

Professor Csillik, the emeritus professor of the Anatomy Department in 2004, together with the staff of the Institute, under the chairmanship of Professor András Mihály.

the post-synaptic membrane in the neuromuscular junction and structural demonstration of its molecular alterations in the course of impulse transmission (Nature, Ann. Histochim., J. Cell Biol.).

1961. Sabbatical at the Department of Anatomy, Sofia, Bulgaria, in the laboratory of Prof. D. Kadanoff, who was the discoverer of numerous (encapsulated) sensory nerve endings.

1962. PhD ("Candidate") of Medical Sciences (Hungarian Academy of Sciences, Budapest).

1962-1963. Sabbatical at the Department of Pharmacology of University of Pennsylvania, Philadelphia, PA, USA, on invitation by Prof. G. B. Koelle, inventor of the acetylthiocholine method for the histochemical detection of acetylcholinesterase.

1964. Associate Professor in the Department of Anatomy, Szeged.

1964. Sabbatical at the Department of Anatomy, Université de Liege, Belgium, on invitation by Prof. M. A. Gerebtzoff, discoverer of fluoride-resistant acid phosphatase.

1965. Publication of the book "The Post-Synaptic Membrane". (Second edition: 1967).

1966. Electron microscopic demonstration of acetylcholinesterase activity in motor end plates (Acta Histochemica).

1968. DSc degree (Doctor of the Hungarian Academy of Sciences, Budapest).

1968. Professor and Chairman of the Anatomy Department, Szeged.

1969-1970. Discovery of the approach of localizing of various enzymes involved in impulse transmission, by locating their specific enzyme inhibitors (with E. Knyihár: Nature, J. Histochem. Cytochem.).

1972-1973. Sabbatical at the Neuroscience Research Program, Boston, MA, USA, in the laboratory of F.O. Schmitt, discoverer of the laminated structure of the myelin sheath.

1975-1978. Discovery of the law of transganglionic degenerative atrophy and regenerative proliferation: biodynamic plasticity of central terminals of sensory neurons, resulting from the blockade of axoplasmic transport of nerve growth factor in the peripheral sensory nerve (with E. Knyihár, in Exp. Brain Res., Z. mikr-anat. Forschg., Experientia, Progr. Neurobiol., Res. Comm. Chem. Path. Pharm.).

1977-1978. Sabbatical at the Department of Neurobiology, Harvard Medical School, Boston, MA, USA, on invitation by Prof. Pasko Rakic, discoverer of the leading role of radial glia in the migration of neuroblasts. Discovery of transient synapses in the developing spinal cord (Science).

1981. Discovery of the role of fluoride resistant acid phosphatase (FRAP) in nociception (Progr. Histochem. Cytochem.).

1982. Discovery of chronic pain treatment via transganglionic degenerative atrophy evoked by transcutaneous iontophoresis of *Vinca* alcaloids, with E. Knyihar and A. Szücs (Neurosci. Lett., J. Neurosci. Res., J. Comp. Neurol., Acta Neurol. Scand., Histochemistry, Recent Results in Cancer Research, Cell Tiss. Res., etc...).

1985. Starting lectures and practicals of Anatomy, Histology and Embryology in English language at the Albert Szent-Györgyi University Medical School.

1982-1992. Successful treatment with Vinca iontophoresis of 923 chronic pain patients in the Pain Clinic of the Albert Szent-György University Medical School.

1983-1993. Discovery of the role of calcium channels in the neuromuscular juntion (Histochemistry, J. Hirnforschg., Ann. New York Acad. Sci. USA, Internat. Rev. Cytology, etc...).

1992-1995. Fogarty Senior Fellow, commisioned by the National Institute of Health, USA, in the Dept. Neurobiology of Yale University, New Haven, USA.

1993. Retirement as Chairman of the Anatomy Department; appointment as Professor of Anatomy at the Harvard University Medical School, Boston, MA, USA and simultaneous promotion to the post of Project Director in the Bay Zoltán Institute of Biotechnology, Szeged.

1994-1999. Publication of the results of the research performed at Yale University, USA.

1999. Returning to the Department of Anatomy as a teaching Emeritus Professor, and giving regular anatomy lectures in German language.

2001. Organizing a new research laboratory in the Department of Anatomy, as an Emeritus Professor of Neuroanatomy.

2002. Discovery of large, calyciform parvalbumin-containing axo-somatic synapses in the reticular nucleus of the rat thalamus (Acta Biol. Hung., Acta Physiol. Hung.).

2005. Discovery of coexistence of GABA and calcium-binding proteins in large, calyciform presynaptic complexes in the reticular nucleus of the rat thalamus (J. Chem. Neuroanatomy, Neuroreport).

2006-2007. Discovery of neogenesis of oncomodulin-immunoreactive regenerating axons in parvalbumin-knockout, young adult animals (Acta Physiol.Hung., IBRO-Congress), in collaboration with Prof. Schwaller, Fribourg, Switzerland.

At present, Professor Csillik is an active member of the teaching- and research staff of the Anatomy Department. He is giving lectures in German, and works on his own scientific project in connection with the thalamic reticular nucleus. We, young and elderly members of the Anatomy Institute, wish him a good health and success in his work, for the benefit of the Department and Szeged University.

Publications of Professor Bertalan Csillik in the past ten years (1998-2007)

Csillik B., Rakic P., Knyihár-Csillik E.: Peptidergic innervation and the nicotinic acetylcholine receptor in the primate

basal nucleus. Eur. J. Neurosci. 10: 573-85 (1998)

Csillik B.: István Apáthy and neurofibrils. Orv. Hetil. 139:1917-9 (1998)

Csillik B., Nemcsók J., Boncz I., Knyihár-Csillik E.: Nitric oxide synthase and the acetylcholine receptor in the prefrontal cortex: metasynaptic organization of the brain. Neurobiology 6: 383-404 (1998)

Knyihár-Csillik E, Vécsei L, Goldman-Rakic PS, Csillik B.: Columnar organization of nitric synthase (NOS) in the prefrontal cortex of primates. Neurobiology 7: 479-80 (1999)

Knyihár-Csillik E., Rakic P., Csillik B.: Development of glomerular synaptic complexes and immunohistochemical differentiation in the superficial dorsal horn of the embryonic primate spinal cord. Anat. Embryol. 199: 125-128 (1999)

Knyihár-Csillik E., Rakic P., Csillik B.: Illusive transience of parvalbumin expression during embryonic development of the primate spinal cord. Int. J. Devl. Neuroscience. 17: 79-97 (1999)

Csillik B., Nemcsók J., Chase B., Csillik A. E., Knyihár-Csillik E.: Infraterminal spreading and extrajunctional expression of nicotinic acetylcholine receptors in denervated rat skeletal muscle. Exp. Brain. Res. 125: 426-434 (1999)

Knyihár-Csillik E., Boncz I., Sáry G., Nemcsók J., Csillik B.,: Parabrachial orgin of calcitonin gene-related peptide-immunoreactive axons innervating Meynert's basal nucleus. Exp. Neurol. 157: 268-76 (1999)

Csillik B., Knyihár-Csillik E.: Degeneration. In: Enclycopedia of Neuroscience (AdelmanG., Smith B.H., editors). Elsevier, 1999, pp 523-528 (könyvfejezet)

Csillik B, Fazekas J, Nemcsók J, Knyihár-Csillik E.: Effect of the pesticide Deltamethrin on the Mauthner cells of Lake Balaton fish. Neurotoxicology 21: 343-52 (2000)

Csillik, B., Kálmán, J., Boncz, I., Knyihár, E., Janka, Z.: Nociception, the c-jun system and the Nerve Growth Factor. Annals of Anatomy, Suppl. 183: 35 (2001)

Csillik, AE., Csillik, B., Okuno, E.,Vécsei, L., Knyihár, E.,: Kynurenin amonotransferase and NMDA receptors in the subplate. Annals of Anatomy, Suppl. 183: 34-35 (2001)

Knyihár-Csillik, E., Tajti, J., Chadaide, Z., Csillik, B., Vécsei, L.: Functional immunohistochemistry of neuropeptides and nitric oxide synthase in the nerve fibers of the supratentorial dura mater in an experimental migraine model. Microsc. Res. Tech. 53: 193-211 (2001)

Samsam, M., Covenas, R., Csillik, B., Ahangari, R., Yajeva, J., Riquelme, R., Narvaez, JA., Tramu, G.: Depletion of substance P, neurokinin A and calcitonin gene-related peptide from the contralateral and ipsilateral caudal trigeminal nucleus following unilateral electrical stimulation of the trigeminal ganglion: a possible neurophysiological and neuroanatomical link to generalized head pain. J. Chem. Neuroanat. 31: 161-169 (2001)

Behrends, S., Knyihár-Csillik, E., Kempfert, J., Scholz, H., Csillik, B., Vécsei, L.: Glyceryl trinitrate treatment up-regulates soluble guanylyl cyclase in rat dura mater. Neuroreport 12: 3993-3996 (2001)

Csillik, AE., Knyihár, E., Okuno, E., Csillik Bertalan, Vécsei, L.: Expression of kyneurine aminotransferase in the subplate of the rat: its possible role in the regulation of programmed cell death. Cereb. Cortex. 12: 1193-1201 (2002)

Csillik Bertalan, Pálfi, A., Gulya, K., Mihály András, Knyihár-Csillik, E.: Somato-dendritic synapses in the nucleus reticularis thalami of the rat. Acta Biol. Hung. 53: 33-41. (2002)

Csillik Bertalan, Pálfi, A., Gulya, K., Samsam, M., Mihály András, Vécsei, L., Knyihár-Csillik, E.: Parvalbumin immunoreactive large presynaptic complexes in the reticular nucleus of the rat. Acta Physiol Hung. 89: 12 (2002)

Csillik Bertalan.: A nociceptio strukturális vonatkozásai. Fájdalom-Pain. 3: 4-13 (2002)

Csillik, AE., Knyihár, E., Okuno, E., Krisztin-Péva Beáta, Csillik Bertalan, Vécsei, L.: Effect of 3-nitropropionic acid on kynurenine aminotransferase in the rat brain. Exp. Neurol. 177: 233-244 (2002)

Bertalan Csillik, Z. Janka, I. Boncz, J. Kálmán, András Mihály, L.Vécsei, E. Knyihár: Molecular plasticity of primary nociceptive neurons: relations of the NGF-c-jun system to neurotomy and chronic pain. Ann. Anat. 185: 303-314 (2003)

Andrea Czigner, M. Samsam, Á. Pálfi, K. Gulya, András Mihály, L.Vécsei, E. Knyihár-Csillik, Csillik, B.: Large calcyform presynaptic complexes in the reticular nucleus of the rat thalamus expressing parvalbumin immunoreactivity. Clinical Neuroscience/Ideggy. Szle; 56 (2) (2003)

Csillik, B., Mihály, A., Knyihár-Csillik, E.: Cytochemi-

cal correlates of the sleep-wake interface: concerted expression of brain-derived nitric oxide synthase (bNOS) and the nicotinic acetylcholine receptor (nAChR) in a columnoid organization of the primate prefrontal cortex. Ann. Anat. 186: 217-21 (2004)

Knyihár-Csillik E., Chadaide Z., Okuno E., Krisztin-Péva B., Toldi J., Varga Cs., Molnár A., Csillik B., Vécsei L.: Kynurenine aminotrasferase in the supratentorial dura mater of the rat: effect of stimulation of the trigeminal ganglion. Exp. Neurol. 186: 242-47 (2004)

Knyihár-Csillik E., Csillik B., Pakáski M., Krisztin-Péva B., Dobó E., Okuno E., Vécsei L.: Decreased expression of kynurenine aminotransferase-I (KAT-I) in the substantia nigra of mice after l-methyl-4-phenyl-1,2,3,6-tetrahydropyridine (MPTP) treatment. Neuroscience 126: 899-914 (2004)

Csillik, B., Mihály, A., Gulya, K., Samsam, M.: Parvalbumin-immunoreactive calyciform presynaptic complexes in the thalamic reticular nucleus. Ann. Anat. Suppl. 186: 40 (2004)

Csillik, B., Rakic, P., Sáry, G., Vécsei, L., Knyihár-Csillik, E.: Cholinergic amplification and calcitonin gene-related peptide in the maintenance of Meynert's basal nucleus. Clinical Neuroscience (Ideggyógyászati szemle) 57: 324 (2004)

Csillik, B., Chadaide, Z., Samsam, M., Knyihár-Csillik, E.: Calcium binding proteins in the reticular nucleus of the thalamus. Acta Physiol. Hung. 91: 283-84 (2004)

Knyihár-Csillik E, Chadaide Z, Mihály András, Krisztin-Péva Beáta, Csillik Bertalan: Effect of electrical stimulation of the reticular nucleus of the rat thalamus upon c-fos immunoreactivity in the retrosplenial cortex. Ann. Anat. 187: 245-9 (2005)

Csillik Bertalan, Mihály András, Krisztin-Péva Beáta, Chadaide Z, Samsam M, Knyihár-Csillik E, Fenyő Róbert: GABAergic parvalbumin-immunoreactive large calyciform presynaptic complexes in the reticular nucleus of the rat thalamus. J Chem. Neuroanat. 30: 17-26 (2005)

Csillik Bertalan, Mihály András, Krisztin-Péva Beáta, Fenyő Róbert, Knyihár-Csillik, E.,: Calcium-binding proteins in GABAergic calyciform synapses of the reticular nucleus. Neuroreport 17: 575-578 (2006)

Knyihár, E., Csillik Bertalan: Plasticity of nociception: recent advances in function-oriented structural pain research. Clinical Neuroscience 59: 87-97 (2006)

Csillik Bertalan, Fenyő Róbert, Mihály András, Chadaide, Z., Vécsei, L., Schwaller, B., Knyihár-Csillik, E.,: Functional structure of GABAergic large calyciform synapses in the reticular nucleus of the thalamus. Acta. Physiol. Hung. 93: 163-164 (2006)

Knyihár-Csillik E, Vécsei L, Mihály A, Fenyő R, Farkas I, Krisztin-Péva B, Csillik B.: Effect of vinpocetine on retrograde axoplasmic transport. Ann. Anat. 189: 39-45 (2007).

Volume 51(1):7-15, 2007
Acta Biologica Szegediensis
http://www.sci.u-szeged.hu/ABS

ARTICLE

Cellular distribution of B-raf protein kinase in the brainstem of the adult rat. A fluorescent immunohistochemical study**

András Mihály*, Gyöngyi Karcsú-Kiss, Mónika Bakos, Erika Bálint

Department of Anatomy, Faculty of Medicine, University of Szeged, Szeged, Hungary

ABSTRACT The Raf-kinases can be activated by growth factors, cytokines and neurotransmitters. Previous studies in our laboratory proved the presence of Raf proteins in the neurons and astrocytes of the forebrain. The present study investigated the localization of B-Raf protein in the brain stem of the rat. Use was made of polyclonal anti-B-Raf serum which detected B-Raf molecules in our Western blotting experiments. Monoclonal tyrosine hydroxylase and dopamine-ß-hydroxylase antibodies were used to identify catecholaminergic brainstem nuclei and to study the co-localization of B-raf protein in them. We found the widespread distribution of B-raf-protein-like immunoreactivity in every segment of the brainstem. Mainly neurons were stained, but weakly immunoreactive glia-like cells were observed, too. Strongest staining was detected in the motor cranial nerve nuclei, the giant neurons of the reticular formation and in the raphe nuclei. The catecholaminergic structures displayed medium-to-weak B-raf-like immunoreactivity. The neurons of the locus ceruleus and the substantia nigra stood out with a conspicuous B-raf-like immunoreactivity. The B-raf protein was localized in the perinuclear cytoplasm and in thick, dendrite-like processes. The ubiquity of B-raf kinase suggests its important contribution to the regulation of the normal cell cycle in these neurons.
Acta Biol Szeged 51(1):7-15 (2007)

KEY WORDS

cellular oncogene
B-raf
immunohistochemistry
brainstem
rat

Protooncogenes are important regulators of cell cycle (Rapp 1991). Their protein products display different localization patterns covering a range of intracellular sites and the outer cell membrane (Rapp 1991). Their main function is to receive and convert extracellular signals, transfer the signal-generated information to the cell nucleus and regulate or modify the expression of different genes (Mihály 1990). These processes are maintained and generated mainly through phosphorylation of specific membrane- and intracellular proteins. Several protein kinases participate in similar intracellular processes, which probably encodes the diversity of the extracellular signals (Zebisch and Troppmair 2006). The different localization of protein kinases could be important in decoding the different kinds of the extracellular information (Mihály et al. 1993). Some of these kinases are able of translocation which further contributes to the versatility of this molecular network (Mihály et al. 1996). The Raf protooncogene products are serine/threonine kinases – different isozymes which exist in different tissues and in different intracellular distribution (Strom et al. 1990; Morice et al. 1999). A very important feature of the cytoplasmic Raf kinases is their ability to translocate from the cytoplasm to the cell membrane (Mihály et al. 1996). The recruitment of Raf to the cell membrane requires the transformation of Ras into a Ras-GTP complex binding Raf molecules, which are then phosphorylated and activated (Kriegsheim et al. 2006). Activated Raf proteins are able to phosphorylate Jun proteins, MAP kinases and MAP kinase kinases (Zebisch and Troppmair 2006). The Northern blotting of mRNAs in different tissues suggested that two isoforms, Raf-1 and B-Raf are present in the brain (Strom et al. 1990; Mihály et al. 1993). B-Raf proteins were detected in rat and guinea pig brain with Western blotting and immunohistochemistry (Mihály et al. 1991, 1993, 1996, 2000; Morice et al. 1999). Mapping of the spinal cord and the cerebral cortex proved the widespread occurrence of Raf-protein-like immunoreactivity (RPI) in neurons and glial cells, mainly astrocytes (Mihály et al. 1993; Mihály and Rapp 1993, 1994; Morice et al. 1999). Ultrastructural immunohistochemistry with preembedding staining proved that the localization of RPI in neurons and astrocytes are mainly cytoplasmic, although postsynaptic densities and dendritic spine apparatuses proved to be immunoreactive, too (Mihály et al. 1991). This preferentially postsynaptic localization points to the importance of Raf kinase in synaptic transmission and in postsynaptic information processing.

Accepted Oct 12, 2007
*Corresponding author. E-mail: mihaly@anatomy.szote.u-szeged.hu
**Dedicated to the honour of Professor Bertalan Csillik, founder of neurohistochemistry in Szeged, on his 80th birthday.

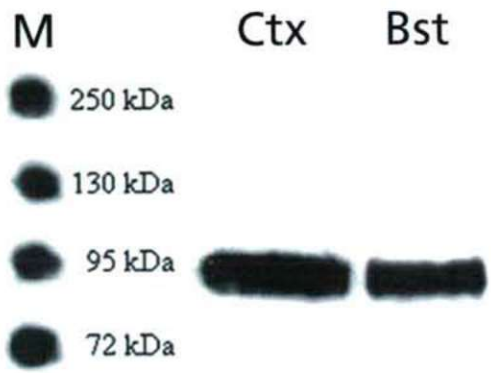

Figure 1. Western blot of homogenates of the neocortex (Ctx) and the brainstem (Bst). Very strong signal is detectable at 95 kDa in cortex and in brainstem samples. M: molecular weight standards.

The present studies were undertaken in order to map the distribution of RPI in the brainstem of the rat. The neurons and their connections in the brainstem are functionally very different; some of the send their axons to the peripheral nervous system (PNS), some of them are of placodal origin (similar to sensory ganglion cells), some are interneurons, some of them have widespread connections to the central nervous system (CNS) – which mean that the chemical informations (trophic factors, transmitters) what they receive are very different, too. It would be interesting to analyze whether these different neurons use similar intracellular molecules in order to process this large diversity of chemical signals. Our presented results, and our previous observations (Mihály et al. 1990, 1991, 1996) suggest, that neurons possess very similar intracellular molecular devices – so probably not the molecules themselves, rather their different intracellular localization, metabolism are responsible for the adaptation of neurons to a changing chemical environment.

Materials and Methods

Monoclonal tyrosine hydroxylase (TH) antibodies were raised against purified TH, isolated from pheochromocytoma cell lines (Semenenko et al. 1986). The monoclonal dopamine-ß-hydroxylase (DBH) antibodies were raised against rat adrenal medulla DBH (Mazzoni et al. 1991). Both antibodies were raised after intrasplenic injection into mice, and fusion of splenocytes and myeloma cell line cells. The characterization of the antibodies has been described in detail (Semenenko et al. 1986; Mazzoni et al. 1991). The antibodies were donated by Professor John V. Priestley.

For the characterization of antibodies raised against B-raf, brain stem and cerebral cortex homogenates were isolated from Wistar rats (200-250 g). Brains were rapidly removed and chopped with a razor blade and homogenized at 4°C with glass-teflon homogenizer in 10 volumes of 0.3 M sucrose, 20 mM TrisHCl (pH 7.4) containing the following protease inhibitors: 2 mM DL-dithiothreitol (DTT), 1 mM pestatin A, 1 mM iodoacetamide, 1 mM phenylmethyl-sulfonyl fluoride (PMSF), 1 mM 1,10-phenanthroline, 2 mM ethylenediamine tetraacetic acid (EDTA). The homogenate was centrifuged at 10,000 g_{max} for 15 min, and the supernatant was investigated. Protein concentrations were estimated with Qubit™ fluorometer, using protein assay kit (Quant-iT™; Invitrogene). The supernatant was processed for electrophoresis and immunoblotting with the polyclonal rabbit anti-B-raf antibody (1:200 dilution; Santa Cruz Biotechnology). The blots were detected with Super Signal West Pico Chemiluminescent kit (Pierce).

Six male Wistar rats (180-200 g body weight) were anesthetized with sodium pentobarbital (Sagatal, M&B; 6 mg per 100 g body weight), and perfused through the ascending aorta with an oxygenated vascular rinse (pH 7.4), followed by 4% paraformaldehyde and 0.1% glutaraldehyde in 0.1 M phosphate buffer (pH 7.4). The brain and the cervical spinal cord were dissected en bloc, and postfixed overnight in the same fixative. The brainstem was cut in three pieces: above the level of the superior colliculi (upper midbrain), at the level of the inferior colliculi (lower midbrain and pons), and at the medulla, above the level of the vagal trigone (medulla oblongata). From each brainstem segment, transverse plane serial vibratome sections were cut at 40 µm and washed in three changes of phosphate buffered saline (PBS; pH 7.4), overnight. Sections were treated with 0.1% sodium borohydride (Sigma) for 15 min, then washed in PBS. The antibody coctails contained 0.1% TritonX-100 (Sigma). Free-floating sections were incubated in 10% normal goat serum for 1 h, then in primary antibody coctails: upper midbrain – anti-tyrosine hydroxylase (TH; 1:50) + anti-B-raf (1:500); lower midbrain-pons and medulla – anti-dopamine-ß-hydroxylase (DBH; 1:50 + anti-B-raf (1:500) for 24 h, at 4°C, with constant agitation. After extensive washes in PBS, sections were incubated in coctails of secondary antibodies: goat anti-rabbit (rhodamine – TRITC – conjugated; 1:100) and goat anti-mouse (fluorescein isothiocyanate – FITC – conjugated; 1:100). Incubation time: 10-12 h at 4°C. The sections were washed, coverslipped and investigated using a Leitz Laborlux epifluorescent microscope. The identification of the structures was helped by a series of touluidine-blue-stained sections, and the stereotaxic atlas (Swanson 1992). Control sections were incubated without the primary antibody – otherwise the same, as written above (Mihály et al. 1993).

The animal experiments conform with the Declaration of Helsinki and the Guide for the Care and Use of laboratory Animals published by the U.S. National Institutes of Health (NIH Publication 85-23, revised 1996).

Results

The specificity of the anti-B-raf antibody was tested by immunoblot analysis of the rat brainstem and cerebral cortex.

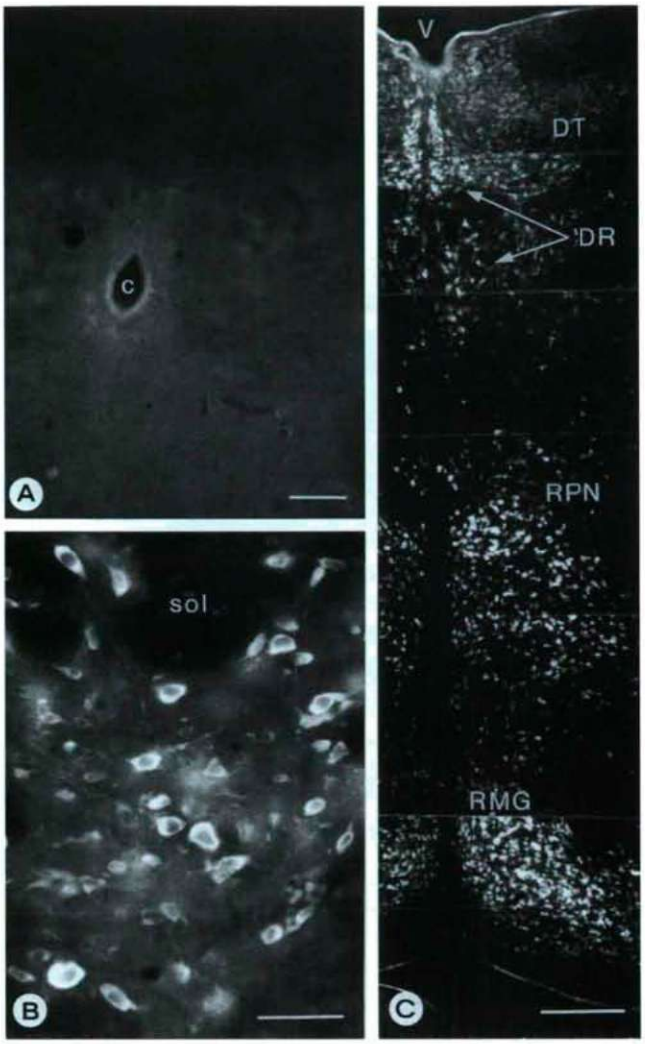

Figure 2. 2A: Section of the lower medulla incubated without primary antibody (c: central canal, bar 50 μm). 2B: in the nucleus of the solitary tract (sol) neurons and neuropil display RPI (bar 50 μm). 2C: pontine raphe displays many RPI-containing neurons (DT: dorsal tegmental nucleus; DR: dorsal raphe nucleus; RPN: raphe pontis nucleus; RMG: raphe magnus nucleus; bar 500 μm).

The antiserum recognized a dominant protein band at 95 kDa in both samples (Fig. 1). The molecular weight of the dominant protein band (95 kDa) corresponds with the previously immunoprecipitated B-raf molecule in brain (Mihály et al. 1991) and cell culture (Kolch et al. 1988). The intensity of the antibody reactions indicated the cytoplasmic localization of the raf protein.

Sections incubated without the primary B-raf serum did not display specific staining (Fig. 2A). Several structures in the medulla displayed RPI. Strong staining of the cell bodies was observed in the nucleus ambiguus, the nucleus retroambigualis and the hypoglossal nucleus. In these structures, mainly the neuronal cell bodies were stained. RPI-containing somata were surrounded by 0.5-2.0 μm thin processes, probably dendrites of motoneurons. The dorsal vagal nucleus and the nuclei of the solitary tract contained strongly- and medium-stained cell bodies (Fig. 2B). Neurons of the inferior olive, and giant neurons of the reticular formation were stained strongly. On the other hand, no cellular immunostaining was observed in the area postrema. In the laminae of the spinal trigeminal nucleus only a few neurons were stained: strongest immunostaining was observed in the marginal layer, where some of the medium-sized neurons contained RPI. The dorsal column nuclei contained scattered immunopositive neurons. The medullary raphe obscurus nucleus contained several strongly-stained neurons.

In the lower pons, the motor nucleus of the facial nerve (Fig. 3D), the abducent nucleus and the lateral vestibular nucleus displayed strong immunostaining. Nuclei of the raphe system contained strongly immunostained neurons as well (Fig. 2C). Neurons of the medial and superior vestibular nuclei and cells of the dorsal cochlear nucleus were medium-weakly stained, with only few RPI-containing neurons present (Fig. 3A,B). The ventral cochlear nucleus contained strongly stained small neurons (Fig. 3C). Neurons of the superior olivary complex and the nucleus of the trapezoid body displayed moderate staining intensity. The large cells of the pontine reticular formation stained more strongly. At higher levels, strong staining was observed in the main motor nucleus of the trigeminal nerve (Fig. 5A). Very few RPI-containing cells were observed in the principal sensory nucleus of the trigeminal nerve (Fig. 5B). The tightly packed neurons of the locus ceruleus (as identified on the basis of strong TH immunoreactivity) displayed medium immunostaining (Fig. 4A,B). The scattered noradrenergic neurons of the subceruleus region and those of the A5 group are brightly stained with TH antibody, but display a weak RPI. Laterally from the locus coeruleus, we observed the first neurons of the mesencephalic nucleus of the trigeminal nerve. These large round cells were strongly stained (Fig. 5C). The large sensory neurons were surrounded by a loose network of TH-containing fibers (Fig. 5D). Many RPI-containing neurons were present in the pontine nuclei.

In the midbrain, motor cells of trochlear and oculomotor nuclei displayed moderate staining. Faintly stained neurons were found in the Westphal-Edinger nucleus. Large cells of the mesencephalic trigeminal nucleus were strongly stained. Strong immunostaining was found in the red nucleus: these neurons stood out due to their staining intensity. Faintly stained small cells were observed in the periaqueductal gray substance or substantia grisea centralis of the midbrain. Scattered stained cells were observed in the substantia nigra and interpeducular nucleus (Fig. 6A-D). The ventral tegmental area contained only a few RPI-positive cells (Fig.

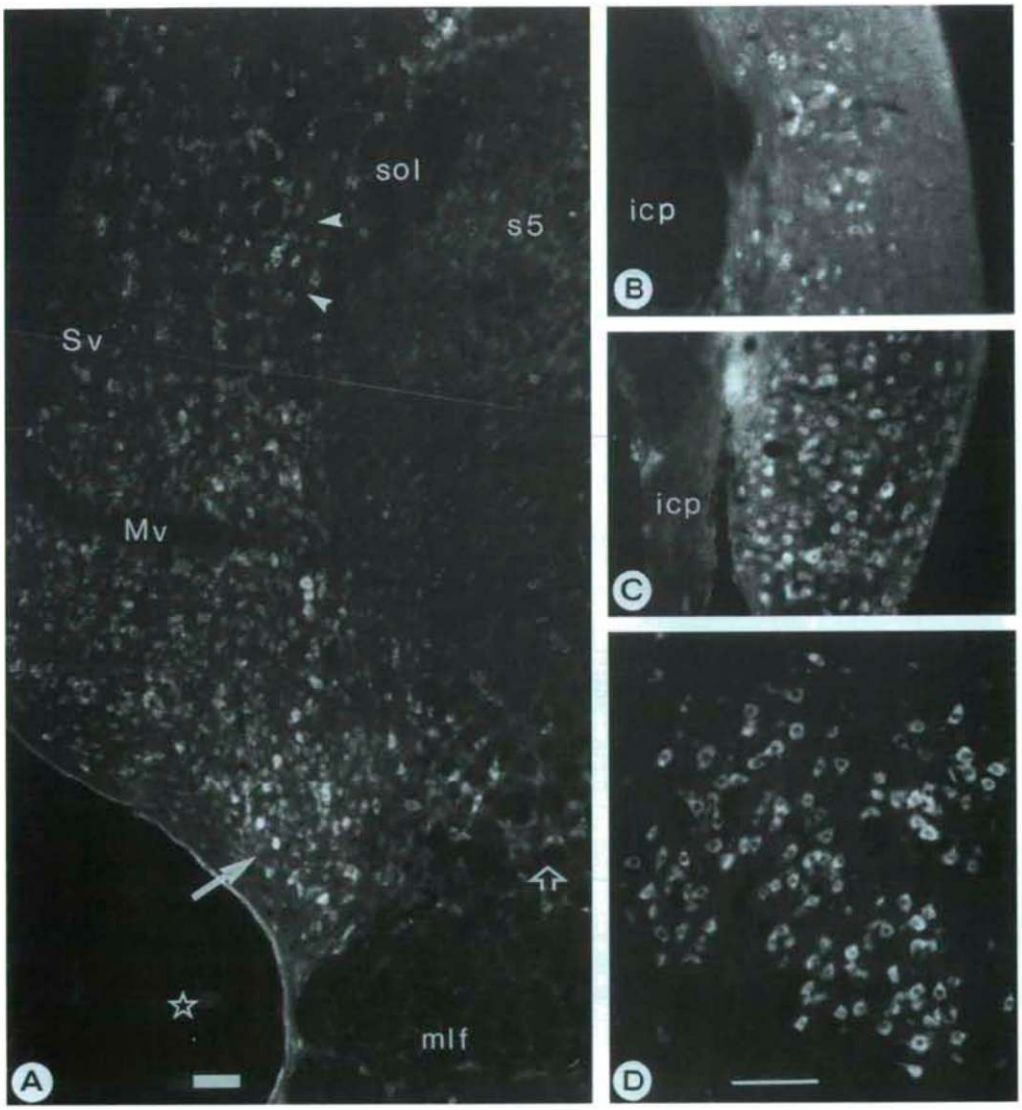

Figure 3A-D. Lower pons structures with RPI. A: superior (Sv) and medial (Mv) vestibular nuclei. Solid arrow: prepositus hypoglossal nucleus; star: fourth ventricle; empty arrow: reticular formation; sol: solitary tract; s5: spinal trigeminal nucleus. B: dorsal cochlear nucleus with a few immunostained cells. C: ventral cochlear nucleus with numerous stained neurons (icp: inferior cerebellar peduncle). D: facial motor nucleus with strongly stained neurons. Bars: 50 μm.

6B). In the superior and inferior colliculi, only a few cells were stained. These neurons appeared to be the larger neurons and were found in the deep layers of the superior colliculus (not shown). Scattered large RPI-containing cells were present in the lateral reticular formation.

The general features of RPI-positivity of cranial nerve nuclei and other brainstem structures are summarized in Figure 7. As a general rule, motor nuclei displayed stronger staining than sensory nuclei. However, the mesencephalic nucleus of the trigeminal nerve, the lateral vestibular nucleus and the ventral cochlear nucleus were exceptions: these sensory structures contained strongly stained neurons. Other structures related to the brainstem auditory pathway, *i.e.* the superior olivary complex and the nucleus of the trapezoid body, similarly contained RPI. Staining was detected in dorsal column nuclei, the locus ceruleus, pontine nuclei, the superior colliculus and the ventral tegmental area. Strong RPI was observed in magnocellular and parvocellular parts of the red nucleus. The neurons of the substantia nigra were moderately stained. All parts of the brainstem reticular formation (including raphe nuclei) contained RPI-positive neurons. When higher dilutions of the antibody were used, staining of perikarya faded more rapidly than that of neuropil (not shown), indicating that the concentration of the antigen was much higher in dendritic processes than in the perikaryon. Finally, stain-

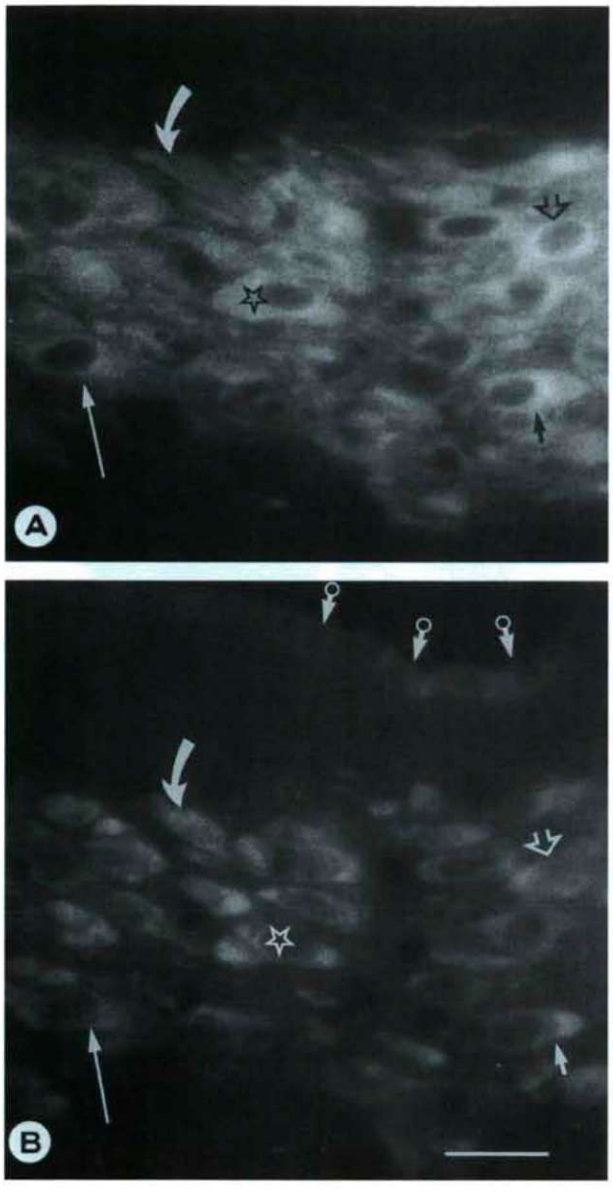

Figure 4A-B. Single section of the locus ceruleus with TH antibody (A) and B-raf serum (B). Star and arrows point to identical neurons. Small arrows with circle on B point to RPI-containing ependyma cells. Bar: 20 μm.

ing intensity depended on the size of cells: larger neurons regularly displayed stronger staining than medium-sized and small neurons.

Discussion

Data are scarcely available on the distribution patterns and possible roles of protooncogenes in the brainstem. The transcription regulator genes are activated and their protein products detected predominantly after stimulation of cranial nerves (Rutherfurd et al. 1992). B-raf belongs to another group of cellular oncogenes, *i.e.* the intracellular, cytoplasmic signal transducers (Rapp 1991). A very important feature of cytoplasmic Raf kinases is their ability to translocate from the cytoplasm to the cell membrane. Recruitment of B-raf to the cell membrane requires transformation of Ras into a Ras-GTP complex binding Raf molecules, which are then phosphorylated and activated (Morrison and Cutler 1997). Activated Raf kinases are able to phosphorylate Jun proteins, MAP kinases and MAP kinase kinases - the latter kinases are often abbreviated as MEK (mitogen- or extracellular-regulated kinase) (Heidecker et al. 1992; Roy et al. 1997). The possibility that they phosphorylate MAP kinases is particularly interesting because this function could explain the presence of B-raf in neuronal processes (Mihály et al. 1991, 1993). The immunohistochemical studies of Fiore et al. (1993) revealed that the localization of p42 MAP kinase was strikingly similar to that of Raf proteins in the forebrain of rat (Fiore et al. 1993; Mihály et al. 1993). The immunohistochemical localization of MEK isoforms also exhibits a distribution pattern that is identical to that of Raf in the brainstem of rat (Flood et al. 1998), with marked immunostaining of neuronal cell bodies in cranial nerve nuclei and other brainstem structures, such as the red nucleus, periaqueductal gray substance, reticular formation, superior olivary complex, inferior olive and dorsal column nuclei (Flood et al. 1998). These findings support the validity of our present observations and point at the importance of the B-raf - MAP kinase cascade in neuronal signal transduction.

Our previous studies of guinea pig spinal cord indicated that motor neurons of the ventral horn, and some medium-sized cells in the dorsal horn (cells in lamina I, nucleus proprius and base of the dorsal horn) were immunopositive with Raf antibodies (Mihály and Rapp 1993). Primary afferent nerve endings were not positive (Mihály et al. 1996). In rats, a large variety (though not all) of dorsal root ganglion (DRG) cells contained B-raf; double labelling revealed that these cells were from every size class (Mihály et al. 1996). On the other hand, we did not find B-raf in the sensory nerve endings of skin and cornea (Mihály et al. 1996). Ligation of the sciatic nerve did not result in accumulation of B-raf on either side, indicating that B-raf molecules are not transported in peripheral nerves in the sensory and motor axons (Mihály et al. 1996). Extrapolation of these results to brainstem allows the conclusion that the B-raf in the cranial nerve nuclei functions in the central nervous system, and does not participate in peripheral signal transduction processes. The signals which travel from the periphery have to reach the cell body first, where they can interact with the B-raf kinase system (Mihály et al. 1996). The strong immunostaining of the trigeminal mesencephalic nucleus is very similar to that of dorsal root ganglion cells (Mihály et al. 1996). On the

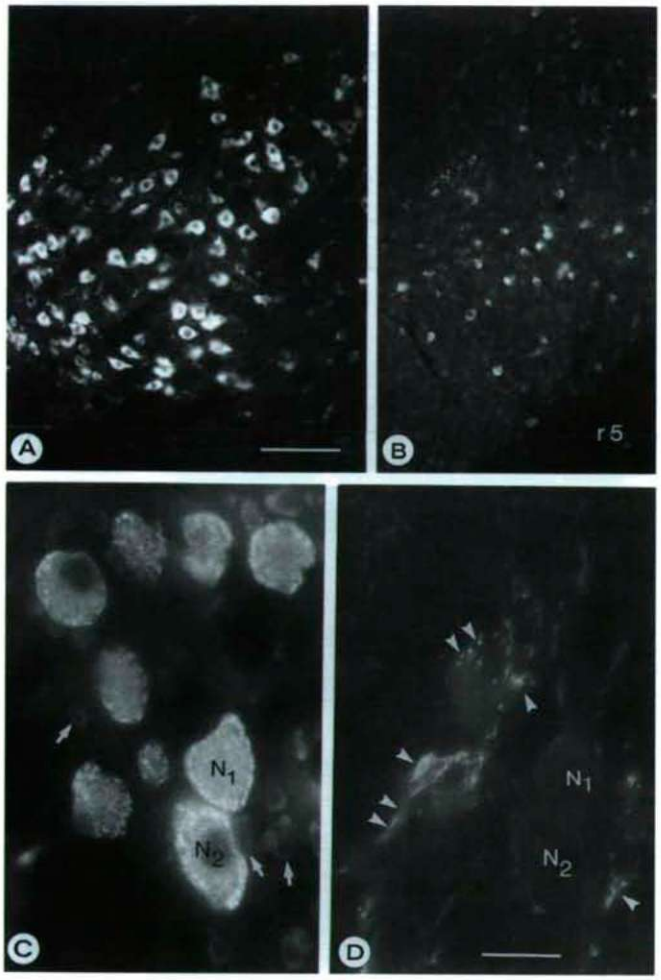

Figure 5A-D. Trigeminal nuclei in upper pons. A: motor nucleus (bar 100 μm). B: principal sensory nucleus (r5: radix of trigeminal nerve; same magnification as A). C: mesencephalic nucleus. Note large sensory cells (N1 and N2) with strong RPI. Small cells (probably glia cells) with weak staining are visible, too (arrows). D: axon network around large sensory neurons contain TH (arrowheads). N1 and N2 are identical with cells on C (bar 50 μm).

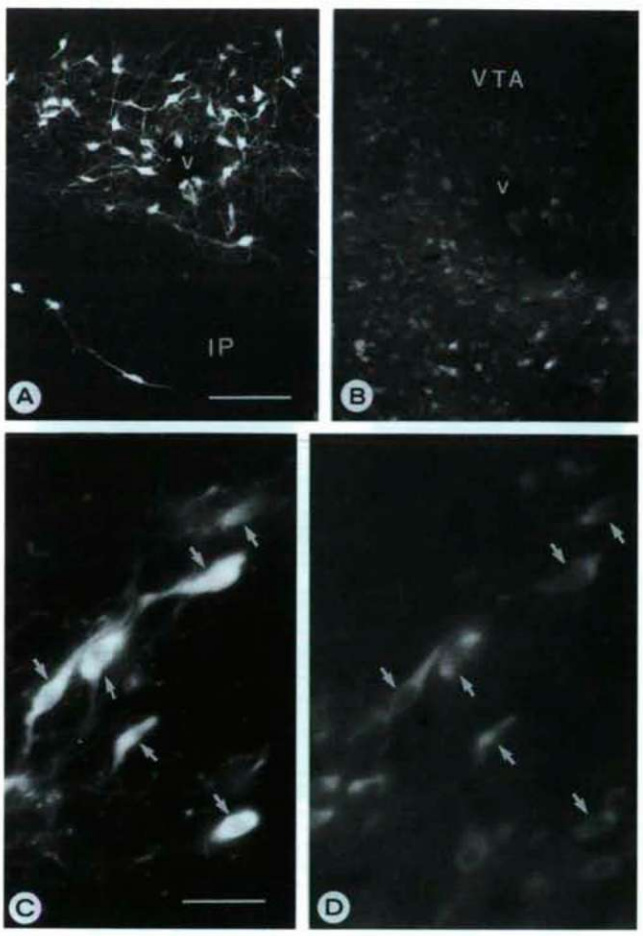

Figure 6A-D. Dopaminergic cells of the midbrain contain RPI (A,B and C,D are identical sections). A: dopaminergic neurons in the ventral tegmental area (VTA; bar for A,B 100 μm). B: some of the dopaminergic cells and neurons of the interpeduncular nucleus (IP) contain RPI (v: blood vessel). C: substantia nigra neurons stained with anti-DBH (arrows; bar for C,D 50 μm). D: the same cells (arrows) contain weak B-raf-like staining.

basis of previous observations (Mihály and Rapp 1994; Mihály et al. 1996; Vossler et al. 1997; Wartmann et al. 1997) and the present data, it can be suggested that B-raf kinase is a cytoplasmic signal transducer, which in the case of neurons is not transported through cranial and spinal nerves to the periphery. It seems that it resides in the cell body and dendrites and receives molecular signals from presynaptic terminals or axons coming from the peripheral nervous system; or coming from the vicinity from other neurons or glial cells. In previous experiments we cut the sciatic nerve, and observed that cytoplasmic B-raf undergoes a characteristic translocation in DRG neurons from the cytoplasm to the periphery of the cell body (Mihály et al. 1996), indicating the sensitivity of B-raf to certain factors arriving via peripheral nerves. This translocation was similar to the membrane translocation described in cell cultures (Leevers et al. 1994). Membrane translocation has been explained on the basis of Raf activation by Ras (Leevers et al. 1994). We think, the our results suggest the ubiquity of B-raf kinase in the central nervous system, indicating that this cytoplasmic signal transducer is not specifically related to synaptic transmission, but is related to other signals coming through growth factor- and cytokine receptors. Platelet-derived growth factor (PDGF; Morrison et al. 1989), epidermal growth factor (EGF; App et al. 1991), nerve growth factor (NGF; Oshima et al. 1991), insulin (Blackshear et al. 1990), interleukins (Carroll et al. 1990) and neuronal angiotensin receptor (Yang et al. 1997) have been found to activate the Ras-Raf-MAP kinase pathway. The question arises, whether the neurons of the brainstem

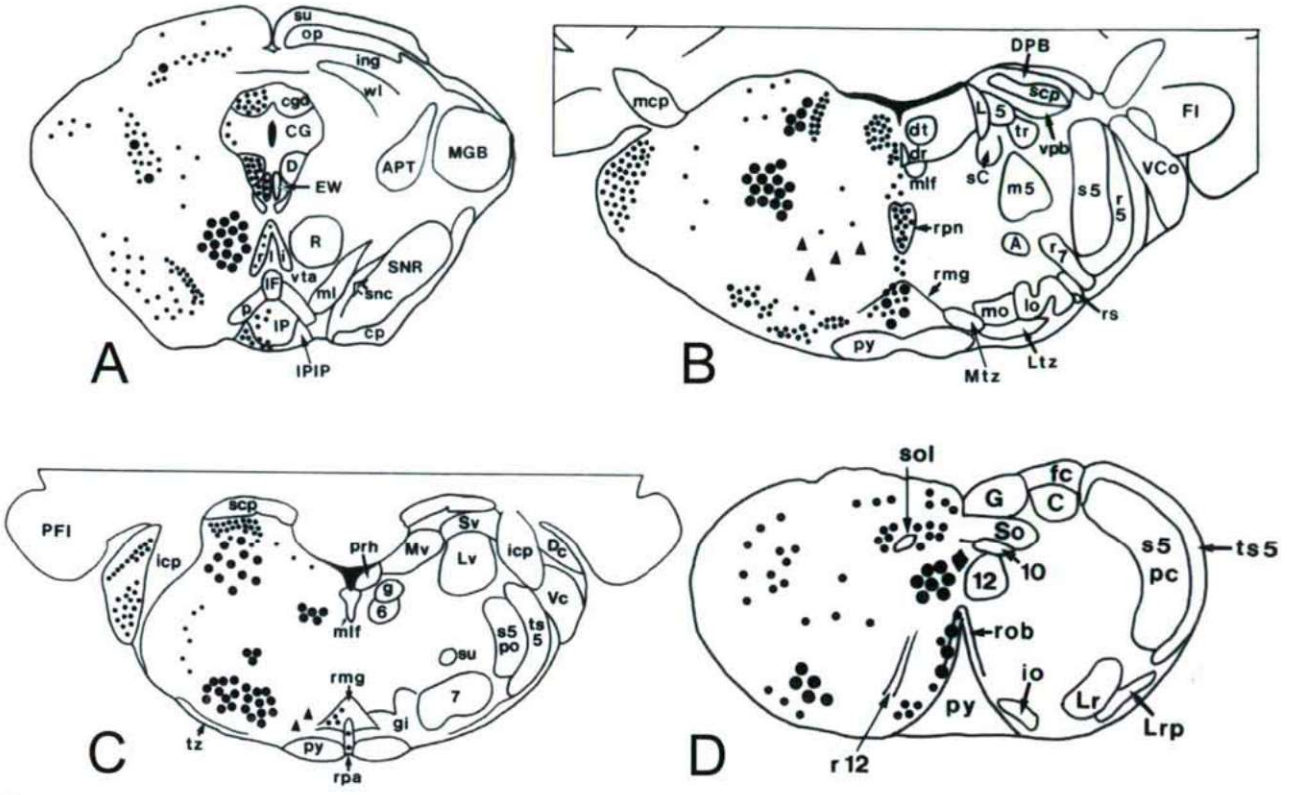

Figure 7A-D. Representative cross sections of the rat brainstem (Swanson 1992). Large dots represent strongly stained neurons, small dots represent medium or faint staining. Triangles represent large nerve cells with outstanding RPI content. A: upper mesencephalon; B: upper pons; C: lower pons; D: lower medulla (closed part). Abbreviations of Fig. 7. 5: mesencephalic nucleus of trigeminal nerve; m5: motor nucleus of trigeminal nerve; s5: principal sensory nucleus of trigeminal nerve; 6: abducens nucleus; g: genu of facial nerve; 7: facial nucleus; 7r: facial nerve root; 10: dorsal motor nucleus of vagus; 12: hypoglossal nucleus; r12: hypoglossal nerve root; APT: anterior pretectal nucleus; A: A5 noradrenaline cells; L: locus ceruleus; sC: subceruleus nucleus; su: superficial gray matter of the superior colliculus (Fig. 7A); op: optic nerve layer of the superior colliculus; ing: intermediate gray layer of the superior colliculus; wl: white layer of the superior colliculus; EW: Edinger-Westphal nucleus; D: nucleus of Darkschewitsch; R: red nucleus; SNR: substantia nigra pars reticulata; snc: substantia nigra pars compacta; MGB: medial geniculate body; IP, IPIP: interpeduncular nucleus; cp: cerebral peduncle; CG, cgd: substantia grisea centralis; rli: raphe, rostral linear nucleus; vta: ventral tegmental area; IF: interfascicular nucleus; p: paranigral nucleus; py: pyramidal tract; dt: dorsal tegmental nucleus; dr: dorsal raphe nucleus; rpn: raphe pontis nucleus; rmg: raphe magnus nucleus; mlf: medial longitudinal fasciculus; mo, lo: medial and lateral superior olivary nucleus; Mtz, Ltz: medial and lateral nucleus of trapezoid body; Vco, Vc: ventral cochlear nucleus; Dc: dorsal cochlear nucleus; DPB: dorsal parabrachial nucleus; vpb: ventral parabrachial nucleus; scp: superior cerebellar peduncle; icp: inferior cerebellar peduncle; mcp: middle cerebellar peduncle; rs: rubrospinal tract; Mv, Lv, Sv: medial, lateral, superior vestibular nucleus; prh: prepositus hypoglossal nucleus; rpa: raphe pallidus nucleus; gi: gigantocellular reticular nucleus; s5po: spinal trigeminal nucleus, pars oralis; s5pc: pars caudalis; ts5: spinal trigeminal tract; su: superior salivatory nucleus (Fig. 7C); sol: solitary tract; So: nucleus of the solitary tract; io: inferior olivary nucleus; rob: raphe obscurus nucleus; Lr, Lrp: lateral reticular nucleus; G: gracile nucleus; C: cuneate nucleus; fc: fasciculus cuneatus.

depend on these growth factors and cytokines, too.

NGF receptors have been found in some of the RPI-containing nuclei: in the mesencephalic trigeminal nucleus, superior colliculus, nucleus ambiguus, medullary raphe nuclei, reticular formation and medial vestibular nucleus in rat (Pioro and Cuello 1990), and visceral solitary tract nucleus in ferret (Henderson et al. 1991). Angiotensin receptors have been detected in brainstem neurons (Richards et al. 1999), and basic fibroblast growth factor (bFGF) in developing and adult brainstem (Grothe et al. 1991). Most of these structures contain RPI as we have shown in the present study. Recently, it was demonstrated that neuronal differentiation and probably regeneration in the adult is mediated by bFGF, and intracellular pathways include the Ras-Raf-MEK pathway (Kuo et al. 1997). This mechanism could also be important in the brainstem auditory system, which has regeneration capacity in rat (Ito et al. 1999). Our present study demonstrated the presence of B-raf in most of the brain stem auditory structures. A further step towards understanding of functions of Raf is the discovery that activated B-raf kinase plays a role in responses to transmitter receptors: cell culture studies have revealed that stimulation of M3 muscarinic receptors with carbachol activates cytoplasmic Raf kinase (Kim et al. 1999). A similar

activation can be achieved with norepinephrine via α- and β-adrenoceptors (Yamazaki et al. 1997). The significance of these findings in adult brainstem is far from understood, but they underline the significance of Raf kinases in neuronal signal transduction, and validate our observations on the widespread localization of the enzyme. It seems that B-raf is a key enzyme in the cell membrane-to-cell nucleus pathway; a number of receptors depend on it, most of them regulating development and regeneration.

Acknowledgement

The authors are grateful to Professor John V. Priestley, Queen Mary and Westfield College, London, for the antibodies. The authors thank Mr. Roland Weiczner, MD, for the construction of Figure 7.

References

App H, Hazan R, Zilberstein A, Ullrich A, Schlessinger J, Rapp UR (1991) Epidermal growth factor (EGF) stimulates association and kinase activity of Raf-1 with the EGF receptor. Mol Cell Biol 11:913-919.

Blackshear PJ, Haupt DMN, App H, Rapp UR (1990) Insulin activates the Raf-1 protein kinase. J Biol Chem 265:12131-12134.

Carroll MP, Clark-Lewis I, Rapp UR, May WS (1990) Interleukin-3 and granulocyte-macro-phage colony-stimulating factor mediate rapid phosphorylation and activation of cytosolic c-Raf. J Biol Chem 265:19812-19817.

Fiore RS, Bayer VE, Pelech SL, Posada J, Cooper JA, Baraban JM (1993) p42 mitogen-activated protein kinase in brain: prominent localization in neuronal cell bodies and dendrites. Neuroscience 55:463-172.

Flood DG, Finn JP, Walton KM, Dionne CA, Contreras PC, Miller MS, Bhat RV (1998) Immunolocalization of the mitogen-activated protein kinases $p42^{MAPK}$ and JNK1, and their regulatory kinases MEK1 and MEK4, in adult rat central nervous system. J Comp Neurol 398:373-392.

Grothe C, Zachmann K, Unsicker K (1991) Basic FGF-like immunoreactivity in the developing and adult rat brainstem. J Comp Neurol 305:328-336.

Heidecker G, Kolch W, Morrison DK, Rapp UR (1992) The role of Raf-1 phosphorylation in signal transduction. Adv Cancer Res 58:53-73.

Henderson Z, Igielman F, Sheriff FE (1991) Organisation of the visceral solitary tract nucleus in the ferret as defined by the distribution of choline acetyltransferase and nerve growth factor receptor immunoreactivity. Brain Res 568:35-44.

Ito J, Murata M, Kawaguchi S (1999) Regeneration of the central auditory pathway in adult rats. Acta Otolaryngol 119:132-134.

Kim JY, Yang MS, Oh CD, Kim KT, Ha MJ, Kang SS, Chun JS (1999) Signalling pathway leading to an activation of mitogen-activated protein kinase by stimulating M3 muscarinic receptor. Biochem J 337:275-280.

Kolch W, Schultz AM, Oppermann H, Rapp UR (1988) Preparation of Raf-oncogene-specific antiserum with Raf protein produced in E. coli. Biochim Biophys Acta 949:233-239.

Kriegsheim Av, Pitt A, Grindlay J, Kolch W, Dhillin AS (2006) Regulation of the Raf-MEK-ERK pathway by protein phosphatase 5. Nature Cell Biol 8:1011-1016.

Kuo WL, Chung KC, Rosner MR (1997) Differentiation of central nervous system neuronal cells by fibroblast-derived growth factor requires at least two signaling pathways: roles for Ras and Src. Mol Cell Biol 17:4633-4643.

Leevers SJ, Paterson HF, Marshall CJ (1994) Requirement for Ras in Raf activation is overcome by targeting Raf to the plasma membrane. Nature 369:411-414.

Mazzoni IE, Jaffe E, Cuello AC (1991) Production and immunocytochemical application of a highly sensitive and specific monoclonal antibody against rat dopamine-β-hydroxylase. Histochemistry 96:45-50.

Mihály A, Endrész V (2000) Neuronal expression of Raf protooncogene in the brainstem of the adult guinea pig. Acta Histochem. 102:203-217.

Mihály A, Priestley JV, Molnár E (1996) Expression of raf serine/threonine protein kinases in the cell bodies of primary sensory neurons of the adult rat. Cell Tissue Res 285:261-271.

Mihály A, Rapp UR (1994) Expression of the raf protooncogene in glial cells of the adult rat cerebral cortex, brainstem and spinal cord. Acta Histochem 96:155-164.

Mihály A, Rapp UR (1993) Neuronal expression of the raf protooncogene in the spinal cord of adult guinea pigs. Acta Histochem 94:189-196.

Mihály A, Endrész V, Oravecz T, Rapp UR, Kuhnt U (1993) Immunohistochemical detection of raf protein kinase in cerebral cortical areas of adult guinea pigs and rats. Brain Res 627:225-238.

Mihály A (1991) The role of raf oncogen in the plasticity of the nervous system. Lege Artis Medicinae (Hung) 1:1196-1202.

Mihály A, Orawecz T, Oláh Z, Rapp UR (1991) Immunohistochemical localization of raf protein kinase in dendritic spines and spine apparatuses of the rat cerebral cortex. Brain Res 547:309-314.

Mihály A, Oláh Z, Krug M, Kuhnt U, Matthies H, Rapp UR, Joó F (1990) Transient increase of Raf protein kinase-like immunoreactivity in the rat dentate gyrus during long-term potentiation. Neurosci Lett 116:45-50.

Morice C, Nothias F, König S, Vernier P, Baccarini M, Vincent JD, Barnier JV (1999) Raf-1 and B-raf proteins have similar regional distribution but differential subcellular localization in adult rat brain. Eur J Neurosci 11:1995-2006.

Morrison DK, Kaplan DR, Escobedo JA, Rapp UR, Roberts TM, Williams LT (1989) Direct activation of the serine/threonine kinase activity of Raf-1 through tyrosine phosphorylation by the PDGF receptor. Cell 58:649-657.

Morrison DK, Cutler JrRE (1997) The complexity of Raf-1 regulation. Curr Op Cell Biol 9:174-179.

Oshima M, Sithanandam G, Rapp UR, Guroff G (1991) The phosphorylation and activation of B-raf in PC 12 cells stimulated by nerve growth factor. J Biol Chem 266:23753-23760.

Pioro EP, Cuello AC (1990) Distribution of nerve growth factor receptor-like immunoreactivity in the adult rat central nervous system. Effect of colchicine and correlation with the cholinergic system - II. Brainstem, cerebellum and spinal cord. Neuroscience 34:89-110.

Rapp UR (1991) Role of Raf-1 serine/threonine protein kinase in growth factor signal transduction. Oncogene 6:495-500.

Richards EM, Raizada MK, Gelband CH, Sumners C (1999) Angiotensin II type 1 receptor-modulated signaling pathways in neurons. Mol Neurobiol 19:25-41.

Roy S, Lane A, Yan Y, McPherson R, Hancock JF (1997) Activity of plasma membrane-recruited Raf-1 is regulated by Ras via the Raf zinc finger. J Biol Chem 272:20139-20145.

Rutherfurd SD, Widdop RE, Sannajust F, Louis WJ, Gundlach AL (1992) Expression of c-fos and NGF messenger RNA in the medulla oblongata of the anesthetized rat following stimulation of vagal and cardiovascular afferents. Mol Brain Res 13:301-312.

Semenenko FM, Cuello AC, Goldstein M, Lee KY, Sidebottom E (1986) A monoclonal antibody against tyrosine hydroxylase: application in light and electron microscopy. J Histochem Cytochem 34:817-821.

Storm SM, Cleveland JL, Rapp UR (1990) Expression of Raf family proto-oncogenes in normal mouse tissues. Oncogene 5:345-350.

Swanson LW (1992) Brain maps: structure of the rat brain. Elsevier, New York.

Yamazaki T, Komuro I, Zou Y, Kudoh S, Shiojima I, Hiroi Y, Mizuno T, Aikawa R, Takano H, Yazaki Y (1997) Norepinephrine induces the Raf-1 kinase/mitogen activated protein kinase cascade through both alpha 1- and beta-adrenoceptors. Circulation 95:1260-1268.

Yang H, Lu D, Raizada MK (1997) Angiotensin II-induced phosphorylation

of the AT receptor from rat brain neurons. Hypertension 30:351-357.

Vossler MR, Yao H, York RD, Pan M-G, Rim CS, Stork PJS (1997) cAMP activates MAP kinase and ELK-1 through a B-Raf and Rap 1-dependent pathway. Cell 89:73-82.

Wartmann M, Hofer P, Turowski P, Saltiel AR, Hynes NE (1997) Negative modulation of membrane localization of the Raf-1 protein kinase by hyperphosphorylation. J Biol Chem 272:3915-3923.

Zebisch A, Troppmair J (2006) Back to the roots: the remarkable RAF oncogene story. Review. Cell Mol Life Sci 63:1314-1330.

Volume 51(1):17-20, 2007
Acta Biologica Szegediensis
http://www.sci.u-szeged.hu/ABS

ARTICLE

Effects of ethanolic extract of *Azadirachta indica* leaves on lipid peroxidation and serum lipids of diabetic Wistar rats

Itemobong S Ekaidem[1]*, Henry D Akpan[2], Itoro F Usoh[2], Oboso E Etim[2], Patrick E Ebong[3]

[1]Department of Chemical Pathology, Faculty of Clinical Sciences, University of Uyo, Uyo, Nigeria, [2]Department of Biochemistry, Faculty of Basic Medical Sciences, University of Uyo, Uyo, Nigeria, [3]Department of Biochemistry, Faculty of Basic Medical Sciences, University of Calabar, Calabar, Nigeria

ABSTRACT The effects of ethanolic extract of *Azadirachta indica* leaves on lipid peroxidation and serum lipids of alloxan-induced diabetic rats were examined to assess the role of the extract in the management diabetic complications. Serum Malondialdehyde (MDA), total cholesterol, triglyceride and blood glucose were measured in diabetic and normal rats with or without 400 mg/kg leaf extract of *A. indica*. The result showed that blood glucose, total cholesterol (TC), triglyceride and MDA concentrations in serum of untreated diabetic rats were significantly ($P<0.05$) higher than that of normal control and diabetic rats treated with the extracts. The extract caused a 55.8%, 27.1%, 16.8% and 64.7% reduction in blood glucose, TC, TG and MDA respectively when compared to untreated diabetic rats. The extract also demonstrated growth promoting effect on normal and diabetic rats. The anti-lipid peroxidative, antihyperglycaemic and serum lipid modulating activities justify the possible use of extract of *A. indica* leaves in the management of diabetic complications.
Acta Biol Szeged 51(1):17-20 (2007)

KEY WORDS

Azadirachta indica,
lipid peroxidation,
serum lipids,
diabetic complications

Lipid peroxidation, a known mechanism of cellular injury, is a chain reaction initiated by oxidant radicals. It is an index of oxidative stress in cells and tissues. The free radical oxidation of lipid molecules proceeds from the fatty acylmethylene group adjacent to a double bond (Frankel 1980) to form lipid hydroperoxides which are capable of further reactions to yield various classes of peroxides. Lipid peroxides are unstable and decompose to form series of complex products including reactive carbonyl compounds. Polyunsaturated fatty acids on oxidation decompose to malondialdehyde (MDA) and 4-hydroxyalkenals (HAE). The levels of these products in serum or tissues have been widely accepted as a measure of lipid peroxidation.

Biological membranes which contain phospholipids rich in polyunsaturated fatty acids are continuously being oxidized by superoxides, hydroperoxyl and peroxyl radicals emanating from exposures to radiations and oxidative reactions involving endogenous and exogenous compounds in the body (Droge 2002). There are, however, some defense systems to prevent injury caused by these free radicals (Hensley et al. 2000). These systems include antioxidant vitamins, reduced glutathione, transport and storage proteins for binding divalent metal irons, and antioxidant enzymes. Oxidative stress which is associated with cellular injury in many pathological conditions occurs when there is an imbalance between free-radical generating and radical scavenging systems (Hensley et al. 2000).

Accepted Sept 5, 2007
*Corresponding author. E-mail: seityjen@yahoo.com

The complications of diabetes mellitus are morphologic consequences of many metabolic pathways which may be associated with increased free radicals and serum lipid production (Lee and Chung 1999; Sheetz and King 2002; Goldberg 2001; Smaoui et al 2004). Intracellular advanced glycated end products (AGE) may stimulate the generation of increased level of reactive oxygen species (ROS) and the activation of NF-kB following binding to specific receptors (Kahler et al. 1993; Stitt et al. 2002). Glucose can be converted to Sorbitol by the enzyme, aldose reductase and eventually to fructose. In this process, intracellular NADPH is used as cofactor and this reduces the availability of NADPH required for the regeneration of reduced glutathione (GSH), a major antioxidant molecule in cells and tissues (Lee and Chung 1999). Sustained hyperglycemia as in diabetes mellitus and progressive depletion of intracellular NADPH by aldose reductase may lead to a compromise of GSH regeneration and thus increase cellular susceptibility to oxidative stress. Protein glycosylation in cells also affect antioxidant reactions catalysed by ROS scavenging enzymes in diabetes mellitus (Stitt et al. 2002).

Accelerated atherosclerosis among diabetics is a major pathologic cause of microvascular and macrovascular complications resulting in increased risk of myocardial infarction, stroke and lower extremity gangrene. Experimental and clinical evidences suggest that these complications are promoted by dyslipidemia (Goldberg 2001). Defects in insulin action have been shown to be responsible for the changes in plasma lipoprotein fractions in patients with diabetes mellitus (Haff-

ner et al. 2000).The oxidized form of low density lipoprotein (LDL)-cholesterol is of prime importance in the formation of foam cells in atherosclerotic plaque (Jilial and Devaraj 1996). Chemical changes of LDL- cholesterol by free radicals generated in macrophages or endothelial cells in the arterial wall yields oxidize LDL thereby implicating oxidative stress in the pathogenesis of atherosclerosis (Reardon and Getz 2001). Antioxidant treatment has however been shown to protect against the development of atherosclerosis in hypercholesterolemic experimental animals (Reardon and Getz 2001) and diabetic models (Jilial et al. 1990; Jilial and Grundy 1992).

Azadirachta indica, also called neem, belongs to the family of meliacea. It is one of the most useful medicinal plants with anti-inflammatory, antibacterial, anti-parasitic and immunomodulatory activities (Kausik and Ranajet 2002). Blood glucose lowering effect of *Azadirachta indica* seed oil and water extract have been reported in various models of diabetic animals (Dixit et al. 1986; Khosla et al. 2000; Halim 2003; Gupta et al. 204). The leaf extract of *A. indica* have been used traditionally in the control of diabetes mellitus in many countries including Nigeria, however, scientific studies on the efficacy and its mechanism of action have not been fully investigated.

This study therefore examines the effects of ethanolic extract of *A. indica* leaves on lipid peroxidation and serum lipids in diabetic rats with a view to ascertaining its involvement in the management of oxidative stress and other complications associated with diabetic mellitus.

Materials and Methods

Plant materials and extract preparation

Fresh matured leaves of *Azadirachta indica* (Neem) were harvested from Endocrine Research Farm of the Department of Biochemistry, University of Calabar, Calabar. The leaves were washed with tap water, rinsed with distilled water and sundried to remove traces of water. The leaves were ground to form paste with an electric blender (Binatone, Japan). One hundred and fifty grams of leaf paste was agitated in 500 ml of ethanol and stored overnight in a refrigerator at 4°C for complete extraction. The suspension was filtered and 50 ml aliquots of the filtrate were poured into separate beakers of known weight. The aliquots were dried at 50°C to constant weight using rotary evaporator. The dry extract was stored in a refrigerator at 4°C. Two grams of the dry extract was resuspended daily in 50 ml of distilled water for administration to the animals. 1.5 ml of the suspension, given to a 150 g rat was equivalent to 400 mg extract per kilogram body weight. The volumes of extract suspension were adjusted accordingly for various weights of the rats.

Animals

Thirty albino wistar rats, weighing 150-200 g, were obtained from the Animal House of the Department of Biochemistry, University of Calabar. The animals were kept in standards plastic cages and placed in a well ventilated room of temperature between 22°C and 27°C. The animals were acclimatized for seven days. During this time and throughout the experimental period, they were fed with commercial rat feed (Pfizer Livestock Co. Ltd, Aba, Nigeria) and tap water *ad libitum* .

Animal treatments

After acclimatization, the animals were assigned into four groups of six rats each as follows: Normal Control (NC), Diabetic Control (DC), Diabetic Treated (DT) and Normal Treated (NT) groups. The animals for DC and DT groups were made diabetic by a single intraperitoneal administration of 150 mg/kg body weight of alloxan (Sigma, St. Louis, USA) dissolved in distilled water (Battel et al. 1999). The animals were left for 7 days after which fasting glucose concentrations were determined in their tail-prick blood samples using One Touch Basic Glucometer (Life Scan, USA). Animals with consistent blood glucose greater than 200 mg/dl for 2 days were considered diabetic and randomly assigned to DC or DT group before administration of extract commenced. Groups DT and NT were treated with 400 mg/kg body weight of the extract twice daily for 7 days by oral gavage while groups DC and NC which served as controls were given distilled water orally. Body weight of the animals and their fasting blood glucose were monitored before and after extract administration.

Collection and preparation of samples

At the end of the 7-day treatment, the animals were anaesthesized under chloroform vapour and sacrificed. Blood samples were obtained by cardiac puncture and poured into plain screw-caped sample bottles and allowed to clot. Serum samples were separated from the clotted blood by centrifugation at 2000 x g for 5 min using an MSE model (England) bench centrifuge. The sera were stored at 4°C and biochemical assays conducted within 24 h.

Biochemical assays

Blood glucose was determined by pricking the tail of rats asceptically with Lancet and placing one drop of blood on a sample strip. The blood on the strip was inserted into the glucometer (Life Scan, USA) and glucose concentration was read (WHO, 1980)

Lipid peroxidation product, malondialdehyde (MDA) was measured by the method of Esterbauer et al (1991) using Bioxytech MDA reagents kit.

Total cholesterol and triglyceride concentrations were determined by enzymatic colourimetric assay using reagents kits from Dialab produktion, France. The absorbances in all analysis were read using spectrophotometer Optima SP-300.

Table 1. Mean values of body weight and blood glucose of normal and diabetic rats on or without extract of *A. indica*.

Group	Body weight(g) Before	After	% Weight gain	Blood Glucose (mg/dl) Before	After
NC	180.2± 5.15	183.5± 8.92	1.83 ± 0.31	106.6 ± 15.10	104.8 ± 18.10
DC	179.3± 6.10	181.0± 8.25	0.95 ± 0.42*	300.4 ± 10.46*	306.5 ± 12.43*
DT	177.5± 6.50	181.1± 9.50	2.03 ± 0.35	302.6 ± 16.48*	133.8 ± 13.75
NT	179.4± 4.25	185.5± 8.20	3.40 ± 0.51*	105.5 ± 18.20	104.5 ± 16.50

Mean ± SD, *Significantly different from normal control at P < 0.05.

Table 2. Malondialdehyde (MDA), total cholesterol (TC) and triglyceride (TG) in serum of normal and diabetic rats on or without extract of *A. indica*.

Group	MDA (μmol/ml)	TC (mg/dl)	TG (mg/dl)
NC	2.07 ± 0.42	92.10 ± 6.17	114.20 ± 6.24
DC	11.51 ± 0.22*	132.00 ± 7.82*	145.71 ± 8.34*
DT	4.06 ± 0.43	96.24 ± 3.42	121.31 ± 7.63
NT	-	94.37 ± 3.47	110.56 ± 5.16

Mean ± SD, *significantly different from normal control at P < 0.05.

Statistical Analysis

Data are presented as mean ± SD. The differences between groups were tested using student's *t*-test. A probability of 0.05 was chosen as a level of significance.

Results and Discussion

The mean values of body weight and blood glucose of normal and diabetic rats before and after treatment with 400 mg/kg of *A. indica* leaf extract is presented in Table 1, while Table 2 shows the effects of the extract on serum malondialdehyde (MDA) and serum lipids of normal and diabetic rats. The percentage weight gain of diabetic and normal rats treated with the extract of *A. indica* leaves were respectively higher than those of diabetic and normal control rats which did not receive the extract. Serum glucose, cholesterol and triglyceride concentrations were significantly ($P < 0.05$) higher in diabetic control rats compared to those of normal control and those receiving extract treatment.

The extract reduced serum glucose, cholesterol and triglyceride concentrations in diabetic rats to about normal levels and also appeared to promote growth of both normal and diabetic rats. The mechanism of growth promotion by the extract is not well known, but may be related to enhanced cellular anabolic processes in which carbohydrates, proteins and lipids are metabolized and stored in tissues. Insulin, a hormone with known anabolic activity, enhances peripheral uptake of glucose and triglyceride from extracellular compartment into cells (Saltiel and Kahn 2001). Thus increase in weight of animals treated with the extract may be the result of enhanced insulin action, especially since extract treatment caused the reduction of serum glucose, cholesterol and triglyceride in the diabetic rats.

The lipid peroxidation product, malondialdehyde (MDA), was significantly ($P<0.05$) higher in the diabetic control rats compared to normal control whereas the MDA of diabetic treated rats was not significantly different from those of normal control. This indicates that the extract of *A. indica* prevents lipid peroxidation reactions in the animals. Fresh mature leaves of *A. indica* have been shown to contain quecretin (a poly-phenolic flavonoid), nimbosterol (β-sitosterol), carotenes and ascorbic acid (Jacobson 1990). Thus, the prevention of lipid peroxidation by the leaf extract could be attributed to the antioxidant activities of the flavonoid, carotenes and ascorbic acid present in the leaves.

Alloxan used in this study for the induction of diabetes mellitus is known to mediate the destruction of β-cells by establishing redox cycles resulting in the formation of reactive free radicals which constitute the major inducer agent for the cell damage and hence diabetes in the rats (Szkuldeshi 2001). The alloxan associated radicals and those generated as a result of hyperglycemia by aldose reductase (Ceriello et al. 1992) and AGE-related (Wolff et al. 1991) activities may be responsible for the increased lipid peroxidation observed in the diabetic control rats. Earlier reports have demonstrated elevated serum lipid peroxides levels and diminished antioxidant status in diabetic subjects (Oberley 1988). It is likely that administration of the extract prevents further destruction of β-cells by terminating the progressive generation of reactive hydroperoxyl radicals. This reduction of lipid peroxidation by the extract appeared to allow for cellular repair and regeneration of β-cells which result in production of insulin as may be evident by the reduction of blood glucose, triglyceride and cholesterol in the diabetic treated rats.

Diabetes mellitus and its complications are associated with free radical mediated celluar injury (Asayama et al. 1993; Lee and Chung 1999) and impaired lipid metabolism (Goldberg 2001). This study have shown that ethanolic extract of *A. indica* leaves demonstrated anti-lipid peroxidative, anti-hyperglycemic, and anti-hypercholesterolemic activities and reduced triglyceride level in diabetic rat model, therefore justifying the possibility of using the extract in management of diabetes mellitus and its complications.

Acknowledgements

The authors wish to acknowledge the research grant awarded to Prof. P. E. Ebong by the Raw Materials Research and Development Council (RMRDC) of the Federal Ministry of Science and Technology, Abuja, Nigeria.

References

Asayama K, Uchida N. Nakane T, Hayashiba H, Dobashi H, Dobashi K, Amemiya S, Kato K, Nakazawa S (1993) Antioxidants in the serum of children with insulin dependent diabetes mellitus. Free Radic Bio Med 15:597-602.

Battel ML, Yuen VG, Verma S, McNeil JH (1999) Other Models of type 1 diabetes. In McNeil JH (ed) Experimental models of diabetes CRC Press LHC. Florida pp. 219-226.

Ceriello A, Quatraro A, Giugliano D (1992) New Insight on non-enzymatic glycosylation may lead to therapeutic approaches for the prevention of the diabetic complications. Diabet Med 9:297-299.

Dixit VP, Sinh R, Tank R (1986) Effect of Neem seed oil on the blood glucose concentration of normal and alloxan diabetic rats. J Ethnopharmacol 17(1):95-98.

Droge W (2002) Free radicals in the physiological control of cell function. Physiol Rev 82:47-52.

Esterbauer H, Schaur RJ, Zollner H (1991) Chemistry and Biochemistry of 4- hydroxynoneral, malondialdehyde and related aldehydes. Free Radic Biol Med 11:81-87.

Frankel EN (1980) Lipid peroxidation. Prog Lipid Res 19:1-22.

Goldberg IJ (2001) Diabetic dyslipidaemia: causes and consequences. J Clin Endocrinol Metab 86(3):965-971.

Gupta S, Kataria M, Gupta PK, Murganandan S, Yashroy RC (2004) Protective role of extracts of neem seeds in diabetes caused by streptozotocin in rats. J Ethnopharmacol 90(2-3):185-9.

Haffner SM, Mykkanen L, Festa A, Burke JP, Stern MP (2000) Insulin resistant prediabetic subjects have more atherogenic risk factors than insulin-sensitive prediabetic subjects: Implication for preventing coronary heart disease during the prediabetic state. Circulation 101:975-980.

Halim EM (2003) Lowering of blood sugar by water extract of Azadirachta indica and Abroma augusta in diabetes rats. Indian J Exp Biol 41(6):636-640.

Hensley K, Robinson KA, Gabbita SP, Salsman S, Floyd RA (2000) Reactive oxygen species, cell signaling, and cell injury. Free Radic Biol Med 28:1456-1461.

Jacobson M (1990) Review of Neem research in the United States. In Proceeding of a workshop on neem potentials, pest management programme USA – ARS, Beltsville, Ad ARS 86:40-44.

Jilial I, Devaraj S (1996) The role of oxidized LDL in atherosclerosis. J Nutri 126:1053s-1057s.

Jilial I, Grundy SM (1992) Influence of antioxidant vitamins on LDL oxidation. Ann NY Acad Sci 669:237-247.

Jilial I, Lena-Veta G, Grundy SM (1990) Physiologic levels of ascorbate inhibit the oxidative modification of LDL. Antherosclerosis 82:185-191.

Kahler W, Kuklinski B, Rublman C, Plotz C (1993) Diabetes mellitus, a free radical-associated disease. Result of adjurant antioxidant supplementation 1. J Gesanite Inn Med 48(4):223-232.

Kausik BI, Ranajit KB (2002) Biological activities and medicinal properties of Neem plant. Current Science 82(11):1336-1345.

Khosla P, Bhanwra S, Singh J, Seth S, Srivastava RK (2000) A study of hypoglycaemic effects of Azadirachta indica (Neem) in normaland alloxan diabetic rabbits. Indian J Physiol Pharmacol 44(1):69-74.

Lee AY, Chung SS (1999) Contributions of Polyol Pathway to oxidative stress in diabetic cataract. FASEB J 13(1):23-30.

Oberley LW (1988) Free radicals and diabetes. Free Radic Biol Med 5: 113-124.

Reardon CA, Getz GS (2001) Mouse models of atherosclerosis. Curr Opin Lipidol 12:167-173.

Saltiel AR, Kahn CR (2001) Insulin signaling and the regulation of glucose and lipid metabolism. Nature 414(6865):799-806.

Sheetz MJ, King GL (2002) Molecular understanding of hyperglycemia's adverse effect for diabetic complications. JAMA 288(20):2579-2588.

Smaoui M, Hummani S, Chaaba R, Affia N, Handa KB, Masmoudi AS, Mahjoub S, Bousslama A, Farhat MB, Hammani M (2004) Lipid and lipoprotein (A) concentrations in Tunisian type 2 diabetic patients: Relationship to glycemic control and coronary heart disease. J Diabetes Complications 18(5):258-263.

Stitt AW, Jenkins AJ, Cooper ME (2002) Advanced glycation end products and diabetic compilations. Expert Opin Invest Drugs 11(9):1205-1223.

Szkudelski T (2001) The mechanisms of alloxan and streptozotocin action in beta-cells of the rat pancreas. Physiol Res 50:536-546.

WHO expert committee on diabetes mellitus. Tech Rep Series No. 646. World Health Organization, Geneva.

Volume 51(1):21-25, 2007
Acta Biologica Szegediensis
http://www.sci.u-szeged.hu/ABS

ARTICLE

Sensitivity of various skinfold sites to fat deposition in adolescent daughters and their mothers

Rashmi Sinha, Satwanti Kapoor*

Department of Anthropology, University of Delhi, Delhi, India

ABSTRACT The present study comprised of 412 adolescent daughters at a yearly intervals from age 11 through 17 years and their mothers who volunteered as subjects. All the subjects belonged to Punjabi speaking Khatri, an endogamous population residing in Delhi, India. A set of five skinfold thickness: biceps, triceps, subscapular, suprailiac and medial calf along with body weight and stature were taken on all the subjects to report the pattern of subcutaneous fat distribution and responsiveness of different skinfold sites to fat deposition with variation in total body fat content. An increase in body mass index (bmi) with age in the present sample with a concurrent increase in the grand mean thickness (GMT) is due to relative increase in fatness. All the skinfold thicknesses, indices of fatness, profile of subcutaneous fat accumulation and sensitivity of each skinfold site showed an increasing fat deposition on trunkal region than on extremities. It was noticed that subscapular site as the most sensitive site followed by triceps and biceps towards fat deposition. The differential rate of fat deposition at various sites in different age groups explains the difference in morphological feature in them.
Acta Biol Szeged 51(1):21-25 (2007)

KEY WORDS

adolescent daughters
fat distribution
mothers
sensitivity of skinfolds

Biological ageing is associated with the number of changes in body composition and body build. The etiology of these changes, all of which are not favorable was unclear up to now. With advancing age, fat free tissue weight decreases whereas fat tissue weight increases. Of the three large tissue components, bone, muscle and fat, the latter shows the greatest change during adulthood in both sexes. The body contours, which are determined by muscle and bone, and the thickness of overlying subcutaneous fat layer undergo a change with fluctuation in body weight. What is of utmost importance and has not gained much attention is the sensitivity of different skinfold sites towards fat accumulation with increase in fat content or with increasing age. Women continue with a largely unchanged fat patterning from puberty to middle age, but with advancing age not only body mass index increases, fat distribution pattern also changes.

The most obvious of the body contour fat patterning an integral aspect of human body has drawn considerable attention recently because of its association with several diseases (Jensen et al. 1989; Bjorntorp. 1990; Kanaley et al. 1993). The importance of the body fatness and its distribution lies in the epidemiological studies and as a clinical marker of health risk among populations. Fat distribution pattern has been extensively studied for decades (Garn 1954; Satwanti et al. 1980; Rimm et al. 1995; Joyce and Kapoor 1996; Sinha and Kapoor 2005), on ethnic variation in fat distribution (Satwanti et al. 1977; Stevens et al. 1992; Wardle et al. 1996) and on level of physical activity and fat distribution pattern (Brown and Jones 1977; Bhalla et al. 1983; Satwanti et al. 1984; Depress et al. 1985). It has become apparent that the fat distribution pattern is population, sex and age specific along with increase in obesity level. The pattern of fat distribution must be evaluated to assess the risk associated with weight gain, as the risk is higher if the fat distribution is already central (Lapidus et al. 1984; Ducimetiere et al. 1986; Kissebah et al. 1988).

The present study was undertaken to report the body mass index- an indicator of obesity and the sensitivity of different skinfold sites for fat deposition with varying body fat content among Indian adolescent girls and their mothers belonging to urban population.

Subjects and Methods

Four hundred and twelve Khatri adolescent girls residing in Delhi, India constituted the study. The girls at a yearly interval from age 11 through 17 years and their mothers 32-50 years volunteered as subjects in the present study. A set of five skinfold thicknesses (biceps, triceps, subscapular, suprailiac and medial calf) along with body weight and stature were taken on all the subjects in the present study. All the measurements were taken according to the techniques described by Weiner and Lourie (1981).

The profile of subcutaneous fat distribution over the body was obtained by arranging the skinfold site in ascending order of their thickness. An indicator of fatness - body mass

Accepted May 21, 2007
*Corresponding author. E-mail: satwanti@yahoo.com

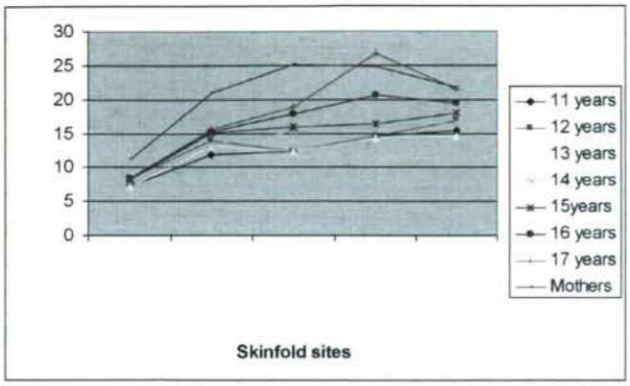

Figure 1. Distribution pattern of subcutaneous fat in adolescent girls and their mothers.

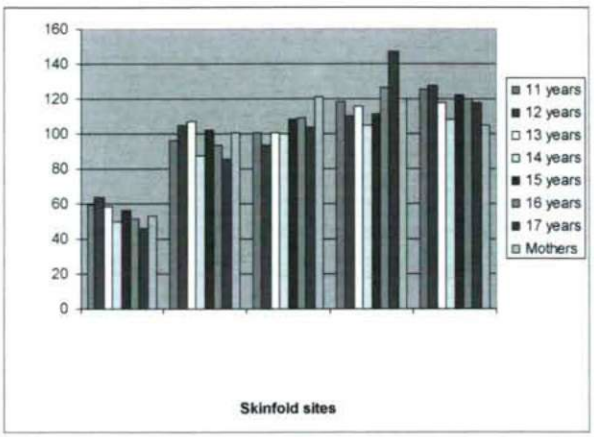

Figure 2. Response of different sites towards accumulation of body fat in adolescent daughters and their mothers.

index was calculated as weight in kg divided by stature in meter square. To study the rate of deposition or sensitivity of subcutaneous fat at different sites, each skinfold thickness was expressed as percent of grand mean thickness (GMT, *i.e.* mean thickness of skinfold at all the sites measured; Satwanti et al.1980). The data was analyzed using SPSS version 7.0.

Results

The means and standard deviations of body weight and stature including BMI for mothers and their daughters are given in Table 1. Skinfold thicknesses and GMT among adolescent daughters and their mothers are presented in Table 2. Table 3 shows the sensitivity of various skinfold sites to fat deposition in adolescent daughters and their mothers. The profile of subcutaneous fat distribution in adolescent girls and their mothers, determined by arranging various sites in ascending order of their thickness is illustrated in Figure 1 and Figure 2 shows the responsiveness of different skinfold site to fat deposition among adolescent daughters and their mothers.

Body weight showed a consistent increase with advancing age (from 11- 32-50 years) as it is evident from Table 1. After 14 years of age increase in body mass index is noticed with advancing age. Stature increased among growing girls with maximum increase in 12 year old subjects. Mothers were marginally shorter than their 17 – year – old daughters.

The distribution of fat pattern in adolescent daughters and their mothers (Table 2, Fig. 1) does not follow similar trend in all the age groups indicating on going tendency of fat redistribution with age, although in all the age groups biceps skinfold site shows the minimum fat, the site of maximum fat varies in different age groups. The distribution pattern of subcutaneous fat in different groups is as follows:

11 years Biceps < triceps < subscapular < suprailiac < medial calf

12 years Biceps < subscapular < triceps < suprailiac < medial calf

13 years Biceps < subscapular < triceps < suprailiac < medial calf

14 years Biceps < triceps < subscapular < suprailiac < medial calf

15 years Biceps < triceps < subscapular < suprailiac < medial calf

16 years Biceps < triceps < subscapular < medial calf < suprailiac

17 years Biceps < triceps < subscapular < medial calf < suprailiac.

Table 1. Basic data of the subjects.

Variable/Age		Adolescent girls (years)							Mothers (years)
		11 (n=54)	12 (n=60)	13 (n=60)	14 (n=62)	15 (n=51)	16 (n=64)	17 (n=61)	32-50 (n=108)
Weight (kg)	Mean	34.32	38.55	47.34	45.0	48.41	48.42	50.95	62.09
	±SD	7.00	8.34	7.40	7.73	5.84	5.11	7.11	12.17
Stature (cm)	Mean	135.8	148.68	151.23	153.57	155.34	155.45	155.80	153.63
	±SD	8.18	7.91	6.21	6.17	5.04	4.25	6.55	4.83
Body mass index (kg/m^2)		18.83	17.36	20.76	19.02	20.15	20.15	20.94	25.84

Table 2. Skinfold thickness and Grand mean thickeness of skinfolds of the subjects.

Skinfold thickness/ /Age		Adolescent girls (years)							Mothers ((years)
		11	12	13	14	15	16	17	35-55
Biceps(mm)	Mean	7.33	8.42	7.20	7.57	8.29	8.31	8.38	11.13
	±SD	3.39	2.69	3.71	2.87	2.92	1.71	2.22	5.51
Triceps(mm)	Mean	11.87	13.93	13.17	13.33	15.05	15.17	15.53	20.90
	±SD	3.85	4.99	4.11	4.80	4.68	4.17	4.57	6.92
Subscapular (mm)	Mean	12.37	12.38	12.37	15.19	15.95	17.76	18.88	25.16
	±SD	6.74	5.18	4.92	6.99	6.59	8.93	7.64	8.83
Suprailiac (mm)	Mean	14.58	14.64	14.26	15.94	16.44	20.58	26.79	24.87
	±SD	7.54	5.89	6.53	7.21	7.33	9.79	4.14	8.81
Medial calf(mm)	Mean	15.48	16.87	14.53	16.49	18.00	19.50	21.40	21.75
	±SD	6.96	6.43	6.92	7.20	6.82	8.09	7.38	8.59
Grand mean thickness(mm)		12.33	13.25	12.31	15.22	13.70	16.26	18.19	20.76

The pattern of subcutaneous fat distribution at 11, 14 and 15 years are same while that at 12 &13 years and 16 &17 years is distinctive of their age. Mothers' subcutaneous fat distribution pattern in ascending order is biceps, triceps, medial calf, suprailiac and subscapular. Both intra and inter group variation in the thickness of fatfold layer was thus depicted. A marked increase in total fat content as calculated by mean of the summing up of the five skinfold thickness (GMT) is found to increase with the advancing age.

The grand mean thickness (GMT) was found to be statistically significant between 13 & 14 years old girls and 17 year old daughters and mothers ($p< 0.05$). In rest of the age groups the difference were found to be statistically non-significant (Table 3).

To understand the reason for this phenomenon the sensitivity of different skinfold sites for accumulation of subcutaneous fat was assessed by expressing each site as percent of GMT (Fig. 2), thus ruling out any inter individual variations solely due to absolute fatness. Theoretically, any change in the GMT would be accompanied by change in the thickness of the skinfold at individual sites. The change thus occurring was not uniform at all sites as some sites gained relatively more fat as compared to others. It was noticed that subscapular site as the most sensitive site followed by triceps and biceps towards fat deposition.

Table 3. Significance of difference in the Grand mean thickness between different age groups.

Age groups (years)	value of 't' with level of significance
11&12	-.760
12&13	.817
13&14	2.35*
14&15	.348
15&16	-1.08
16&17	-1.56
17&,Mothers	-2.07*

*p<0.05

Discussion

There is a consistent increase in the body weight with advancing age from adolescence to middle aged mothers. The subcutaneous fat as assessed from skinfold thickness taken at various sites over the body and GMT (grand mean thickness) showed fluctuation in the study. The 17 year old daughters were found to be taller than their mothers reflecting the presence of secular trend due to improved nutritional status and living conditions of the population in the present study. There have been studies showing the increase in height and weight of people increasing with succeeding generations (Kapoor et al. 1984; Gordon-Larsen et al. 1997; Khanna and Kapoor 2004), a reflection of better nutrition, fewer diseases and better medical facilities (Tanner 1978). The Khatri daughters (17 year old) of the present sample were taller than their mothers. As mothers (mother vs. 17 year daughters) BMI were higher than of daughter, a major contribution in their weight gain could be attributed to gain in fatness, lending further support to "well founded concept of fat gain with ageing" (Nirmala and Reddy 1997; Tungdim et al. 2002). The higher value of GMT in mothers further supports this phenomenon.

The fluctuation in the skinfold thickness among girls could be a reflection of fluctuation for energy stores as fat is depleted in case of faster growth phase (Parizkova 1977; Kapoor et al. 1998; Sinha and Kapoor 2006). There are many changes during adolescence taking place; hence the body calls upon fat stores as and when required. Whereas continuously increasing body weight with age can be attributed to increase in muscle and skeletal mass which is at the cost of stored fat in the body. Juvenile obesity warrants early intervention because

the pattern of unhealthy behaviour is formed in adolescence and young adulthood (Riberio et al. 2004).

Adult fat distribution in females start manifesting itself from early pubertal period (Forbes 1990), supported by present study too. There is a relative loss of extremity fat from preadolescence through adulthood (Ramirez and Mueller 1980) as illustrated in the present study too. Skinfold thickness measurements in the study of Guilford et al. (2001) suggested a central pattern of body fat distribution. Young et al. (1962) claimed that at adolescence girls begin to assume fat distribution of a young woman with greater concentration on the lower trunk. The fat mass of body increases with age and also re-distribution of fat in body takes place in later age resulting in centripetal adiposity (Orden and Oyhenart 2006; Sinha and Kapoor 2006). The active role of children as social architects of their own biology should provide novel and important understanding of biocultural construction of childhood nutrition (Brewis and Gartin 2006).

The increase in BMI, an index of overweight/ obesity and a simultaneous increase in the GMT of skinfold thickness with age would entail this increase in weight due to increase in fatness. Higher values of all the five skinfold thickness of mothers as compared to the adolescent daughters in the present study also indicated an increase in fatness with age. All the skinfold thicknesses, indices of fatness, profile of subcutaneous fat accumulation and sensitivity of each skinfold site showed an increasing fat deposition on trunkal region than on extremities. The varying rate of fat deposition at various sites in different age groups explains the difference in morphological feature in them.

A consistent increase in fatness establishes the fact that fat content in females continously increase throughout life. This means reflection of increase in the measure of skinfold thickness at individual site. But this increase was not uniform at all the sites, as some sites seemed to gain proportionately more fat as compared to other sites with increase in the body fat. This phenomenon could be determinant of change in physique.

Sensitivity of the five skinfold site towards deposition of fat showed variation in different sites in different age groups. Subscapular was found to be most sensitive site towards fat deposition followed by triceps and biceps. This further strengthens the fact that even during the late adolescent period not only continues to increase in fat content but also favors redistribution of fat away from extremity towards the trunk and that adolescents (17 year old daughter) still does not have the same pattern of subcutaneous fat as the middle aged women (mothers).

In the present study all the fatness pointer/measure/indicator showed an increasing fat in favor of trunkal region. The differential rate of fat deposition at various sites in different age groups explains the difference in morphological feature in them and may have epidemiological significance.

Acknowledgements

We owe our sincere gratitude to Professor I.P. Singh for his unconditional and invaluable guidance. The financial assistance offered by Indian Council of Medical Research is gratefully acknowledged. The authors are thankful for cooperation extended by the subjects during data collection.

References

Bhalla R, Kapoor AK, Satwanti, Singh IP (1983) The distribution of subcutaneous fat with reference level of physical activity in adult females. Z Morph Anthropol 24:191-197.

Bjorntorp P (1990) The association between obesity, adipose tissue distribution and disease. Acta Med Scand 723:121-134.

Brewis A, Gartin M (2006) Biocultural construction of obesogenic ecologies of childhood:Parent feeding versus child eating strtigies. Am J Hum Biol 18:203-213.

Brown WJ, Jones PRM (1977) The distribution of body fat in relation to habitual activity. Ann Hum Biol 4:537-550.

Depress JP, Bouchard C, Trembley A, Savard R, Marcotte M (1985) Effect of aerobic training on fat distribution in male subjects. Med Sc Sports Exerc 17:113-118.

Ducimetiere P, Richard J, Cambien F (1986) The pattern of subcutaneous fat distribution in middle aged man and the risk of coronary heart disease: The Paris prospective study. Int J Obes 10:229-240.

Forbes GB (1990) The abdomen: Hip ratio normative data and observation on selected patients. Int J Obes 14:149-157.

Garn SM (1954) Fat patterning and fat intercorrelation in adult males. Hum Biol 26:59-69.

Godon-Larsen P, Zemel BS, Johnston FE (1997) Secular change in stature, weight, fatness,overweight and obesity in urban African American adolescents from mid 1950's to mid 1990's. Am J Hum Biol 9:675-688.

Guilford MC, Mahabir D, Rocke B, Chinn S, Rona R (2001) Overweight, obesity and skinfold thicknesses of children of African or Indian descent in Trinidad and Tobago. Int J Epidemiol 30:989-998.

Jensen MD, Haymond MW, Rizza RA, Cryer PE, Miles JM (1989) Influence of body fat distribution on free fatty acid metabolism in obesity. J Clin Invest 83:1168-1173.

Joyce KP, Kapoor S (1996) Pattern of subcutaneous fat distribution, its variation with age among young Rajput females of Pauri Garhwal, India. J Hum Ecol 7:45-49.

Kanaley JA, Andersen–Reid ML, Oenning LV, Kottke BA, Jensen MD (1993) Differential health benefits of weight loss in upper –body and lower body obese. Amer J Clin Nutr 57:20-26.

Kapoor S, Kapoor AK, Kumbnani HK, Bhalla R (1984) Anthropometry of newborns: change over a decade. Acta Med Auxol 16:223-226.

Kapoor S, Patra PK, Sandhu S, Kapoor AK (1998) Fatness and its distribution pattern among Jat Sikhs. J Ind Anthrop Soc 33:223-228.

Khanna G, Kapoor S (2004) Secular trend in stature and age at menarche among Punjabi Aroras residing in New Delhi, India. Coll Anthropol 28:571-575.

Kissebah AH, Peiris A, Evans DJ (1988) Mechanisms associating body fat distribution to glucose intolerance and diabetes mellitus.. In: Bouchard C, Johnston FE, Alan R (Eds): Fat Distribution during Growth and later Health Outcomes. Liss. New York. pp. 203-220.

Lapidus L, Bengtsson C, Larsson B, Pennert K, Rybo E, Sjostrom L (1984) Distribution of adipose tissue and risk of cardiovascular disease and death: A 12-y follow up of participants in the population study of women in Gothenberg, Sweden. Brit Med J 289:1257-1260.

Nirmala A, Reddy PC (1997) A study of blood pressure on the aged. In: Life in Twilight Years. Quality Book Company Publishers, Calcutta, India. p. 223-228.

Orden AB, Oyhenart EE (2006) Prevalence of overweight and obesity among Gurani-Mbya from Misiones,Argentina. Am J Hum Biol 18:590-599.

Parizkova J (1977) Body fat and physical fitness. The Hague, Martinus Nijhiff, B. V. Med. Div. 1

Ramirez ME, Mueller WH (1980) The development of density and fat patterning in Tokelau Children. Hum Biol 52:675-687.

Riberio JC, Gurra S, Oliveira J, Anderson LB, Dyarte JA, Mota J (2004) Body fatness and clustering of cardiovascular disease risk factors in Portuguese children and adolescents.Am J Hum Biol 16:556-562.

Rimm EB, Stampfer MJ, Giovannucci E, Ascherio A, Spiegelman D, Golditz GA, Willet WC (1995) Body size and fat distribution as predictors of coronary heart disease among middle –aged and older US men. Am J Epidemiol 141:117-1127.

Satwanti, Bharadwaj H, Singh IP (1977) Relationship of body density to body measurements in young Punjabi women: Applicability of body composition prediction equations developed for women of European descent. Hum Biol 49:203-213.

Satwanti, Singh IP, Bharadwaj H (1980) Fat distribution in lean and obese young Indian women: A densitometric and anthropometric evaluation. AJPA 53:611-616.

Satwanti, Kapoor AK, Bhalla R, Singh IP (1984) A study of the distribution pattern of fat in male gymnasts. Anthrop Anz 42:131-136.

Sinha R, Kapoor S (2005) Fat patterning among Indian adolescent Boys and Girls. Ind J Phy Anthrop Hum Genet 24:135-141.

Sinha R, Kapoor S (2006) Parent-Child Correlation for Various Indices of Adiposity in an Endogamous Indian Population. Coll Antrop 30:291-296.

Stevens J, Keil JE, Rust PF, Tyroler HA, Davis CE, Gazes PC (1992) Body Mass Index and body girths as predictors of mortality in black and white women. Arch Intern Med 152:1257-1262.

Tanner JM (1978) Foetus into man: physical growth from conception to maturity. London: Open Books.

Tungdim MG, Kapoor S, Kapoor AK (2002) Morpho-physiological changes among high altitude aged. Ind J Med Res 16:329-343.

Ulijaszek SJ, Strickland SS (1996) Body Mass Index and fat patterning of adults in rural Sarawak. Mal J Nutr 2:128-136.

Wardle J, Wrightson K, Gibson L (1996) Body fat distribution in South Asian Children. Int J Obes 20:267-271.

Weiner JS, Lourie JA (1981) Human Biology. A guide to field methods. IBP Handbook no 9. Oxford Blackwell Sci Publication.

Young CM, Martin MEK, Tensuan RS, Blondin J (1962) Predicting specific gravity and body fatness in young women. J Am Diet Assoc 40:102-107.

Young CM, Martin MEK, Tensuan RS, Blondin J (1962) Predicting specific gravity and body fartness in young women. J Am Diet Asso 40:102-107.

Volume 51(1):27-32, 2007
Acta Biologica Szegediensis
http://www.sci.u-szeged.hu/ABS

ARTICLE

Fluorescence induction reveals organization of antenna and reaction center in photosynthetic bacteria

László Gerencsér, Péter Maróti*

Department of Biophysics, University of Szeged, Szeged, Hungary

ABSTRACT The photochemical phase of the bacteriochlorophyll fluorescence induction generated by rectangular shape of laser diode illumination was measured in different organization levels (whole cell, chromatophore and isolated reaction center protein) of carotenoidless mutant of purple photosynthetic bacterium *Rhodobacter sphaeroides* R-26.1. While the antenna containing species showed large and positive variable fluorescence (F_v) relative to the constant (initial) fluorescence (F_0) (F_v/F_0 ~ 4.5 in whole cell), the isolated RC had smaller and negative change (F_v/F_0 ~ -0.6). The variable fluorescence of the cells increased steadily in the function of the age of the cultivated bacterium: F_v/F_0 ~ 2 for young cells and F_v/F_0 ~ 4.5 for old cells while the rise time of the fluorescence induction remained constant (~ 2 ms). In chromatophore, 7 times higher rate was measured than in isolated reaction center under identical experimental conditions. The results obtained under different conditions are interpreted by an extended version of the Lavergne-Trissl model where the simultaneously measured fluorescence inductions from the antenna and the RC can be separately expressed.
Acta Biol Szeged 51(1):27-32 (2007)

KEY WORDS

harvesting the sun
photosynthesis
chromatophore
bacteriochlorophyll
fluorescence

Photosynthetic organisms convert the light energy of the sun to other forms of free energy manifested mainly by chemical energy of useful chemical products. The overall yield of the conversion is low. Based on the amount of carbon fixed by a field of corn during a typical growing season, only about 1 - 2% of the solar energy falling on the field is recovered as new photosynthetic products. The photosynthetic efficiency of uncultivated plant is even less, about 0.2%. In sugar cane, which is one of the most efficient plants, about 8% of the light absorbed by the plant is preserved as chemical energy. In contrast to the relatively low efficiency of the overall photosynthesis, the yield of the initial photophysical processes (capturing the light by antenna, funneling to the reaction center (RC) protein and primary charge separation) is high: for example, close to 100% of the excited (bacterio)chlorophyll dimer of the RC (P*) makes charge separation (Wraight and Clayton 1974). The efficient photophysics is due mainly to the optimal organization of the antenna system and the RC.

The photosynthetic apparatus of the bacterium *Rhodobacter (Rba.) sphaeroides* (wild type) consists of three membrane-bound pigment-protein complexes: light-harvesting complexes I (LH I or B875) and II (LH II or B800-850), and the RC, along with the associated components required for subsequent electron transport and energy transduction (Fig. 1). The pigment-protein complexes B875 and B800-850 harvest solar energy and funnel it to the RC. Approximately 14 B875 complexes surround and contact the RC whereas the B800-850 complexes are positioned around the B875-RC complex (Cogdell et al. 2003; Roszak et al. 2003). The B800-850 complex has a minimal unit consisting of three BChl molecules and two carotenoids noncovalently bound to two low-molecular-weight hydrophobic apoproteins labeled as α and β (Zuber and Brunisholz 1993). Two of the BChls are bound in close proximity to each other in the protein and are responsible for the absorption at 850 nm, while the remaining monomeric BChl is responsible for the absorption at 800 nm.

The LHII antenna complex (B850 complex) of the carotenoidless mutant of *Rba. sphaeroides* (R-26.1) is similar in polypeptide composition to the wild-type B800-850 complex, but lacks both carotenoids and the 800 nm absorbing bacteriochlorophyll. The optical absorption spectra of cellular suspension show the typical broad and intense absorption band at ~865 nm due to the overlapping of both LHI and LHII bacteriochlorophyll molecules (B875 and B850, respectively). At 800 nm, a weak absorption peak can be detected due to the RC bacteriochlorophyll monomers.

Although the components of the light harvesting system are tightly packed and energetically well coupled, small portion of the transferred energy is escaped in form of (bacterio)chlorophyll fluorescence. If the photosynthetic organism is exposed to sudden change from dark to light of constant intensity, complex kinetics of the (bacterio)chlorophyll

Accepted Aug 6, 2007
*Corresponding author. E-mail: pmaroti@sol.cc.u-szeged.hu

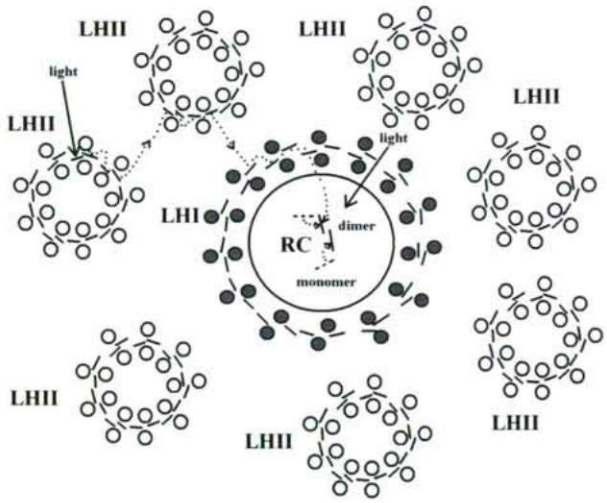

Figure 1. Schematic view of the structural arrangement of the bacterial photosynthetic light gathering complex in *Rba. sphaeroides* cells. The reaction center protein (RC) is surrounded by the core (LHI) and peripheral (LHII) light harvesting complexes. The porphyrine rings of the BChls are represented by short lines in RC (dimer, P and monomer (dashed line)), in LHI (B875) and in LHII (B800-850). The antenna BChls are sandwiched between the inner and outer arrays of the transmembrane α-helices (filled and open circles in LHI and LHII, respectively, end-on view). The complexes are shown in plane of membrane. Both the antenna and the RC pigments can be excited by light. The way of migration of the exciton from the place of absorption (antenna pigment and/or monomer in RC) to the dimer of the RC is indicated by dotted line. (Constructed after Koblizek et al. (2005).)

fluorescence (fluorescence induction) can be observed. The phenomenon was discovered by Müller (1874) and quantitatively studied for the first time by Kautsky and Hirsch (1931) in oxygenic phototrophs and by Vredenberg and Duysens (1963) in anoxygenic phototropic purple bacteria. It has become one of the most frequently used tools in photosynthesis research of green plants to study the organization of the light harvesting system and the molecular mechanisms of energy capture and conversion to chemical energy (Dau 1994; Govindjee 2004; Cser and Vass 2007). In comparison with chlorophyll fluorescence, the use of fluorescence induction of bacteriochlorophyll is much more limited, probably due to the widespread use of kinetic absorption spectrometers to monitor the redox reactions in photosynthetic bacteria (Osváth et al. 1996; Trissl 1996, 1999; Koblizek et al. 2005).

In this work, we measured kinetic traces of fluorescence induction of the carotenoidless mutant of *Rba. sphaeroides* (R-26.1) in different levels of organization (whole cells, chromatophores and isolated RCs) in the (sub)millisecond time range under rectangular shape of intense illumination. The variable fluorescence of the bacterium showed remarkable variation during cultivation. The simplest possible explanation includes simultaneous excitation and detection of fluorescence from both RC and antenna and variable energetic coupling between the components of the light gathering system. This view offers qualitative reasons for the observed widespread changes of the kinetics of bacteriochlorophyll fluorescence induction of the photosynthetic bacteria. By comparison of the rise times of the fluorescence induction in chromatophores and in isolated RC under otherwise identical conditions, the effect of antenna size and the absorption cross section parameters can be directly analyzed in the light harvesting process.

Materials and Methods

Whole cells

The cells of the carotenoidless mutant (R-26.1) of the photosynthetic bacterium *Rba. sphaeroides* were anaerobically cultivated in the light of four tungsten lamps (40 W) under 1.3 mW/cm^2 light intensity measured by Spectra Physics 404 power meter that had flat spectral response between 450 nm and 900 nm. The bacteria were harvested in different phases of the growth. The concentration of the cells (N) was determined either by counting the number of cells under microscope or by measuring the optical density (OD_{obs}) in a 1 cm cuvette at 535 nm (where the cell has minor absorption, therefore the scattering dominates). The following polynomial approach of calibration (Italiano 2007) was used:

$$OD_{obs}(535\ nm) = 0.0119 + 1.61 \cdot N - 0.548 \cdot N^2 + 0.0817 \cdot N^3$$

where N is normalized to 10^9 active cells/ml (that corresponds to $OD_{obs} = 1.16$).

Chromatophores

Chromatophores were obtained by mechanical rapture (sonication) of the cells harvested in the stationary phase of cell growth as previously described (Maróti and Wraight 1988). By this procedure, most of the water-soluble c type cytochromes were lost. The chromatophores were used immediately or kept at -14°C in a glycerol-containing (60:40 (v/v)) buffer (50 mM sodium glycyl-glycine (Fluka)) at pH 7.5. The absorption at 860 nm is the measure of the bacteriochlorophyll content in the chromatophore that can be determined spectroscopically following extraction in polar solvents (acetone/methanol, 7:2 v/v) and using an extinction coefficient of 75 $M^{-1}cm^{-1}$ at 775 nm.

Reaction center protein

The reaction center protein was yielded from chromatophore by standard procedure reported earlier (Maróti and Wraight 1988).

Fluorescence measurements

For recording the kinetics of the fluorescence upon rectan-

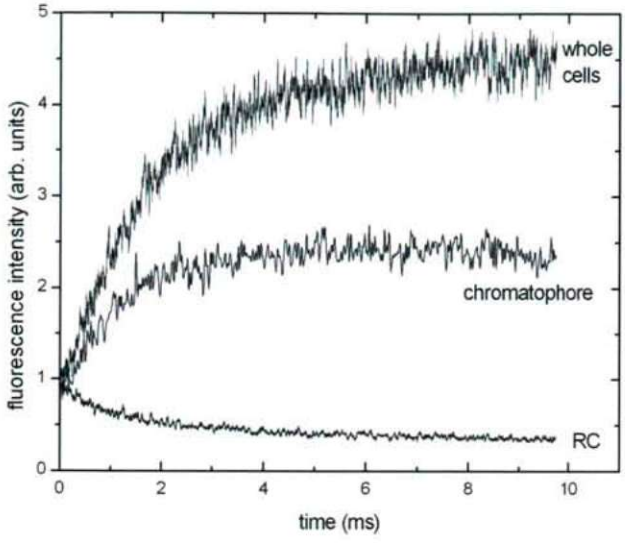

Figure 2. Typical fluorescence induction kinetics in whole cells, chromatophore and isolated RC. The fluorescence levels were normalized to the same initial values (F_0) and were excited by different light intensities to bring the kinetics to the same time scale.

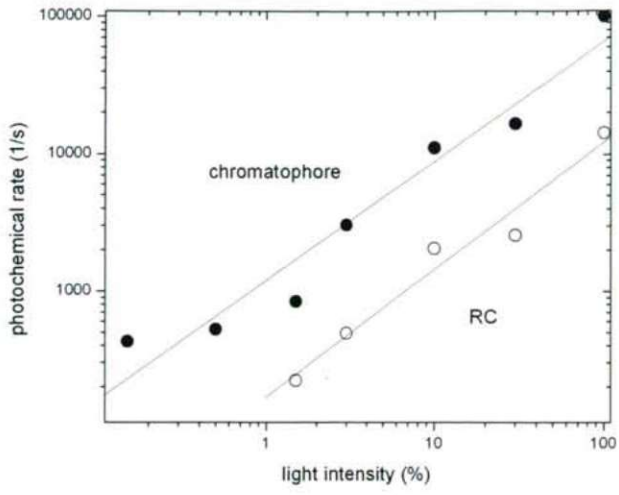

Figure 3. Comparison of the rates of the photochemical phase of the fluorescence induction excited by the same light intensities in chromatophores (●) and isolated RCs (○). The light intensities were attenuated by calibrated neutral density filters. In double logarithm representation, the slopes are 0.87 (chromatophore) and 0.93 (RC) and the rate is 7 times higher in chromatophore than in isolated RC under identical light intensity.

gular shape of illumination, we used a home-built spectrofluorometer with laser diode excitation (808 nm, maximum power 1 W) described previously (Osváth et al. 1996). The duration and intensity of the laser pulse could be adjusted arbitrarily. Fluorescence ($\lambda > 850$ nm) was detected at 90° with respect to the excitation light. The optical densities of the samples in the 1x1 cm cuvette were kept low (OD (865 nm) ~ 0.4) to minimize the secondary effects (scattering, re-absorption of BChl fluorescence, secondary fluorescence, etc.). Addition of 120 μM terbutryne (Chem Service) to RC or chromatophores blocked the electron transfer between the quinones and assured the transfer of only one electron to the acceptor quinone complex. The fluorescence kinetic traces were recorded after single illumination (duration 1-10 ms) at room temperature.

Results

After switching on the exciting light of constant intensity, the fluorescence of BChl *a in vitro* (in solution) appeared immediately and its intensity did not changed during the excitation. On the contrary, BChl *a*-containing photosynthetic organisms show complex time-courses of the fluorescence. The fastest and the more obvious phase of the fluorescence induction is the photochemical phase whose rise time is controlled by the exciting light intensity. We will concentrate here on this phase only. As BChl *a* pigments are major constituents of the bacterial RC and the light harvesting (antenna) system, one can expect different fluorescence induction kinetics in different organization levels of the bacterium. Indeed, we observed significantly different types of curves in isolated RC, membrane fragments (chromatophores) and in whole cells (Fig. 2).

One of the major differences is the direction of change of the fluorescence in whole cells (or chromatophore) and in isolated RC. While the fluorescence increases in the antenna-containing species, it decreases if the antenna is removed. There is a small spectral shift in fluorescence: the peaks of the fluorescence are at 890 nm and 920 nm for the antenna and the RC, respectively (De Klerk et al. 1969; Osváth et al. 1996). Significant difference is observed in the levels of variable fluorescence (F_v) relative to that of initial (constant) fluorescence (F_0): the ratio F_v/F_0 is high for whole cells (> 4) and much less (≈ 2.5) in chromatophore. As the kinetic traces were detected after single illumination, the signal-to-noise ratio is not high enough to make clear-cut distinction between the exponential and sigmoidal shape of the fluorescence induction in whole cells or chromatophores (Trissl 1996, 1999). The decay of fluorescence yield in isolated RC follows the exponential kinetics of charge separation (Osváth et al. 1996).

The photochemical nature of the fast phase of the fluorescence induction is demonstrated by determination of the rate of rise (chromatophore) or decay (RC) at different light intensities (Fig. 3). Attenuation of the exciting light intensity was achieved by calibrated neutral density filters. In double logarithm representation, straight lines with slopes close to 1.0 were obtained for both chromatophores and isolated RC indicating that only photochemical reactions determine the rise (chromatophore) and decay (RC) of the fluorescence in

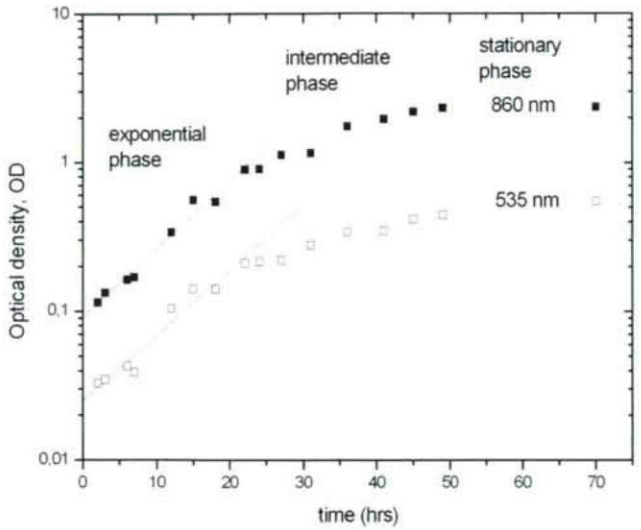

Figure 4. Growth curves of the culture. After inoculation of the cells, the culture is set to light. The optical densities measured in 1 cm cuvette at wavelengths of 860 nm and 535 nm are characteristics of the BChl content and cell population of the culture, respectively. The duplication time of culture in the exponential phase is 6 hrs. OD(535 nm) = 0.1 corresponds to $5.5 \cdot 10^7$ active cells/ml (see M&M).

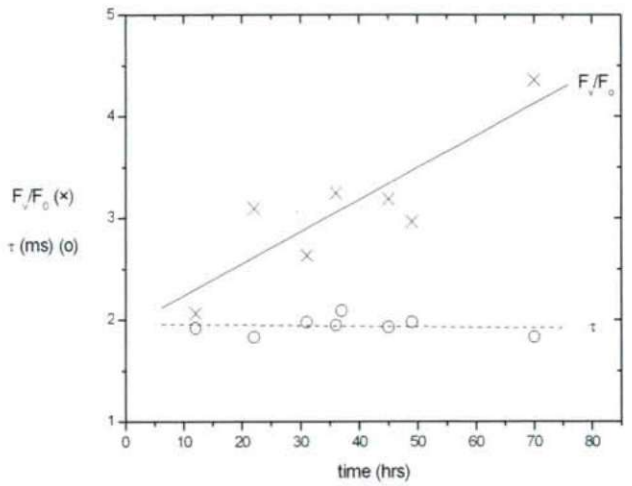

Figure 5. Ratio of the variable to initial fluorescence (F_v/F_0) and rise time (τ) of the fluorescence induction during growth of the culture.

this time range. As the conditions for excitation ($\lambda = 808$ nm) and observation ($\lambda > 850$ nm) were the same (there is only slight difference in spectral properties of the fluorescence from the antenna and the RC), the ratio of the observed rates should be characteristics of the antenna function. Under these conditions, the presence of the antenna complex in chromatophore assured 7 times higher rate of the photochemistry than in isolated RC.

The photochemical phase of the fluorescence induction is the signature of organization of BChl pigments in the photosynthetic apparatus. One of the most demonstrative examples is the change of fluorescence characteristics during assembly (Koblizek et al. 2005) and age (de Klerk et al. 1969) of the photosynthetic unit. To show these variations of numbers, connectivity and distribution of the pigments during cultivation of R-26.1 strain of *Rba. sphaeroides*, we present typical growth curve measured after inoculation of the cell into culture medium in photochemostat (Fig. 4). The cell population is proportional to the turbidity of the sample measured by the optical density (OD) at 535 nm. At this wavelength, the absorption is negligible and the observed optical density is mainly due to light scattering. After proper calibration, the value of OD(535 nm) can be used to determine the number of cells (see M&M). Similarly, the optical density at the peak of the absorption spectrum (860 nm) is the measure of the BChl-a content of the cells, and its concentration can be determined by extraction (see M&M). Three distinct phases can be defined. In the exponential phase, the cells are dividing at maximum rate (the doubling time is 6 hrs), in the intermediate phase, only a portion of the cell population is growing at maximum rate and in the stationary phase, the net growth rate is zero. As the two curves of OD(860) and OD(535) run parallel during the growth phases, the ratio of the amount of BChl-a synthesized and the number of cells remains almost constant. Similarly, the rate of the photochemical rise of the variable fluorescence does not show major change during the growth (Fig. 5). In contrary, striking increase in the ratio of variable to constant fluorescence is observed. The older are the cells the greater is the ratio. While F_v/F_0 is only 2 in younger cells, it increases above 4.5 in older cells. However, care should be taken to assign the increase of F_v/F_0 solely to the age of the bacterial cells. Alternative effect of decreasing exciting light intensity may have its role. As the cells are growing under constant light conditions and the culture becomes more dense in the intermediate and stationary phases, the intensity of exciting light reaching a given cell decreases. It has been long known that decreased light intensity can increase the BChl-a synthesis and can modify the distribution of the pigments (Cohen-Bazire et al. 1956).

Discussion

Generally, the reason of the studies of the fluorescence induction is to translate the observed characteristics of the kinetics into physiological parameters. The theory of fluorescence induction of antenna containing species (mainly for PSII) has been elaborated in great details including two major transitions of the RC: photochemistry ($PQ \rightarrow P^+Q^-$), and radical-pair mechanism ($P^* \leftrightarrow P^+H^-$) and restricted transfer of excitation energy from closed RC to an open RC (Lavergne and Trissl 1995). Based on this sophisticated theory, the functional absorption cross-section and connectivity of the photosynthetic complexes (see the shape of the induction curve), the

quantum yield of primary charge separation (see F_v/F_0) and the efficiency of light harvesting by the photosynthetic units (see the rate of the rise) can be deduced. In the presence of antenna, its fluorescence will dominate the observed signal as the absorption cross section (size) of the antenna is much larger than that of the RC. In these cases, the open RC serves only as trap for the excitons in the antenna pigment bed and the fluorescence from RC is not detected.

Here, we try to extend the simplified version of the Lavergne-Trissl model by consideration of the contribution of the fluorescence originating from the RC. It can have not only theoretical but also practical significance in weakly coupled system of RC and antenna, where the two components of the observed fluorescence induction may be commeasurable. Based on this extended model, reasonable explanation can be given to fluorescence changes observed in our experiments. Only qualitative view will be given but it can be treated in quantitative terms, as well.

The exciting photon can be absorbed both by one of the antenna BChl molecules and by the RC itself determined by their absorption cross sections (Fig. 1). The excited state (exciton) in the antenna is rapidly distributed in the pigment bed and finally finds the way to the open RC (redox pigment state is PQ_A) that becomes closed ($P^+Q_A^-$). The trap will be similarly closed if the photon is directly absorbed by the RC. These processes are accompanied by loss of the excited states by different other mechanisms including fluorescence. The observed variable fluorescence originates both from the RC and from the antenna and reflects the redox status of the RC.

In accordance with Figure 2, the antenna fluorescence is the inverse process of the trapping mechanism: initially when the photochemical trapping is most effective, the fluorescence is low (F_0). Later, when the trap disappears, the fluorescence is high (F_M). The rise time of the fluorescence increase depends on the effectiveness of the light harvesting and the extent of the rise (F_M/F_0) on the coupling of the light harvesting pigments to the RC. Both quantities could be modified in our experiments.

In intact cells, we measured larger variable fluorescence than in chromatophores (Fig. 2). During mechanical fracture of the cells and break of the natural membranes into fragments (chromatophore), the connection of the light harvesting system is impaired and the open RC became less effective trap for the excitons in the antenna. As the role of competitive processes (including also fluorescence) increased in comparison to photochemistry, the constant fluorescence (originating from detached pigments of the antenna) enhanced in expense of the variable fluorescence.

Similar changes were observed during aging of the cells. The BChl pigments might have severe re-distribution from young to old cells as the old cells showed significantly larger fluorescence induction (Fig. 5). In young cells, the pigments are arranged in loose structures that can be visualized by loosely attached and/or not properly well developed LHII units around the core complex (Koblizek et al. 2005). In old cells, the light harvesting complex becomes more compact assuring effective transfer of electronic excitation energy to the open RC. This process is accelerated not only by age of the cell but the decrease of the internal light intensity, as well.

Contrary to the relatively simple picture of the antenna fluorescence, the temporal change of the RC fluorescence is more difficult (Fig. 2) and less elaborated (Osváth et al. 1996). The observed fluorescence can arise from one BChl dimer (P), two BChl monomers and some residual (unknown) pigments left after protein purification. Initially, the RC is open and the dimer is ready to absorb photon and emit fluorescence. However, if the RC becomes closed ($P^+Q_A^-$), the dimer cannot be excited anymore and cannot emit fluorescence. The simple drop of the RC fluorescence during closure of the RC is modified by the BChl monomers in the RC. They contribute to the more efficient utilization of the photon (open RC) and to the residual RC fluorescence (closed RC). If they absorb the photon, they would transfer the electronic excitation energy to the closely placed dimer of the open RC. Thus, the monomers increase the absorption cross section of the RC. However, if the RC is closed, they emit the electronic excitation energy in form of fluorescence whose quantum yield depends on the redox states of the nearby cofactors (P, Q_A and Q_B, see Osváth et al. 1996). The fluorescence intensities from the dimer (P) and the BChl monomers in $P^+Q_A^-$ redox state of the RC are almost the same (Fig. 2).

The antenna fluorescence is usually much more intense than the RC fluorescence due mainly to two reasons: 1) the antenna has about 100 times more BChl pigments than the RC and 2) the quantum yield of the BChl fluorescence in the antenna (1-2%, van Grondelle and Duysens 1980, but $1 \cdot 10^{-3}$, Borisov and Godik 1972) is much larger than in the RC ($4 \cdot 10^{-4}$, Zankel et al. 1968). The difference is due to the effectiveness of the photochemical trap in the two cases. If the absorption cross section of the antenna is artificially decreased then commeasurable fluorescence can be observed from the antenna and the RC. In our experiments, the wavelength of the laser diode excitation was 808 nm that matched the BChl monomers of the RC but not the LHII of R-26.1 that lacked the B800 pigment. Under this condition, the photochemical rise of the fluorescence induction of the chromatophore was only 7 times faster than in isolated RC. The large number of pigments in the antenna was compensated by the favorable excitation of the RC. The positive outcome of this experiment encourages us to use this method to lower the fluorescence level of the antenna close to that of the RC and to detect the simultaneous fluorescence induction from the antenna and the RC. This will assure firm experimental background to test the quantitative consequences of the extended Lavergne-Trissl model.

Acknowledgements

This work was supported by OTKA, MTA-CNR and TéT. We thank Ms. R. Kékesi for her help in our preliminary measurements and Mrs. J. Laskay-Tóth for the culturing of the bacteria.

References

Borisov AYu, Godik VI (1972) Energy transfer to the reaction centers in bacterial photosynthesis. II. Bacteriochlorophyll fluorescence lifetimes and quantum yields for some purple bacteria. J Bioenerg Biomembr 3(6):515-523.

Cogdell RJ, Isaacs NW, Freer AA, Howard TD, Gardiner AT, Prince SM, Papiz MZ (2003) The structural basis of light harvesting in purple bacteria. FEBS Lett 555:35-39.

Cohen-Bazire G, Sistrom WR, Stanier RY (1956) Kinetic studies of pigment synthesis by non-sulfur purple bacteria. J Cell Comp Physiol 49:25-68.

Cser K, Vass I (2007) Radiative and non-radiative charge recombination pathways in Photosystem II studied by thermoluminescence and chlorophyll fluorescence in the cyanobacterium *Synechocystis* 6803. Biochim Biophys Acta 1767:233-243.

De Klerk H, Govindjee, Kamen MD, Lavorel J (1969) Age and Fluorescence Characteristics in some Species of Athiorhodaceae. Proc Nat Acad Sci USA 62:972-978.

Dau H (1994) Molecular mechanisms and quantitative models of variable Photosystem II fluorescence. Photochem Photobiol 60(1):1-23.

Italiano F (2007) Exploring anoxygenic photosynthesis as tool for heavy metal removal: the metabolic response and bioremediation potentialities of the photosynthetic bacterium *Rhodobater sphaeroides*. PhD Thesis, University of Bari, Italy.

Kautsky H, Hirsch A (1931) Neue Versuche zur Kohlensäureassimilation. Naturwissenschaften 48:964.

Koblizek M, Shih JD, Breitbar SI, Ratcliffe EC, Kolber ZS, Hunter CN, Niederman RA (2005) Sequential assembly of photosynthetic units in *Rhodobacter sphaeroides* as revealed by fast repetition rate analysis of variable bacteriochlorophyll *a* fluorescence. Biochim Biophys Acta 1706:220-231.

Lavergne J, Trissl HW (1995) Theory of Fluorescence Induction in Photosystem II: Derivation of Analytical Expressions in a Model Including Exciton-Radical-Pair Equilibrium and Restricted Energy Transfer Between Photosynthetic Units. Biophys J 68:2474-2492.

Maróti P, Wraight CA (1988) Flash-induced H^+ binding by bacterial photosynthetic reaction centers: Comparison of spectrometric and conductometric methods. Biochim Biophys Acta 934:314-328.

Müller NJC (1874) Beziehungen zwischen Assimilation, Absorption und Fluorescenz im Chlorophyll des lebenden Blattes. Jahrb Wiss Bot 9:42-49.

Osváth Sz, Laczkó G, Sebban P, Maróti P (1996) Electron transfer in reaction centers of *Rhodobacter sphaeroides* and *Rhodobacter capsulatus* monitored by fluorescence of the bacteriochlorophyll dimer. Photosynth Res 47:41-49.

Papageorgiou GC, Govindjee (editors) (2004) „Chlorophyll Fluorescence: A Signature of Photosynthesis. Advances in Photosynthesis and Respiration." Kluwer Academic Publishers, Dordrecht.

Roszak AW, Howard TD, Southall J, Gardiner AT, Law CJ, Isaacs NW (2003) Crystal structure of the RC-LH1 core complex from *Rhodopseudomonas palustris*. Science 302:1969-1972.

Trissl HW (1996) Antenna organization in purple bacteria investigated by means of fluorescence induction curves. Photosyth Res 47:175-185.

Trissl HW (1999) Theory of fluorescence induction. An introduction. http://www.biologie.uni-osnabrueck.de/biophysik/trissl/Teaching/fi.PDF.

Van Grondelle R, Duysens LN (1980) On the Quenching of the Fluorescence Yield in Photosynthetic Systems. Plant Physiol 65:751-754.

Vredenberg WJ, Duysens LNM (1963) Transfer of energy from bacteriochlorophyll to a reaction centre during bacterial photosynthesis. Nature (London) 197:355-357.

Wraight CA, Clayton RK (1974) The absolute quantum efficiency of bacteriochlorophyll photooxidation in reaction centers. Biochim Biophys Acta 333:246-260.

Zankel KL, Reed DW, Clayton RC (1968) Fluorescence and photochemical quenching in photosynthetic reaction centers. Proc Natl Acad Sci USA 61:1243-1249.

Zuber H, Brunisholz RA (1993) „The Chlorophylls," Sheer H., Ed.; CRC: Boca Raton, Fl.

Volume 51(1):33-38, 2007
Acta Biologica Szegediensis
http://www.sci.u-szeged.hu/ABS

ARTICLE

Photosynthetic electron transport activity of light and shade-acclimated field grown grapevine leaves

Péter Teszlák*, Krisztián Gaál, Pál Kozma Jr.

Ministry of Agricultural and Rural Development, Research Institute for Viticulture and Oenology, Pécs, Hungary

ABSTRACT The light response curves of relative electron transport rate (ETR) in field grown grapevine (Vitis vinifera L.) leaves were studied on different canopy exposure. The daily course of incident photosynthetic photon flux density (PPFD) was measured by means of ceptometer configured in segmented mode and inserted through the canopy. We compared the photosynthetic activity of shaded leaves and leaves exposed to sunlight on the eastern and western sides of canopy by North-South row direction. Moreover, we studied the seasonal influence of change in daily mean temperature and precipitation frequency on ETR light response curves. The different sides of canopy showed significant differences with regard the incident PPFD value, the western side received with 30% higher maximum PPFD values compared to eastern leaves. However, despite these differences we did not find any significant differences in the ETR light response curves between east and west- positioned leaves. The favourable water condition with lower daily mean temperature (≤20°C) resulted in significant lower ETR values in all leaf types. Based on seasonal fluctuation of ETR light curves we can hypothesized that low temperature have higher impact on photosynthetic electron transport activities of grapevine leaves than moderate water deficit.
Acta Biol Szeged 51(1):33-38 (2007)

KEY WORDS

grapevine,
sun and shade leaves,
electron transport rate,
light response curves

Canopy microclimate is one of the most important with regard to fruit composition and wine quality, in which the effects of soil, climate and cultural practices are summarized (Smart 1985). In general, commercial vineyards are characterized by high plant density, large shoot numbers with closed canopy (Smart 1985; Bertamini and Nedunchezhian 2002). In the different cordon training systems the shoots of individual vines are positioned vertically and include leaves forming a continuous canopy wall in the rows. During the canopy development the leaves are exposed to different light conditions (Smart 1988), the young leaves expand at direct sunlight and later they are shaded through shoot growing and the development of neighbouring immature leaves (Bertamini and Nedunchezhian 2003). Shade conditions can result rapid senescence of interior leaves or photosynthetic performance is acclimate to shade and the senescence process follows the natural way (Schultz 1991; Wells 1991). Generally used operations in canopy management, e.g. defoliation, significantly alter light distribution (Mabrouk et al. 1997), photosynthetic performance (Candolfi-Vasconcelos et al. 1994; Poni et al. 2006) and growth compensation (Hunter 2000) of the canopy system. These studies concluded that removed leaves from different canopy sides are not all the same. We must select those leaves for the defoliation that represent insignificant share from the total photosynthetic performance of canopy. It seems to be clear that chlorophyll fluorescence measurements are very useful tools for descriptions and estimation of grapevine leaf photosynthesis in field studies (Bálo et al. 1992; Flexas et al. 2000; Iacono and Sommer 2000; Ortoidze and Düring 2001; Cifre et al. 2005; Christen et al. 2007). Recent studies are emphasizing important differences between leaf photosynthesis on the southern and northern canopy sides at common East-West row direction (Mabrouk et al. 1997; Escalona et al. 2003), but light distribution of canopy wall and photosynthetic activity of different leaf exposures for the North-South row direction (on steep slopes) are less well understood. In this paper we characterized the light interception of external and internal sides of canopy by the way of daily course measurements of PPFD at North-South row direction and described photosynthetic activity of light (on eastern and western exposures) and shade-acclimated leaves using ETR light response curves during the growing season.

Accepted June 20, 2007
*Corresponding author. E-mail: teszlakp@szbki-pecs.hu

Materials and Methods

Plant material and experimental site

The study was carried out in the Szentmiklós vineyard of Research Institute for Viticulture and Oenology Pécs, in Hungary. The experimental site is located on steep slopes of Mecsek Hills (latitude: 46°07' N, longitude: 18°17' E, 230-260 m above sea level) in non-irrigated field conditions. The eight-year-old vines of cultivar Sauvignon blanc (Vitis

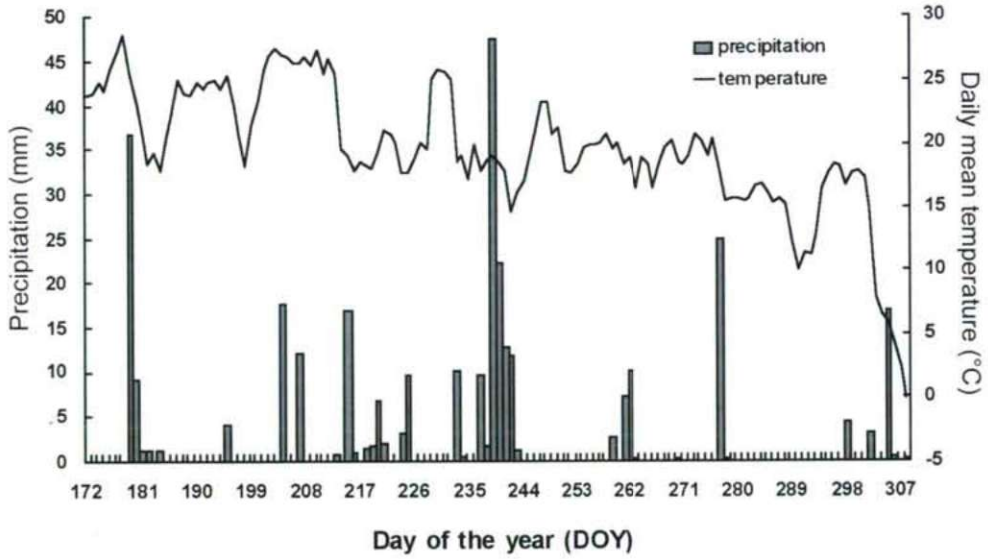

Figure 1. Precipitation frequency and daily mean temperature of air in 2006 (MARD Research Institute for Viticulture and Oenology Pécs).

vinifera L. convar. occidentalis, subconvar. gallica, provar. microcarpa) was grafted on Berlandieri x Riparia Teleki 5C rootstocks and planted in North-South row direction of steep slope. The soil is Ramann type brown forest soil on red sandstone. The training system was mid-high cordon with 2.2 x 0.8 m row and vine spacing and average pruning level was 8 buds per square metre. We measured only healthy mature leaves were taken from randomly chosen vines and 4-5th nodes of shoots near clusters. The leaf samples were collected from the eastern external side, internal side and western external side of canopy in three repetitions of different exposures between June and November in six measurement days (DOY 178, 194, 223, 251, 286, 306).

Meteorological parameters

Weather conditions, *i.e.* precipitation frequency and air temperature were registered by means of an automatic weather station (Lufft HP-100, Fellbach, Germany) situated in the experimental vineyard. The meteorological data were recorded continuously every 12 minutes per day.

PPFD measurements in the canopy

Daily course of PPFD values on different canopy exposures were measured using a linear PAR/LAI ceptometer (Model P-80 AccuPAR, Decagon Devices, WA, USA). The ceptometer was situated on two plastic columns in the row and inserted horizontal through the canopy near the cluster zone. In the course of measurements, we used unattended mode of device and chose the segmented option (Operator's manual AccuPAR 2001). Within this option the measurements were programmed as follows: start time 7:50, stop time 20:00, sampling interval 5 min, with night shutdown (sleep 20:30 and wake 4:30). The full length of ceptometer (0.8 m) was segmented to 3 segments like 0.20 m on the external sides and 0.40 m in the interior of canopy. Reported values were evaluated as average of five diurnal course measurements during the mid growing season.

Chlorophyll fluorescence measurements

Pulse modulated chlorophyll a fluorescence measurements were made in detached leaves using a PAM-2100 fluorometer (Heinz Walz GmbH, Effeltrich, Germany) connected to a notebook computer with data acquisition software (PamWin v 1.17, Heinz Walz GmbH, Effeltrich, Germany). The leaf samples were dark-adapted for 30 min in field conditions and detached before the end of the dark adaptation. The measurements were performed immediately after the detachment at normal temperature and pressure (20°C, 101 kPa) under laboratory conditions. For inclusions of ETR light response curves, we used the "rapid light curves" option of PamWin software with the pre-programmed operating parameters. The initial PPFD of measurements was lower than 0.1 μmol m^{-2} s^{-1} at the leaf surface. Each light response curve consist of 10 illumination steps (20 s per step) with increasing PPFD values between 0 and 2000 μmol m^{-2} s^{-1}. The values of ETR_{max} were estimated from the last point of rapid light curves (between 1400 and 1500 μmol m^{-2} s^{-1} of PPFD). Minimum (F_0) and maximum fluorescence (F_m) was measured by switching on the modulated radiation of 0.6 kHz and 20 kHz, respectively and induced with a 0.8 s saturating flash of 6000 μmol m^{-2} s^{-1}. The actual PPFD values were measured on-line with a micro quantum sensor (4 mm^2 of the total 80 mm^2 measur-

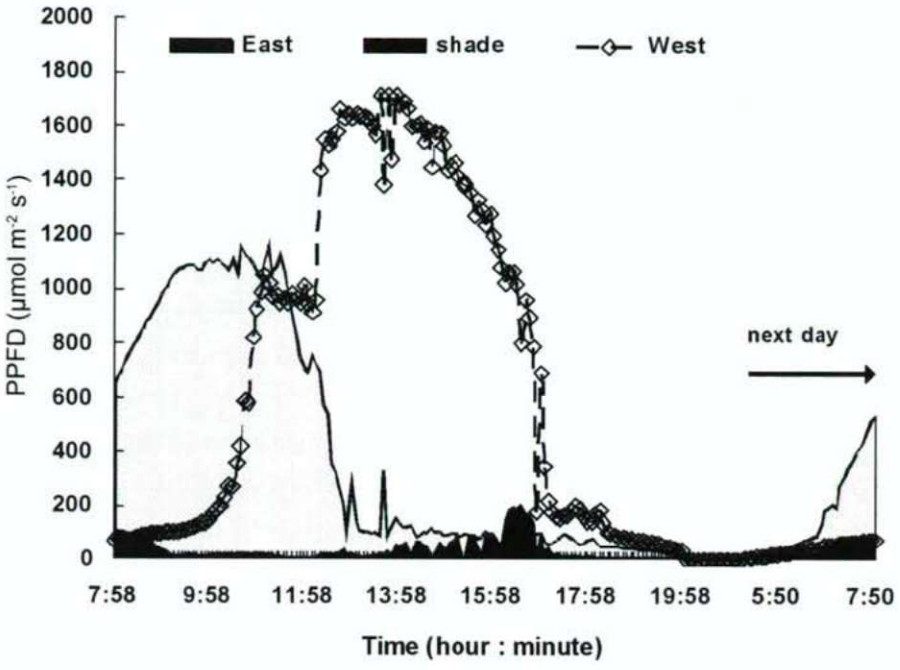

Figure 2. Diurnal course of incident PPFD values in the different leaf exposures of canopy, where East is the eastern external segment, shade is the internal segment and West is the western external segment of ceptometer inserted through the canopy.

ing area) integrated into the Leaf-Clip Holder 2030-B. The ETR light curves were fitted on the basis of the well-known photosynthesis model (Eilers and Peeters 1988; Eilers and Peeters 1993). Electron transport rate was estimated as ETR = $F/F'_m \times PAR \times 0.5 \times ETR$ factor, where F/F'_m is the effective quantum yield of irradiated sample (variable fluorescence/effective maximum fluorescence), PAR is photosynthetically active radiation, and ETR factor corresponds to the fraction of incident radiation absorbed by green leaves (value of 0.84) (Schreiber et al. 1994).

Statistical analysis

Statistical analysis was carried out using Excel (Microsoft Corp., Redmond, USA). Paired samples t-test was performed on all data sets with 95% confidence interval between the ETR values of different leaf types.

Results and Discussion

Analysis of meteorological background

In the mid growing season the studied site received less precipitation compared to the 50 years average (Research Institute for Viticulture and Oenology Pécs 2007) after well-watered periods of April and June. Rapidly developing drought stress conditions were observed in July (DOY 182-212; Fig. 1). In this period the daily mean temperature often fluctuated above 25°C (with 28°C maximum value) and the amount of monthly precipitation was 46% of the total long-term average. After this drought stress period, the august (DOY 213-243) showed untypical conditions, average air temperature was lower by 1.9°C and precipitation was higher with 112% than the 50 years average. We evaluated the air temperature and precipitation changes 14 and 7 days before the fluorescence measurements. These values were as follows: precipitation in the previous 14 days was 0 mm, average of daily mean temperatures in the previous 7 days was 25°C (DOY 178); precipitation in the previous 7 days was 0 mm, average of daily mean temperatures in the previous 7 days was 24°C (DOY 194); precipitation in the previous 7 days was 30 mm, average of daily mean temperatures in the previous 7 days was 19°C (DOY 223); precipitation in the previous 7 days was 0 mm, average of daily mean temperatures in the previous 7 days was 21°C (DOY 251); precipitation in the previous 7 days was 0 mm, average of daily mean temperatures in the previous 7 days was 16°C (DOY 286); precipitation in the previous 7 days was 20 mm, average of daily mean temperatures in the previous 7 days was 10°C and actual air temperature before sunrise was -0.5 °C (DOY 306).

Light interception of different leaf exposures

Diurnal course of incident PPFD values showed significant differences in the different leaf exposure of canopy. The western leaves of external canopy received the highest PPFD between 12:18 and 15:38 at local time (Fig. 2). In the morn-

ing, the PPFD values of eastern canopy side increased earlier than western side or canopy interior. This leaves intercepted efficient light conditions from 7:58 till 12:18 and duration of stage at maximum PPFD (above 600 μmol m^{-2} s^{-1}) was very similar to the western side. However, on the western side a 30% higher photon flux density was measured compared to the eastern side. The initial and ending slopes of the respective curves were very similar in the external canopy sides during the diurnal PPFD course and during the initial slopes. Then they increased exponentially, but we found a stationary phase between 11:03 and 12:13 in the curve of western side (Fig. 2). After noon, the incident PPFD values showed a rapid decreasing on the eastern side because of change in actual zenith angle. The low values from 13:00 to 20:00 resulted suboptimal light conditions for the eastern leaves of external canopy. This light distribution suggested that eastern sun leaves have lower potential of the photosynthetic performance in North-South row direction. Eastern sun leaves have shorter illumination period with 1 hour from PPFD values above 200 μmol m^{-2} s^{-1} compared to the other side. We characterized the different canopy sides by means of gas exchange parameters (data not shown) and measured 12 μmol m^{-2} s^{-1} of average CO_2 assimilation rate on eastern leaves in the mid growing season. In our estimation, the shorter illumination period of 1 hour causes lower carbon assimilation yield (approximately 1kg per 100 vines) on eastern leaves when the half of average leaf area index was 2 m^{-2} m^{-2} and when the both leaf types were grown in the same conditions (Teszlák, unpublished data). However, the estimation of canopy carbon balance is more difficult, the photosynthetic performance of external leaves on western canopy side becomes adverse via increasing air temperature and leaf surface temperature after noon. In spite of longer illumination period of western side the leaves have a disadvantaged status because the higher leaf surface temperature inhibited photosynthetic processes and the daily course of photosynthesis is postponed compared to the leaves on eastern or southern exposures. In the canopy interior, the incident PPFD values were drastically reduced due to the light absorption of leaves on external canopy surface. During the diurnal course of photosynthetically active radiation the shade-acclimated leaves received less than 100 μmol m^{-2} s^{-1} of PPFD in the internal canopy side. In the case of canopy interior, a short period to be found almost 200 μmol m^{-2} s^{-1} of PPFD between 16:13 and 16:48 (Fig. 2), but the time and length of illuminated period and the light intensity may alter because of different positions and frequency of canopy gaps. It is well known that heavily shaded leaves do not contribute to canopy photosynthesis, they turn yellow and abscise (Smart 1973; 1988; Schultz 1991). We observed similar process in shade leaves such as the first visible reaction of vine canopy to moderate drought stress in July. However, we can not leave out of consideration the function of interior leaves, because due to several steps of canopy management the available canopy structure is altering (Candolfi-Vasconcelos et al. 1994; Mabrouk et al. 1997; Poni et al. 2006) and this change reduces the potential CO_2 assimilation surface on the external canopy sides (Smart 1985, 1988; Hunter 2000). Since the shade-acclimated leaves are functioning at lower dark respiration level over a large part of the growing season (Schultz 1991), they may play a significant role in carbohydrate balance of the total canopy. The light microclimate of shade leaves is not widely known and theirs important role needs further verifications, where we can recommend this application.

ETR light response curves of sun and shade leaves

There were high significant differences between sun leaves and shade-acclimated leaves for each measurement date. In spite of different light microclimate of eastern and western canopy sides ETR light response curves showed very similar values in leaves of both exposures (Fig. 3).

The ETR increased with light intensity in light and shade-acclimated leaves, maximum values of sun leaves were distinctly higher than shade leaves. On the basis of the last points of light curves (between 1400 and 1500 μmol m^{-2} s^{-1} of PPFD) Sauvignon blanc leaves showed normal ETR_{max} values that are characterized some white varieties (Ortoidze and Düring 2001). The average ETR_{max} values of shade-acclimated leaves were lower with 68% compared to the sun leaves at the first measurement date (DOY 178), after starting drought period lasting for 14 days precipitation deficit and at average 25°C of daily mean temperature (Fig. 1; Fig. 3). Photosynthetic activity of both leaf types changed with enhanced drought conditions in July (DOY 194), moderate drought resulted in lower ETR_{max} of sun leaves with 20% and increasing ETR_{max} in shade-acclimated leaves with 32% compared to the previous record. This change of potential electron transport efficiency indicated that light-acclimated leaves can not keep their photosynthetic activity at the starting level, but shade-acclimated leaves have a capacity to increase ETR when precipitation deficit is on the increase. On the other hand, the approach of the different light response curves means that the vine canopy has alternative possibility to balance of its total photosynthetic performance by means of shade-acclimated leaves. There is non-negligible importance of shade leaves and their PSII electron transport capacity considering that they are functioning hardily shaded conditions (below 200 μmol m^{-2} s^{-1} of PPFD) with short illumination period per day (Fig. 2). Our results of shade-acclimated leaf behaviour are particularly in agreement with previous research, which described chloroplast acclimation in the canopy interior with decreasing chlorophyll a/b ratio, increasing maximal fluorescence values and better light perception based on fluorescence induction curves (Bálo et al. 1992). At the third measurement date (DOY 223), light and shade-acclimated leaves showed lower ETR_{max} values with 20% and 40% compared to former

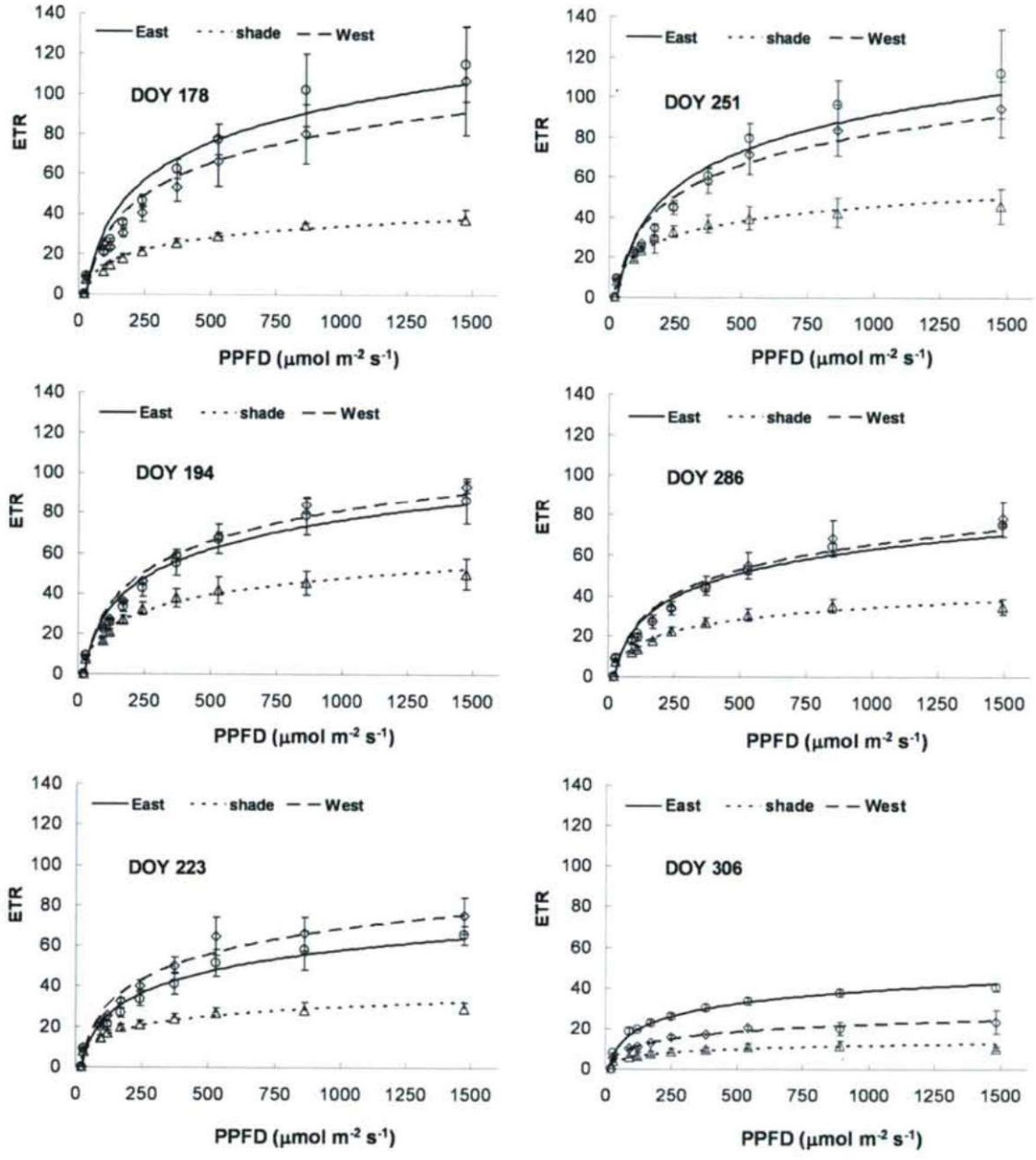

Figure 3. Light response curves of ETR in eastern external (East), interior (shade) and western external (West) leaves of canopy. DOY number indicates the days of year during the growing season and vertical bars represent standard deviation of mean (n = 3).

record. There are significant responds of photosynthetic apparatus to decreasing air temperature (7 days average of daily mean temperature was 19°C with minimum of 12 °C) under favourable water conditions (7 days average of precipitation was 30 mm). After the unusual cold and rainy period daily mean temperature increased above 20 °C with negligible precipitation values developed favourable conditions for ripening of grapes. The apparent electron transport rate showed significant increase with rising daily mean temperature (32°C of maximum) in light (48%) and shade-acclimated (55%) leaves (Fig. 1; Fig. 3). On the basis of increasing ETR light response values (DOY 251) we can find a high reversibility of moderately depressed PSII electron flow at the phenological stage of ripening. This change suggested that shade-acclimated leaves have significant potential to enhance photochemical activity of the total canopy system. At late growing season (post-harvest period, DOY 286) there were medium low ETR_{max} in light and shade-acclimated leaves, but light-

acclimated leaves showed stronger decrease as a response to low daily mean temperature with average of 16°C and with minimum of 10°C during the previous 7 days. In this period shade-acclimated leaves showed lower ETR_{max} with 57% compared to the sun leaves. In spite of this decrease, there was no significant difference between ETR_{max} of eastern and western light-acclimated leaves indicating a similar response to low temperature. The light-acclimated leaves on the different canopy sides showed significant differences only at last measurement date (DOY 306), when we recorded a cold shock effect (Fig. 1), which resulted in severe decreasing of ETR light response curves (Fig. 3). The highest ETR_{max} value was found in the light-acclimated leaves for the eastern canopy side that indicated a slighter chilling-induced photoinactivation of PSII. The western leaves and shade-acclimated leaves had significantly lower ETR_{max} values (with 42% and with 75%) compared to the eastern leaves. These results correspond with recent studies (Bálo et al. 1986; Hendrickson et al. 2004; Bertamini et al. 2005), that reported significantly reduced ribulose-1,5 bisphosphate carboxylase activity and PSII activity due to loss of D1 protein at low temperature (5°C). Based on results of ETR light response curves we can suppose that light-acclimated leaves have similar photochemical potential on the eastern and western sides of canopy in North-South row direction, but eastern sun leaves indicated lower photoinhibition for chilling temperature.

Acknowledgements

The authors gratefully acknowledge Mr. Jörg Kolbowski (the writer of PamWin software, Walz, Effeltrich, Germany) for the help in pws file operations and Dr. Martin Pour Nikfardjam for improving the manuscript and correcting the English version.

References

Bálo B, Mustárdy LA, Hideg É, Faludi-Dániel A (1986): Studies on the effect of chilling on the photosynthesis of grapevine. Vitis 25:1-7.

Bálo B, Váradi Gy, Pölös E, Happ I (1992) Effect of shading on the photosynthetic apparatus of Chardonnay vine leaves. Proc. of IV Simposio Int. di Fisiol. della Vite, San Michele all' Adige, Torino, Italy. pp. 555-558.

Bertamini M, Nedunchezhian N (2002) Leaf age effects on chlorophyll, Rubisco, photosynthetic electron transport activities and thylakoid membrane protein in field grown grapevine leaves. Plant Physiol 159:799-803.

Bertamini M, Nedunchezhian N (2003) Photoinhibition of photosynthesis in mature and young leaves of grapevine (Vitis vinifera L.). Plant Science 164:635-644.

Bertamini M, Muthuchelian K, Rubinigg M, Zorer R, Nedunchezhian N (2005) Low-night temperature (LNT) induced changes of photosynthesis in grapevine (Vitis vinifera L.) plants. Plant Phys Biochem 43:693-699.

Candolfi-Vasconcelos MC, Koblet W, Howell GS, Zweifel W (1994) Influence of defoliation, rootstock, training system, and leaf position on gas exchange of Pinot noir grapevines. Am J Enol Vitic 45:173-179.

Christen D, Schönmann S, Jermini M, Strasser RJ, Defago G (2007) Characterization and early detection of grapevine (Vitis vinifera) stress responses to esca disease by in situ chlorophyll fluorescence and comparison with drought stress. Environ Exp Bot 60:504-514.

Cifre J, Bota J, Escalona JM, Medrano H, Flexas J (2005) Physiological tools for irrigation scheduling in grapevine (Vitis vinifera L.). An open gate to improve water-use efficiency? Agirc Ecosys and Environ 106:159-170.

Escalona JM, Flexas J, Bota J, Medrano H (2003) Distribution of leaf photosynthesis and transpiration within grapevine canopies under different drought conditions. Vitis 42:57-64.

Eilers PHC, Peeters JCH (1988) A model for the relationship between light intensity and rate of photosynthesis in phytoplankton. Ecol Mod 42:199-215.

Eilers PHC, Peeters JCH (1993) Dynamic behaviour of a model for photosynthesis and photoinhibition. Ecol Mod 69:113-133.

Flexas J, Briantais JM, Cerovic Z, Medrano H, Moya I (2000) Steady-state and maximum chlorophyll fluorescence responses to water stress in grapevine leaves: A new remote sensing system. Remote Sens Environ 73:283-297.

Hendrickson L, Förster B, Furbank RT, Chow WS (2004) Processes contributing to photoprotection of grapevine leaves illuminated at low temperature. Phys Plant 121:272-281.

Hunter JJ (2000) Implications of seasonal canopy management and growth compensation in grapevine. S Afr J Enol Vitic 21:81-91.

Iacono F, Sommer KJ (2000) Response of electron transport rate of water stress-affected grapevines: Influence of leaf age. Vitis 39:137-144.

Mabrouk H, Sinoquet H, Carbonneau A (1997) Canopy structure and radiation regime in grapevine. II. Modelling radiation interception and distribution inside the canopy. Vitis 36:125-132.

Ortoidze T, Düring H (2001) Light utilization and thermal dissipation in light- and shade-adapted leaves of Vitis genotypes. Vitis 40:131-136.

Poni S, Casalini L, Bernizzoni F, Civardi S, Intrieri C (2006) Effects of early defoliation on shoot photosynthesis, yield components, and grape composition. Am J Enol Vitic 57:397-407.

Research Institute for Viticulture and Oenology Pécs (MARD) (2007) Annual review for "K+F" research activities. Institutional Public Library. 4 Pazmany P., Pécs H-7643, Hungary

Schreiber U, Bilger W, Neubauer C (1994) Chlorophyll fluorescence as a non-intrusive indicator for rapid assessment of in vivo photosynthesis. In: Schulze E-D, Caldwell MM (eds) Ecophysiology of Photosynthesis. Springer-Verlag, Berlin, pp 49–70.

Schultz HR (1991) Seasonal and nocturnal changes in leaf age dependent dark respiration of grapevine sun and shade leaves. Modelling the temperature effect. Vitic Enol Sci 46:129-141.

Smart RE (1973) Sunlight interception by vineyards. Am J Enol Vitic 24:141-147.

Smart RE (1985) Principles of grapevine canopy microclimate manipulation with implication for yield and quality. A review. Am J Enol Vitic 36:230-239.

Smart RE (1988) Shoot spacing and canopy microclimate. Am J Enol Vitic 39:325-333.

Wells R (1991) Soybean growth response to plant density: Relationships among canopy photosynthesis, leaf area, and light interception. Crop Sci 31:755–761.

Volume 51(1):39-42, 2007
Acta Biologica Szegediensis
http://www.sci.u-szeged.hu/ABS

ARTICLE

Carrot flowering initiation: light effect, photosynthetic pigments, carbohydrates

Giedre Samuoliene*, Gintare Sabajeviene, Akvile Urbonaviciute, Pavelas Duchovskis

Laboratory of Plant Physiology, Lithuanian Institute of Horticulture, Babtai, Kaunas district, Lithuania

ABSTRACT The present study was aimed at the investigation of the influence of illumination spectrum on physiological processes in carrots (*Daucus carota* L.) during their evocation, flower initiation and differentiation. The process of flower initiation and morphogenesis was studied in a phytotron facility under treatment with different illumination spectra. The dominating 640-nm component and supplementary components (455-nm, 660-nm and 735-nm). High-performance liquid chromatography with a refractive-index detector was used for the detection and separation of carbohydrates. Total quantification of photosynthetic pigments was performed by spectrophotometric method. A considerable influence of illumination spectrum on physiological processes in the carrot, especially on the morphogenesis rate, was observed. We conclude that flower initiation processes in carrots can be controlled by tailoring the illumination spectrum and photon flux density. This enables one to accelerate plant cultivation in phytotron conditions. Conclusions: (i) The elimination of both red and far-red or only blue light appeared to suppress floral initiation, under such conditions carrots grew vegetative. In contrary, the elimination of solely far-red light resulted in faster flowering differention. (ii) The elimination of solely red or blue light resulted in a low synthesis rate of photosynthetic pigments and conditioned high sucrose content in carrot root. Meanwhile, the elimination of solely far-red light resulted in the opposite effect. (iii) Dominating 640-nm light was found to considerably contribute to the excitation of the carotenoid antennal complex of the photosynthetic system.
Acta Biol Szeged 51(1):39-42 (2007)

KEY WORDS

carrots,
carbohydrates,
carotenoids,
chlorophyll,
evocation

Light quality (spectral composition), quantity (photon flux density), and duration (photoperiod) have a profound influence on the morphogenesis of biennial plants. However, there is very little knowledge on how to control flower initiation processes of biennial plants using LEDs. Flowering induction and evocation consist of two periods. The first period of flowering induction is photoinduction. During photoinduction, metabolites of the photomorphogenetic system are transported to apical meristems where they can de-block the genes of the inflorescence axis formation. This moment is the starting point of the Ist evocation period, which is accomplished with the formation of the inflorescence axis. The second period of flowering induction of wintering plants is thermoinduction. The induction metabolites determine the formation of inflorescence axis structures (the evocation period II). These processes require flower initiation and differentiation (Duchovskis 2004). The carrot plant is known to flower only after vernalization, *i.e.* low temperatures are needed for flower initiation (Gláucia et al. 1994). The role of illumination spectrum in these processes is not known well enough. Therefore, the growth, development and flowering initiation of different species of plants grown under specific wavelengths and narrow bandwidth must be characterized and understood.

Light is the energy source for photosynthesis, and it controls many aspects of the plant development. In recent studies photomorphogenetic responses of plants to red and blue light from broad spectrum sources were examined (Brown et al. 1995; Yorio et al. 1995). Pepper, lettuce, radish, spinach, broccoli, cabbage, wheat, strawberry, etc. have been successfully grown under red and blue light applied typically within vegetative growth (Kim et al. 2006; Tarakanov 2006; Yanagi et al. 2006). However, little is known on the use of light-emitting diodes to support plants after flowering induction (after vernalization) through the further life cycle.

Photosynthetically active radiation (PAR) referred to as blue light (from 400 to 500 nm) and red light (600 – 700 nm) is involved in photosynthesis, photomorphogenesis, and chlorophyll synthesis. Far-red irradiance, the spectral band from 700 to 800 nm is not important for photosynthesis but considerably influences photomorphogenesis (Casal and Sanchez 1994). Both red light, via phytochrome, and blue light, via photoreceptor(s), is effective in inducing photomorphogenetic responses. Although red light has great potential to drive photosynthesis, plants are adapted to utilize a wide-spectrum of

Accepted May 4, 2007
*Corresponding author. E-mail: g.samuoliene@lsdi.lt

Table 1. Illumination conditions for 6 growth treatments.

Treatment	455 nm	640 nm	660 nm	735 nm
L1	7.6 (4.5%)	150 (89.7%)	7.1 (4.3%)	2.5 (1.5%)
L2	1.4 (0.8%)	159 (94.5%)	7.5 (4.5%)	0.0
L3	7.6 (4.7%)	150 (93.7%)	0.0	2.5 (1.6%)
L4	0.0	159 (93.8%)	7.5 (4.4%)	3.0 (1.8%)
L5	0.0	150 (100%)	0.0	0.0
L6	1.4 (4.5%)	159 (95.5%)	0.0	0.0

Table 2. Orgagenesis as a function of treatments.

Treatment	Organogenesis stages according to Kuperman (%)			
	II	III	IV	V
L1		65	25	
L2		27	35	38
L3		40	60	
L4	22	11	67	
L5	100			
L6	100			

light to control photomorphogenetic responses (Kendrich and Kronenberg 1994). Carbohydrate-dependend regulation of photosynthetic gene expression is believed to occur through hexokinase, which is a sugar sensor (Jang et al. 1997).

It is well-known that phytochrome is light sensing protein that plants require for developmental responses and that plays an important role as a photoreceptor in the photoperiodic reaction of floral initiation (Thomas and Vince-Prue 1997).

In this study we present results on manipulation of carrot flowering initiation by blue, red and far-red light, and the links with the variation in carbohydrates and photosynthetic pigment contents.

Materials and Methods

Carrots *Daucus carota* L. var. *Garduolė 2* were initially grown in vegetative tumbler, 54x34x15 cm in size, placed in a greenhouse (16 h photoperiod and 21/16°C day/night temperature). Peat (pH ≈ 6) was used as a substrate. Carrots with 9 leaves in rosette were removed from the greenhouse and kept in phytotron chambers under low temperature (4°C) for 120 days. Subsequently evocation, flower initiation and differentiation processes were investigated under illumination with the photoperiod of 16 h and 21/16 ± 2°C day/night temperatures maintained for one month. Illumination with different spectra was generated by an light-emitting diodes based illuminator (Table 1). The dominating 640-nm component delivered by AlGaInP LEDs and supplementary components from AlGaN (455-nm) and AlGaAs (660-nm and 735-nm) LEDs (Tamulaitis et al. 2005). After a month of growth under different regimes of illumination, all plants were grown under a high-pressure sodium lamp (Son-T Agro, *Philips*), and their further development was studied. The level of plant development was determined according to Kuperman (1982).

Carbohydrates sample preparation: 1-2 g of fresh tissue per sample was grounded and diluted with 4 ml bidistilled water. The samples were pre-purified using 0.2 μm syringe filters.

Analysis of fructose (Fru), glucose (Glu), sucrose (Suc) and maltose (Mal) were performed on a Shimadzu 10A HPLC model equipped with a refractive index detector (RID 10A), column oven (CTO-10AS VP), degasser (DGU-14A), and pump (LC-10AT VP). Separations were performed on an Adsorbosil NH_2-column (150 mm x 4.6 mm). Mobile phase: 75% acetonitrile. Flow rate: 1 ml/min.

Spectrofotometric analysis (spectrophotometer Genesis 6, USA) and quantification of total chlorophylls a and b and carotenoids was performed at 440.5nm, 662 nm, and 644 nm wavelengths, respectively. Photosynthetic pigment samples preparation: 0.2 g of fresh weight (from roots and leaves) was grounded with $CaCO_3$ and extracted in 100% acetone, according to Vetsthtein (Gavrilenko 1975).

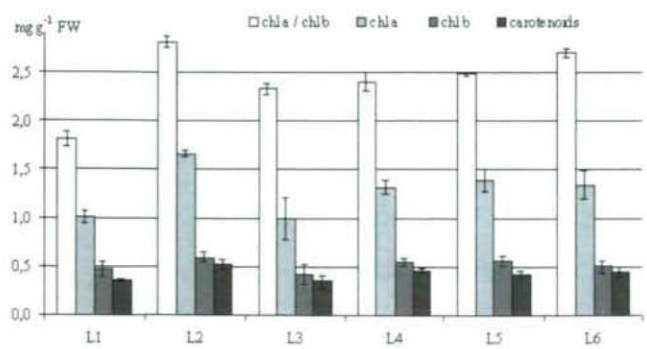

Figure 1. Effects of illumination spectrum on photosynthetic pigment contents.

Results

Different effects of illumination spectrum on the carrots physiological process, especially on morphogenesis rate during evocation, flower initiation and differentiation, were observed, as illustrated in Table 2. All plants passed the flower initiation and evocation process in growth runs L1, L2 and L3. Under treatment without blue component (L4), 22% of plants remained in the vegetative state (organogenesis stage II). Carrots treated under solely red LEDs (640 nm, L5) and under combination of red and blue LEDs (640 nm and 455 nm, L6) generally showed no development and all 100% remained in the vegetative stage (Table 2).

The influence of different illumination spectrum on the content of the photosynthetic pigments indices was established (Fig. 1). The lowest contents of all pigments were

Figure 2A, B. Effects of treatments on sugar content.

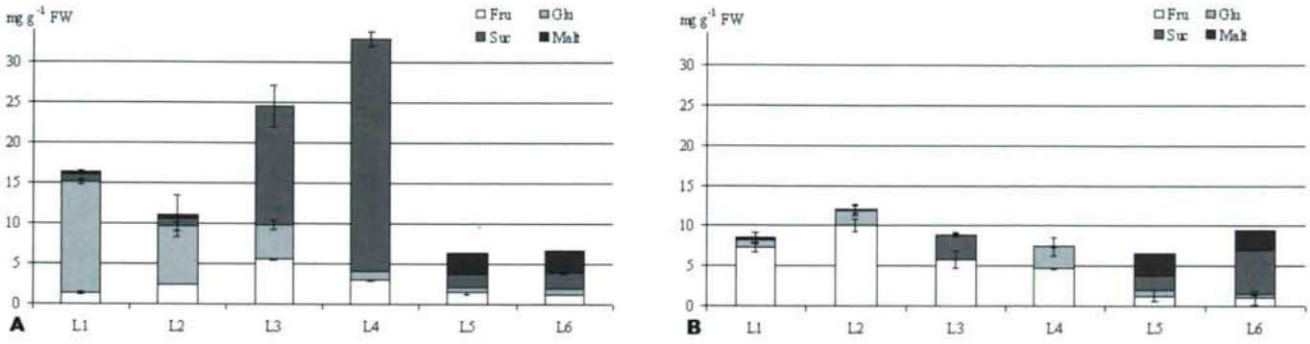

found in growth runs L1 (with all four spectral components) and L3 (without 660 nm). The highest concentrations of chlorophylls a and b and carotenoids were detected in L2 runs, where plants were treated without far-red light. The lowest and the highest chlorophyll a/b ratios were observed in growth runs L1 and L2 respectively. No significant differences in photosynthetic pigment concentrations in growth runs L4 (without blue light), L5 (only with 640 nm component) and L6 (without 660 nm and 735 nm components) were found.

Figure 2 shows that though the variation between fructose and glucose and between sucrose and maltose in different growth treatments was different, but we found that when the total amount of monocarbohydrates is high, the levels of dicarbohydrates are low (L1, L2, L3 and L4). Contrarily where the concentrations of monocarbohydrates were low, the amount of dicarbohydrates were high (L5 and L6). Considering dicarbohydrates, the sucrose concentration significantly increased in carrot root in growth runs L3 and L4, although maltose was not detected here (Fig. 2A). In the carrot leaves (Fig. 2B) maltose also was not detected in growth treatments L3 and L4. Also sucrose was not present in leaves in treatment L4. Different behavior was observed for monocarbohydrates. Contrary to carrot leaves, roots exhibited higher glucose and lower fructose levels (L1 and L2). In growth treatments L5 and L6 the carbohydrate distribution between roots and leaves are the same.

Discussion

In agreement with other authors (Yanagi et al. 2006), our results show that the elimination of both red (660 nm) and far-red (735 nm) light that is utilized in the reversible transformation at phytochrome (growth runs L5 and L6) suppresses floral initiation. Although plants were treated by low positive temperatures required for floral induction, after treatment with above-mentioned illumination (L5 and L6) carrots remained in the vegetative stage (Table 2). Also, for these treatments the sugar concentration was low and distribution of mono and dicarbohydrates was the same in roots and in leaves. The elimination of only far-red (L2), red (L3) or blue (L4) light did not have such a dramatic effect on the suppression of plants flowering (Table 2). These results imply that at least far-red is required to invoke floral initiation, probably mediated by phytochrome response. The effect of the absence of blue light (L4) might be lower than that of the absence of far-red light (Table 2). Similarly to our results a study of the light wavelength range required for floral induction, because floral initiation by red and far-red lighting seems to be mild in strawberry plants (Yanagi et al. 2006). In higher plants there are general pathways in the transduction of photoperiodic/photomorphogenetic signals. Effects of different environmental stimuli (e.g., flowering occurs in response to long photoperiod as well as to low red : far-red ratio) often result in the same developmental or morphogenetic pattern depending on the plant life strategy. According to our results, when red: far-red ratio was equal to zero (L2 treatment) even 38% reached V^{th} organogenesis stage. In treatments L1, L3 and L4 red : far-red ratio was equal to 50, and development of carrots was lower (Table 2). In other words, photoperiodic and photomorphogenetic light signals trigger similar stress-avoidance response. In long-day plants with competitor strategy the same conditions influence rapid flowering and bolting response (Tarakanov 2006).

Photosynthetic system plays an important role in plant development. In photoperiodic plants, there is strong experimental evidence that leaves produce promoters and inhibitors of flowering when exposed to favorable and unfavorable conditions, respectively (Bernier and Prilleux 2005). These signals are transported from the leaves to the apical meristem with metabolites of photosynthesis process. Plants are adapted to utilize a wide-spectrum of light to control photomorphogenetic responses (Kendrick and Kronenberg 1994). Various parts of light spectrum serve as signals providing organism with important information from their environment. Appropriate combinations of red and blue light have great potential for use as a light source to drive photosynthesis due to the ability to tailor irradiance output near the peak absorption

regions of chlorophyll. There are close relations between plant photosynthesis and photoperiodic response based on source-sink relations (Tarakanov 2006). Chlorophyll b and inactive phytochrome form (P_r) have absorption spectrum at 660 nm, the elimination of this red light (L3) resulted in a low photosynthetic pigments synthesis rate (Fig. 2) and conditioned a high sucrose content in carrot root (Fig. 2A). In the contrary, the elimination of far-red light (L2) stimulated synthesis of chlorophylls and carotenoids (Fig. 1). The absorption spectrum of carotenoid and chlorophyll a is at blue light region. The elimination of this blue light did not influence the content of chlorophyll a but dramatically influenced sucrose distribution: a high level was found in carrot root (Fig. 2A) and no sucrose was found in leaves (Fig. 2B). The transported sucrose is effective as a florigen even if its main action is the energy supply (King 2006). Conversion of sucrose to glucose can control flowering. According to Bernier and Perilleux (2005), mutants that block photosynthetic carbon metabolism usually exhibit late flowering as could be expected for a plant that shows flowering due to a photosynthetic response.

During the reproductive phase of development a lot of new structures are formed, the photosynthetic apparatus is complete. Photosynthetic pigments can participate like structural material for carbohydrates biosynthesis. Both, light quantity and quality are known to affect the contents and the ratio of individual proteins and pigment-protein complexes of the photosynthetic apparatus. It is well known that blue light promotes stomatal opening and influences the biochemical properties of photosynthesis. Menard et al. (2005) showed that plants grown under blue fluorescent lamps had higher chlorophyll a/b ratios, smaller amounts of light-harvesting chlorophyll a/b-binding protein of photosynthetic system II per unit chlorophyll content, and higher ribulose-1.5-bisphosphate carboxygenase/oxygenase activities per unit leaf area compared to plants grown under red fluorescent lamps. According to our results the elimination of blue light (L4) had no such influence on chlorophyll a/b ratio (Fig. 2). The stability of photosynthetic pigment contents in growth runs without blue (L4), both red (660nm) and far-red (L6) and only with 640 nm lighting (carotenoid absorption maximum) shows very strong participation of photosynthetic system antennal complex (Fig. 1). Antennas permit organisms to increase greatly the absorption cross section for light without having to build an entire reaction center and associated electron transfer system for each pigment, which would be very costly in terms of cellular resources.

To summarize, the following conclusions can be drawn. (i) The elimination of both red (660 nm) and far-red (735 nm) or only blue (455 nm) light appeared to suppress floral initiation, under such conditions carrots grew vegetative. In contrary, the elimination of solely far-red light resulted in faster flowering differention. (ii) The elimination of solely red (660 nm) or blue (455 nm) light resulted in a low synthesis rate of photosynthetic pigments and conditioned a high sucrose content in carrot root. Meanwhile, the elimination of solely far-red light resulted in the opposite effect. (iii) Dominating 640-nm light was found to considerably contribute to the excitation of the carotenoid antennal complex of the photosynthetic system.

Acknowledgments

The work was supported by the Lithuanian State Science and Studies Foundation under HORTILED project.

References

Bernier G, Prilleux C (2005) A physiological overview of the genetics of flowering time control. Plant Biotechnol J 3:3-16.

Casal JJ, and Sanchez RA (1994) Impaired stem-growth responses to blue-light radiance in light-grown transgenic tobacco seedlings overexpressing Avena phytochrome A. Physiol Plant 91:268-272.

Duchovskis P (2004) Flowering initiation of wintering plants. Horticulture and vegetable growing 23(2):3-11.

Gavrilenko VY (1975) Big practice of growing physiology. Moscow. (in Russian).

Gláucia M, Dias-Tagliacozzo and Válio FM Ivany (1994) Effect of vernalization on fowering of *Daucus carota*. R Bras Fisiol Veg 6:71-73.

Jang JC, Leon P, Zhou L, Sheen J (1997) Hexokinase as a sugar sensor in higher plants. The Plant Cell 9:5-19.

Kendrick RE, Kronenberg GHM (1994) Photomorphogenesis in plants, 2nd edn. The Netherlands: Kluwer Academic Publishers.

Kim HH, Wheeler RM, Sager JC (2006) Evaluation of lettuce grown using supplemental green light with red and blue light-emitting diodes in a controlled environment –a review of reseach at Kennedy Space Center. Acta Horticulturae 711:111-119.

King R (2006) Light-regulated plant growth and flowering; from photoreceptors to genes, hormones and signals. Acta Hort 711:227-233.

Kuperman FM, Rzhanova EI, Murashev VV, L'vova IN, Cedova EA, Akhundrova VA, Shcherbina IP (1982) Biology of cultivated plants development. 'Vischaia shkola', Moscow (in Russian).

Menard C, Dorais M, Hovi T, Gosselin A (2006) Development and physiological responses of tomato and cucumber to aditional blue light. Acta Hort 711:291-296.

Tamulaitis G, Duchovskis P, Bliznikas Z, Breive K, Ulinskaite R, Brazaityte A, Novickovas A, Zukauskas A (2005) High-power light-emitting diode based facility for plant cultivation. J Phys D 38:3182-3187.

Tarakanov IG (2006) Light control of growth and development in vegetable plants with various life strategies. Acta Hort 711:315-321.

Thomas B, Vince-Prue D (1997) Photoperiodism in Plants, 2nd ed. Academic Press, San Diego.

Yanagi T, Yachi T, Okuda N, Okamoto K (2006) Lihgt quality of continuous illuminating at night to induce floral initiation of Fragaria chiloensis L. CHI-24-1. Sci Hortic 109:309-314.

Yorio NC, Mackowiak CL, Wheeler RM, Sager JC (1995) Vegetative growth of potato under high-pressure sodium, high-pressure sodium SON-T Agro, and metal halide lamps. HortScience 30:374-6.

Volume 51(1):43-46, 2007
Acta Biologica Szegediensis
http://www.sci.u-szeged.hu/ABS

ARTICLE

Increased carotenoid content of *Xanthophyllomyces dendrorhous* cultivated in plant oil supplemented media

Árpád Csernetics[1], Linka Beáta[1], Judit Krisch[2], Csaba Vágvölgyi[1] and Tamás Papp[1]*

[1]Department of Microbiology, Faculty of Sciences, University of Szeged, Szeged, Hungary, [2]Institute of food Engineering, Faculty of Engineering, University of Szeged, Szeged, Hungary

ABSTRACT Carotenoid pigments (particularly astaxanthin) of the red yeast *Xanthophyllomyces dendrorhous* (*Phaffia rhodozyma*) have economical importance as food and feed colouring additives. Application of nutrients stimulating astaxanthin synthesis would improve the pigment production of the fungus. Vegetable oils contain various unsaturated fatty acids and isoprenoids, among them different precursors of the carotenoid biosynthesis. The effect of seven different, commercially available vegetable oils (sesame seed oil, corn seed oil, wheat germ oil, palm oil, pumpkin seed oil, coconut oil and olive oil) on the carotenoid production of two strains representing the teleomorph *X. dendrorhous* and the anamorph *P. rhodozyma* was examined. The two strains responded to the presence of the oil additives distinctly. Sesame seed and coconut oil stimulated the pigment production in the *X. dendrorhous* isolate only, whereas palm oil increased the production of both tested strains.
Acta Biol Szeged 51(1):43-46 (2007)

KEY WORDS

astaxanthin
Phaffia
Xanthophyllomyces
culturing conditions
carotenoid biosynthesis

Astaxanthin (3,3′-dihydroxy-β,β-carotene-4,4′-dione) is a very effective flesh pigmenter and has great economical importance as feed colouring additive in salmon, trout and crustacean, as well as poultry, farming (Nelis and De Leenheer 1991; Dufossé 2006). Astaxanthin is closely related to other well-known carotenoids, such as β-carotene, zeaxanthin and lutein, so that they share many of the metabolic and physiological functions attributed to carotenoids. It exhibits strong free radical scavenging activity and protects against lipid peroxidation and oxidative damage of LDL-cholesterol, cell membranes, cells, and tissues; it also has an anti-cancer activity and enhances the immune system (Guerin et al. 2003). All these properties of astaxanthin share it an importance in the human diet which could lead to extended commercial applications. Today, most of the industrial astaxanthin production is performed by chemical synthesis, but serious efforts are made to develop strains and techniques for achievement of the microbial production. The red pigmented basidiomycetes yeast, *Xanthophyllomyces dendrorhous* (*Phaffia rhodozyma*) is one of the best candidates as a natural source of astaxanthin and other carotenoid compounds. The original taxonomic description defined this red yeast as an anamorphic species and it was named as *Phaffia rhodozyma* (Miller et al. 1976). Later, Golubev (1995) discovered the sexual cycle of the yeast and introduced the new species *Xanthopyllomyces dendrorhous* (Basidiomycetes). *P. rhodozyma* was considered to be con-specific with *X. dendrorhous* and the latter became the commonly accepted species name. However, a number of data have accumulated later on suggesting that the teleomorph *X. dendrorhous* and the anamorph *P. rhodozyma*, would be separate species (Kucsera et al. 1995; Fell and Blatt 1999). For this reason, two isolates representing *X. dendrorhous* and *P. rhodozyma* were involved in the present study and their responses to the application of different plant oils were compared.

In the last decade, strain improvement studies were carried out to elevate the pigment production of *Xanthophyllomyces* to an economic level, among others by mutagenesis and screening (Fang and Cheng 1993; Sun et al. 2004; Palágyi et al. 2006), protoplast fusion (Chun et al. 1992) or by means of metabolic pathway engineering (Visser et al. 2003). Besides development of carotenoid overproducing strains, application of nutrients stimulating carotenoid synthesis, through enzyme induction or by exerting a general positive effect on the fungal growth, could also improve the carotenoid production. Vegetable oils may contain various unsaturated fatty acids and isoprenoids, among them precursors of the astaxanthin biosynthesis. In earlier studies, several lipids and lipid derivatives were used successfully to increase β-carotene synthesis in the Zygomycetes fungi, *Phycomyces blakesleeanus* and *Blakeslea trispora* (Ciegler and Arnold 1959 a,b; Lampila et al. 1985). The aim of the present work was to investigate the effect of different, commercially available vegetable oils on the carotenoid pigment production of *X. dendrorhous/P. rhodozyma*.

Accepted August 7, 2007
*Corresponding author. E-mail: pappt@bio.u-szeged.hu

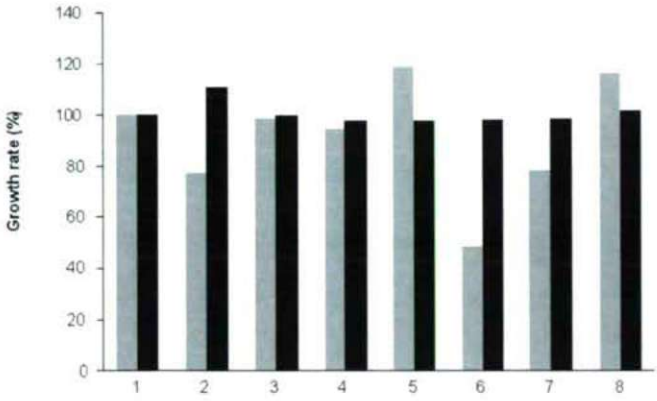

Figure 1. Effects of different vegetable oils on the astaxanthin production of *P. rhodozyma* and *X. dendrorhous*. ■: *P. rhodozyma* CBS 5905; ■: *X. dendrorhous* CBS 6938. 1: control; 2: sesame seed oil; 3: corn germ oil; 4: wheat germ oil; 5: palm oil; 6: pumpkin seed oil; 7: live oil; 8: coconut oil. Media contained 1% of the oils in every case.

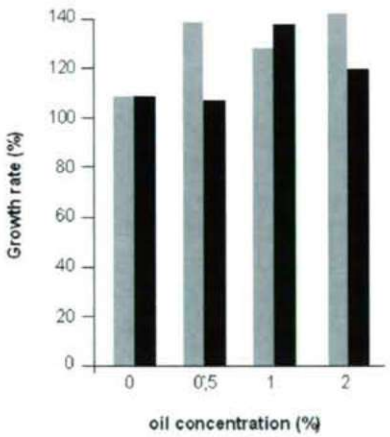

Figure 2. Effect of palm oil on the astaxanthin production of *P. rhodozyma* and *X. dendrorhous*. ■: *P. rhodozyma* CBS 5905; ■: *X. dendrorhous* CBS 6938.

Materials and Methods

Strains and culture conditions

P. rhodozyma CBS 5905 and *X. dendrorhous* CBS 6938 were cultured in 25 ml of yeast-peptone-glucose (YPG: 1% glucose, 0.25% peptone, 0.25% yeast extract) liquid medium supplemented with the appropriate vegetable oil for 4 days at 20°C under continuous shaking (200 rpm). The tested plant oils were as follows: sesame seed oil (Sigma); corn seed oil (Sigma); wheat germ oil (Sigma); palm oil (cooking oil); pumpkin seed oil (Sigma); coconut oil (cooking oil) and olive oil (extra virgin). The latter two were commercially available standard brands.

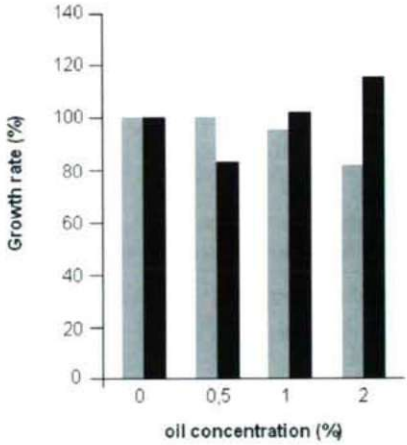

Figure 3. Effect of coconut oil (grease) on the astaxanthin production of *P. rhodozyma* and *X. dendrorhous*. ■: *P. rhodozyma* CBS 5905; ■: *X. dendrorhous* CBS 6938.

Measurement of the pigment content

After cultivation, cells were collected from 1 ml culture by centrifugation (5 min, 10 000 rpm) and washed twice with distilled water. The cell pellet was freeze-dried and treated with 1 ml of pre-heated dimethyl sulfoxide (DMSO) for 10 min at 55°C. Samples were centrifuged again (5 min, 12 000 rpm), and the total carotenoid content was measured in the supernatant by recording the absorbance at 492 nm. Dry-weight of cells harvested by centrifugation from 1 ml of each the cultures was also determined and the pigment content was related to dry cell mass. The carotenoid contents of the control extracts obtained from cultivation on YPG without oil supplements were regarded as 100%.

Thin layer chromatography (TLC) analysis

Pigment samples were obtained by the modified method of Sedmack et al. (1990). To 3 ml carotenoid extract in DMSO, equal volume of diethyl ether was added in a separator funnel. It was placed on ice for 3 min and then 0.5 ml of water was added. The lower phase was removed and 5 ml of acetone and then 5 ml of 10% (v/v) ether-petrol were added. To achieve the separation of phases, 10 ml of water was added. The upper phase was decanted, washed with water (10 ml) and dried in a stream of N_2. Samples were redissolved in ethyl acetate and subjected on silica gel ($60F_{254}$, Merck) for TLC, which was developed with acetone-petroleum ether (20:80).

Results

In a primer experiment, effects of 1% of 7 plant oils (sesame seed oil, corn seed oil, wheat germ oil, palm oil, pumpkin seed oil, coconut oil and olive oil) added into the cultivation media were tested (Fig. 1). Elevated carotenoid production

was detected in *X. dendrorhous* with the application of sesame seed oil; the total pigment content increased by 11%. At the same time, sesame seed oil and olive oil caused about 20% decrease in the carotenoid content of *P. rhodozyma*. Palm and coconut oil, in contrast, stimulated the pigment production of *P. rhodozyma*: an increment of 20% and 16% was observed, respectively. These compounds did not affect significantly the pigment production of *X. dendrorhous*. Pumpkin seed oil had no effect on *X. dendrorhous*, but decreased the carotenoid production of *P. rhodozyma* by 48%. The other oils tested seemed to have no effec on the carotenoid production in either organism.

After this preliminary experiment, the effect of coconut and palm oil was studied in more detail (Fig. 2-3), applying the oil supplements in 3 different concentrations (0.5; 1 and 2%). Palm oil stimulated the carotenoid production in both strains, but the effect of the same palm oil concentration in the two tested strains was different (Fig. 2). Carotenoid content of *P. rhodozyma* was increased by 20-29% depending on the oil concentration; the best result was observed if 2% of oil was added. In case of *X. dendrorhous*, a 25% increment of the total pigment content was observed on adding 1% palm oil, while 2% oil led to a lower increment (10%). The application of coconut oil exerted an opposite effect on the pigment production of *P. rhodozyma* and *X. dendrorhous*. Coconut oil decreased the carotenoid production in *P. rhodozyma* proportionally to the applied concentration. At the same time, the production in *X. dendrorhous* was increased (Fig. 3). The highest production (115%) was observed at 2% coconut oil concentration.

Samples extracted from the cultures containing sesame seed, palm and coconut oil were examined also with TLC (results not shown). Although the analysis detected the changes in the carotenoid – mainly astaxanthin – content, alterations in the carotenoid spectra were not observed.

Discussion

Phaffia rhodozyma and *Xanthophyllomyces dendrorhous* are the most promising fungal sources of the carotenoid astaxanthin. The commercial demand for astaxanthin increases, and although the biological production is still not economic, there is a continuous progress in improving strains as well as and fermentation methods. In our study on the effect of seven different oil extracts (all of them produced industrially in high quantity) as potential stimulators of the pigment production of these fungi, it was found that sesame seed, palm and coconut oils exerted significant effect on the pigment production. However, the two involved strains, representing the anamorph (*Phaffia*) and the teleomorph (*Xanthophyllomyces*) states, reacted to the applied oils very differently. This result supports the suggestion, based mainly on DNA sequence analysis data, that *Phaffia* is not just an anamorph state of *Xanthophyllomyces*, but a separate species (Kucsera et. al. 1998; Fell and Blatt; 1999, Lukács et al. 2006).

Extracts of palm oil generally contain several isoprenoid derivatives, such as β-carotene, different, cyclic and acyclic carotenoids and sterols, in high amounts (Lo and Choo 2003). Beta-carotene can be rapidly oxidised on exposure to light and in the presence of oxygen, but it is supposed that the lipid compounds of the palm oil can protect and conserve it. Together with other carotenoids, β-carotene is a precursor of astaxanthin, so the presence of these compounds in the oil additive could be one of the explanations of its stimulating effect on the astaxanthin production.

Acknowledgements

This research was supported in part by grants from the Hungarian Scientific Research Fund (OTKA D48537) and the J. Bolyai Research Scholarship of the Hungarian Academy of Sciences.

References

Chun SB, Chin JE, Bai S and An G-H (1992) Strain improvement of Phaffia rhodozyma by protoplast fusion. FEMS Microbiol Lett 93:221-226.

Ciegler A, Arnold M and Anderson RF (1959a) Microbiological production of carotenoids.IV:Effect of various grains on production of beta-carotene by mated strains of Blakeslea trispora. Appl Microbiol 7:94-97.

Ciegler A, Arnold M and Anderson RF (1959b) Microbiological production of carotenoids.V:Effect of lipids and related substances on production of beta-carotene. Appl Microbiol 7:98-101.

Dufossé L (2006) Microbial production of food grade pigments. Food Technol Biotechnol 44:313-321.

Fang TJ and Cheng Y-S (1993) Improvement of astaxanthin production by Phaffia rhodozyma through mutation and optimization of culture conditions. J Ferment Bioeng 75:466-469.

Fell JW, Blatt GM (1999) Separation of the strains of the yeasts Xanthophyllomyces dendrorhous and Phaffia rhodozyma based on rDNA IGS and ITS sequence analysis. J Ind Microbiol Biotechnol 23:677-681.

Golubev WI (1995) Perfect state of Rhodomyces dendrorhous (Phaffia rhodozyma). Yeast 11:101-110.

Guerin M, Huntley ME, Olaizola M (2003) Haematococcus astaxanthin: applications for human health and nutrition. Trends Biotechnol 21:210–216

Kucsera J, Pfeiffer I, Ferenczy L (1998) Homothallic life cycle in the diploid red yeast Xanthophyllomyces dendrorhous (Phaffia rhodozyma). Anton Leeuw Int J G 73:163-168.

Lampila LE, Wallen SE and Bullerman LB (1985) A review of factors affecting biosynthesis of carotenoids by the order Mucorales. Mycopathologia 90:65-80

Loh SK and Choo YM (2003) Palm-based chiral compounds. Journal of Oil Palm Research 15:6-11.

Lukács Gy, Linka B, Nyilasi I (2006) Phaffia rhodozyma and Xanthophyllomyces dendrorhous: astaxanthin-producing yeasts of biotechnological importance. Acta Aliment 35:99-107.

Miller MW, Yoneyama M, Soneda M (1976) Phaffia, a new yeast genus in the Deuteromycotina (Blastomycetes). Int J Syst Bacteriol 26:286-291

Nelis HJ and De Leenheer AP (1991) Microbial sources of carotenoid pigments used in foods and feeds. J Appl Bacteriol 70:181-191.

Palágyi Zs, Linka B, Papp T, Vágvölgyi Cs (2006) Isolation and characterization of Xanthophyllomyces dendrorhous mutants with altered carotenoid content. Acta Aliment Hung 35:223-228.

Sedmak J J, Weerasinghe DK and Jolly SO (1990) Extraction and quantification of astaxanthin from Phaffia rhodozyma. Biotechnol Technol 4:107-112.

Sun N, Lee S and Song KB (2004) Characterization of a carotenoid-hyper-producing yeast mutant isolated by low-dose gamma irradiation. Int J Food Microbiol 94:263-267.

Visser H, van Ooyen AJJ and Verdoes JC (2003) Metabolic engineering of the astaxanthin-biosynthetic pathway of Xanthophyllomyces dendrorhous. FEMS Yeast Res 4:221-231.

Volume 51(1):47-52, 2007
Acta Biologica Szegediensis
http://www.sci.u-szeged.hu/ABS

ARTICLE

Auxin autotrophic tobacco calli with modified aldehyde oxidase isoenzyme activities show enhanced abiotic stress tolerance

Jolán Csiszár[1]*, Margit Szabó[1], Dorica Botau[2], László Erdei[1], Irma Tari[1]

[1]Department of Plant Physiology, University of Szeged, Szeged, Hungary, [2]Institute of Plant Biotechnology, Banat's University of Agricultural Sciences, Timisoara, Romania

ABSTRACT The growth, abiotic stress resistance and aldehyde oxidase (AO) activities of auxin autotrophic and heterotrophic tobacco calli were compared. The auxin-independent autotrophic calli maintained their growth rate even at 35°C temperatures, showed enhanced abiotic stress resistance in the presence of 50-300 mM NaCl, 0.1-5 mM KNO_2 or 0.1-10 mM H_2O_2. 0.1-5 mM H_2O_2 caused a higher increase in glutathione S-transferase (GST) and glutathione peroxidase (GPOX) activities of heterotrophic calli, however these enzymes worked in an elevated level in autotrophic lines under control circumstances and were induced differently under oxidative stress, indicating an altered signalling mechanism. AO activity could be detected by activity staining after native PAGE with indole-3-acetaldehyde (IAAld) substrate in both calli, which means that the enzyme catalyzing the last step in IAA biosynthesis is present in both tissues. Contrary to heterotrophic calli, in the auxin autotrophic cultures an isoenzyme with low mobility (AO1) was detectable. 100 mM NaCl enhanced the AO1 activity and a new isoenzyme (AO2) was observed. The increase of the activities of these isoenzymes were higher in the autotrophic lines suggesting that the enhanced IAA biosynthesis can play a role in the recovery of growth under stress conditions.
Acta Biol Szeged 51(1):47-52 (2007)

KEY WORDS

auxin heterotrophic and autotrophic calli,
aldehyde oxidase,
glutathione S-transferase and peroxidase,
oxidative stress resistance

The requirement for auxin and cytokinin to maintain the growth of plant tissue cultures has long been known. Under certain conditions, however, proliferation can take place on medium containing no exogenous auxin and/or cytokinin; these hormone-independent cultures are referred to as autotrophic or habituated tissues, the process - in which the cells regain the hormone synthesizing capacity - is the habituation. Habituation defined as an epigenetic change, the sequence of DNA is not altered, but the DNA methylation patterns and expression of genes, posttranslational modifications can be different. It is extremely stable and heritable at cellular level.

Several processes can lead to an elevated auxin level, such as the enhanced or altered biosynthesis of indoleacetic acid (IAA; Jackson and Lyndon 1990; Szabó et al. 1994; Michalchuk and Druart 1999), or the different levels of IAA conjugation or degradation (Bouchet et al. 1978; Syono 1979; Michalchuk and Druart 1999).

Plants usually synthesize IAA from L-tryptophan, but there is evidence for tryptophan-independent IAA production (Crozier et al. 2000). The first enzymatic step of the major tryptophan-dependent pathway is catalyzed by aminotransferases with broad substrate specificities (Wightman and Forest 1978; Koshiba et al. 1993). The produced indole-3-pyruvic acid is extremely unstable and can be easily decarboxylated enzymaticaly or non-enzymaticaly to indole-3-acetaldehyde (IAAld). The last step is the conversion of IAAld to IAA by indole-3-acetaldehyde oxidase enzyme, this enzyme belongs to the aldehyde oxidase (AO) multigene family.

In plants, different isoforms of AO enzimes have been identified which have a rather broad substrate specificity and show organ specific distribution. AO enzymes can also oxidize indole-3-aldehyde (IAld) to indole-3-carboxylic acid in the peroxidative decarboxylation pathway of IAA causing an irreversible loss of IAA. AO oxidizes abscisic aldehyde to abscisic acid (ABA) either. Since members of the AO enzyme family catalyze the final step in the biosynthesis of phytohormones, plant AOs may have an important role in plant development and adaptation to environmental stresses (Koshiba et al. 1996; Sagi et al. 1998; Zdunek-Zastocka et al. 2004).

Glutathione S-transferases (GSTs) with high affinity for auxins and cytokinin have also been suggested to contribute to hormone homeostasis and responses to different stress factors, because this enzymes not only catalyze conjugation of reduced glutathione (GSH) with natural products and xenobiotics, but they function in the homeostasis of hormones and

Accepted Aug 14, 2007
*Corresponding author. E-mail: csiszar@bio.u-szeged.hu

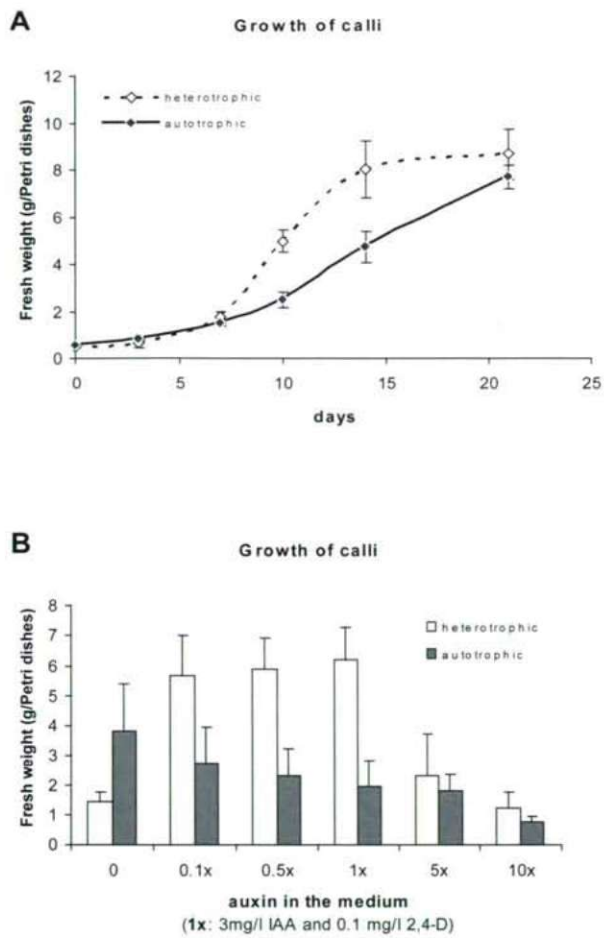

Figure 1. A: Growth of calli on RM media containing 17 µM IAA and 0.5 µM 2,4-D (in the case of auxin heterotrophic calli) or without exogenous auxins (for autotrophic calli). B: Growth of the auxin heterotrophic (□) and autotrophic (■) calli on 0.1-10 times external auxin containing RM media after 2 weeks. The amount of auxins for growing heterotrophic lines usually is 17 µM IAA and 0.5 µM 2,4-D (1x).

catalyze alternative GSH-dependent biotransformation reactions (Marrs 1996; Edwards et al. 2000, Basanti and Srivastava 2007). It was reported previously that the auxin autotrophic tobacco calli can be characterized with an elevated antioxidant activities and GSTs and glutathione peroxidases (GPOX) play an important role in their tolerance to 100 mM NaCl (Csiszár et al. 2004). In this paper we compared the growth and AO activities of auxin heterotrophic and autotrophic tobacco callus cultures under different conditions and evaluated the effect of exogenous H_2O_2 on the two types of calli.

Materials and Methods

Plant material

The callus cultures originated from protoplasts of *Nicotiana tabacum* SR1 plants (Csiszár et al. 2001). The auxin-requiring cultures were grown on a solid MS medium (Murashige and Skoog 1962) containing 2 µM kinetin, 17.5 µM IAA and 0.45 µM 2,4-D, and the auxin autotrophic cultures were transferred onto the same medium without auxin. Each Petri dish contained 25 inocula; the weight of one inoculum was approximately 20 mg. The cultures were kept in a growth chamber at 25°C, under 8.4 Wm^{-2} warm white fluorescent light (Tungsram F29 lamps, Hungary), and were analyzed in a 3-week period. Abiotic stress treatments were carried out by growing the calli in the growth chamber (Conviron) at 15-35°C, or by supplying the culture media with 50-300 mM NaCl or 0.1-5 mM KNO_2. H_2O_2 was added aseptically in the final concentrations of 0.01-10 mM just before the medium became solid, and the inocula were plated immediately.

Investigation of aldehyde oxidase in native gel

Two g of 2-week-old calli were homogenized with 2 ml of ice-cold extraction medium containing 250 mM Tris(hydroxymethyl)aminomethane hydrochloride (TRIS-HCl), pH 8.5, 1 mM ethylenediaminetetraacetic acid (EDTA), 10 mM reduced glutathione (GSH), and 2 mM dithiothreitol (DTT). The homogenized plant material was centrifuged at 10 000 g and 4°C for 25 min. The resulting supernatant was subjected to native polyacrylamide gel electrophoresis (PAGE) on 1.5-mm-thick slabs of 7.5% polyacrylamide gels in a Laemmli buffer system (Laemmli 1970) in the absence of SDS at 4°C. The gels were loaded with 100 mg protein. After electrophoresis, AO activity staining was developed at room temperature in a mixture containing 0.1 M TRIS-HCl, pH 7.5, 0.1 mM phenazine methosulphate, 1 mM MTT (3[4,5-dimethylthiazol-2-yl]-2,5-diphenyltetrazolium-bromide), and 1 mM indole-3-acetaldehyde (IAAld) or indole-3-aldehyde (IAld) substrate. AO activity was estimated on the basis of MTT reduction, which resulted in the development of specific formazan bands. The relative intensity of formazan bands was directly proportional to enzyme activity (Sagi et al. 1998). When IAAld was used as a substrate, the gel instantly became dark purple (Koshiba et al. 1996) however, we could definitely distinguish bands. Native PAGE was carried out with a Hoefer SE 600 (Amersham Pharmacia Biotech, USA).

Activity measurements of glutathione S-transferase and peroxidase enzymes

The enzyme activities were determined 2 weeks after the transfer onto the MS medium. Two g of callus tissues was homogenized on ice in 4 ml extraction buffer (50 mM phosphate buffer pH 7.0, containing 1 mM EDTA, 1 mM phenylmethylsulfonyl fluoride and 1% polyvinyl-polypirrolidone). The homogenate was filtered through two layers of cheese-cloth and centrifuged for 25 min at 15 000 g at 4°C. The supernatant was used for enzyme activity assays.

GST activity was determined spectrophotometrically

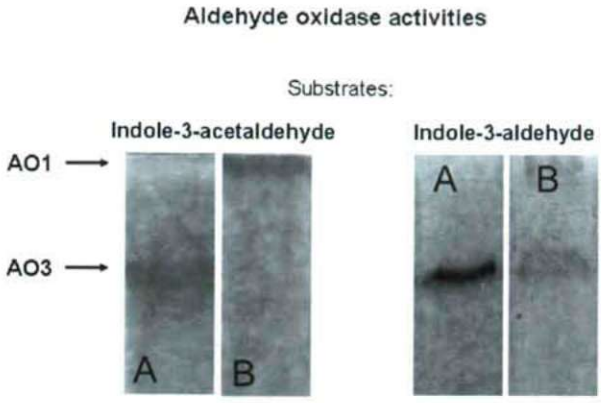

Figure 2. Aldehyde oxidase activities of 2-week-old tobacco calli with IAAld and IAld substrates after native-PAGE. A: auxin heterotrophic calli grown on RM medium containing 17 μM IAA and 0.5 μM 2,4-D; B: auxin autotrophic calli grown on RM medium without exogenous auxin.

by using an artificial substrate, 1-chloro-2,4-dinitrobenzene (CDNB), according to Habig et al. (1974). Reactions were initiated by the addition of CDNB, and the increase in A_{340} was determined. One enzyme unit (U) is the amount of enzyme producing 1 μmol conjugated product in 1 min, $\varepsilon_{340} = 9.6\ mM^{-1}cm^{-1}$.

Glutathione peroxidase (GPOX) activity was measured by the method of Awasthi et al. (1975), with cumene hydroperoxide as substrate. The reaction mixture contained 4 mM GSH, 0.2 mM NADPH, 0.05 U of glutathione reductase (GR, Type II from wheat, Sigma), 100 μl enzyme extract and 0.5 mM substrate in phosphate buffer (0.1 M, pH 7.0) in a total volume of 1 ml. The decrease of NADPH was followed by measuring the A_{340}; the non-specific NADPH decrease was corrected for by using additional measurements without substrate. $\varepsilon_{340} = 6.22\ mM^{-1}\,cm^{-1}$. One U is the amount of enzyme converting 1 μmol NADPH in 1 min. The protein contents of the extracts were determined by the method of Bradford (1976). The results are means ±SD of three independent experiments.

Results and Discussion

Growth and AO activities of the auxin heterotrophic and autotrophic calli

The growth of the autotrophic cells exhibits a longer logarithmic, "rapid growth" phase: the fresh weight of the tissues growing on auxin-free medium were less than that of the heterotrophic calli growing in the presence of IAA and 2,4-D, but at the end of the 3rd week the difference disappeared (Fig 1A). The maximum growth of the heterotrophic calli was found in the presence of 17 μM IAA or 2.5 μM 2,4-D in the medium (Fig. 1B). Higher auxin concentrations proved supraoptimal. In the autotrophic tissues, all the used auxin concentrations inhibited the growth (Fig 1B). Their sensitivity to the auxin content in the medium had been changed suggesting a possible difference in auxin-dependent gene regulation.

Investigation of the hormone metabolism in auxin autotrophic cultures revealed that their endogenous free auxin level can be higher than that in the heterotrophic lines (Nakajima et al. 1979). The major pathway for IAA biosynthesis appears to proceed via indole-3-acetaldehyde in plants, the final step is catalyzed by AO. We compared the isoenzyme pattern in the two types of calli by activity staining for AO after native PAGE.

AO activity could be detected both in the auxin heterotrophic and autotrophic calli using IAAld substrate, however the auxin autotrophic line contained a different AO isoenzyme (Fig. 2). Because this activity is present in the heterotrophic calli, our results demonstrate that the lack of the IAA synthesis of the cultured cells is not due to the limiting AO activity. However, in the autotrophic calli a new isoenzyme (AO1) was detected, which had considerable activity toward IAAld substrate.

Seo et al. (1998) reported that the auxin overproducing *Arabidopsis sur1* (*superroot1*) mutant had three AO isoenzymes (AO1-3). AO1 had the lowest mobility, and its activity was significantly higher in mutant seedlings. The activity of this enzyme toward IAAld substrate was about 5 times higher in the extract of the *sur1* plants, supporting the possible role of AO1 in IAA biosynthesis in *Arabidopsis* seedlings, but this isoenzyme showed also a relatively high activity with IAld substrate (Seo et al. 1998). Koshiba et al. (1996) found that maize AO had a high affinity for IAAld (K_m 3-5 μM), indicating that even if a low concentration of IAAld was present in cells, the aldehyde could be converted into IAA. It is possible, that the newly activated enzyme, which is regulated presumably in a different way, in our auxin autotrophic calli is involved in the synthesis of IAA and in the auxin-independent growth of the autotrophic tissues. In our experiments the second isoenzyme (denoted by AO3) exhibited a very strong staining with indole-3-aldehyde (IAld) substrate in the heterotrophic tissues, suggesting that in the IAA degradation pathway the oxidation of IAld catalysed by AO3 has an important role (Fig. 2). This activity determinate the IAA levels not directly, because it is the last step of the peroxidases-initiated IAA inactivation pathway.

The growth rate of the calli at different temperatures and in the presence of abiotic stressors

The effect of temperatures on the growth of calli were investigated on MS media used for maintaining the cultures; it contained 17 μM IAA and 0.5 μM 2,4-D for auxin heterotrophic calli, or no exogenous auxins in the case of autotrophic tissues. The growth rate of heterotrophic calli increased with increasing temperatures till 30°C, above this

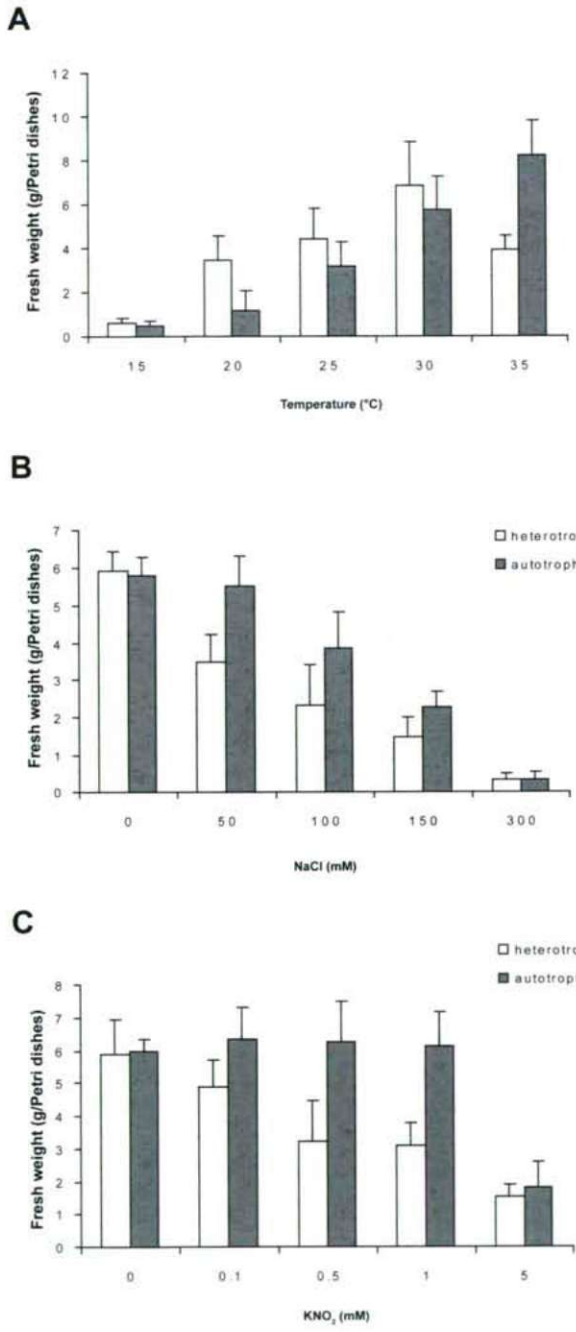

Figure 3. Effect of different temperatures (A), 50-300 mM NaCl (B) and 0.1-5 mM KNO_2 (C) on the fresh weight of 2-week-old auxin heterotrophic and autotrophic calli The used media are the same as in Fig. 1A.

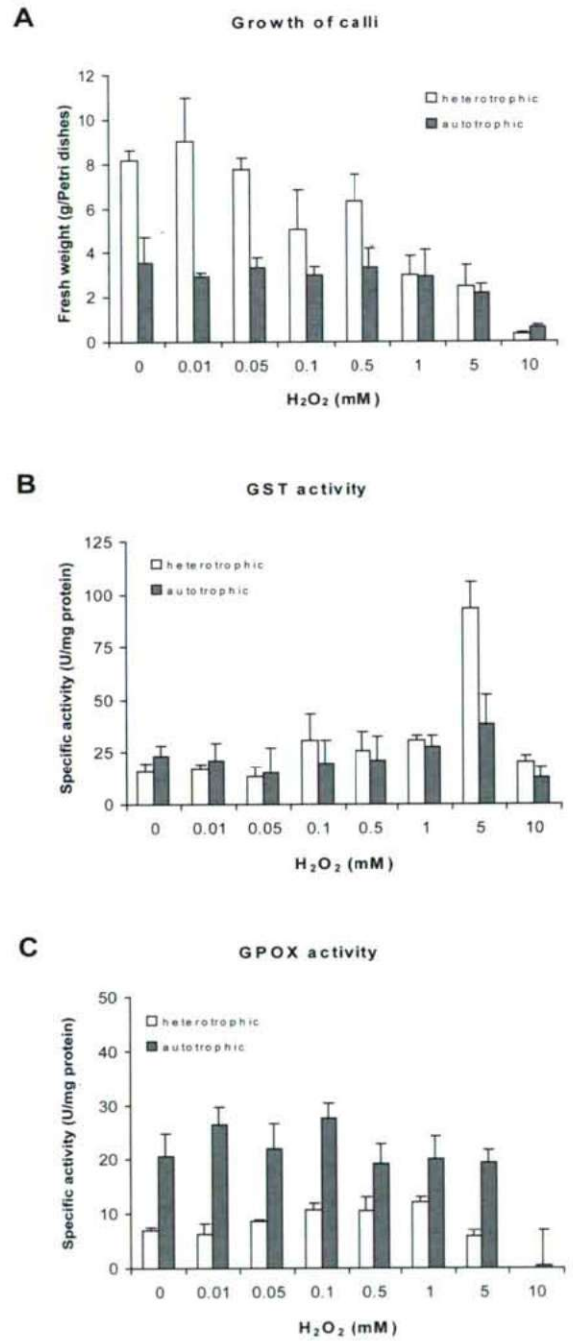

Figure 4. Effect of exogenous H_2O_2 on the growth (A), glutathione S-transferase (B) and glutathione peroxidase (C) activities of 2-week-old auxin heterotrophic and autotrophic calli

it was inhibited (Fig. 3A). Decrease in the growth rate may be an adaptation strategy for unfavourable circumstances; its role may be the reservation of the energy for defence mechanisms (May et al. 1998). The growth rate of auxin autotrophic calli showed an increasing tendency in our experiments; the fresh weight of the 2-week-old calli at 35°C was even higher than that of the heterotrophic tissues. This indicates the enhanced stress tolerance of autotrophic tissues to high temperature.

Supplying the medium with 50-300 mM NaCl and 0.1-5 mM KNO_2 concentrations resulted in significant differences

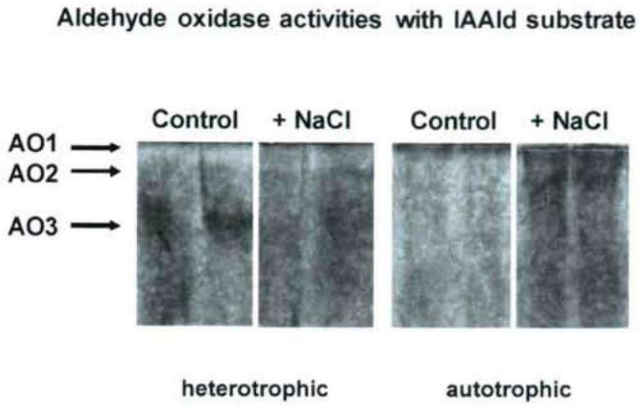

Figure 5. Aldehyde oxidase activities of 2-week-old auxin heterotrophic and autotrophic calli grown on RM media supplied with 100 mM NaCl with IAAld substrate. RM media contained 17 μM IAA and 0.5 μM 2,4-D for the heterotrophic and no exogenous auxins for the autotrophic cultures.

in the growth of the two cultures and veryfied the enhanced abiotic stress resistance of the auxin autotrophic lines (Fig. 3B, C).

The effect of exogenous H_2O_2 on the growth, GST and GPOX activities of calli

The common element of these different abiotic stressors is that they can, at the cellular level, enhance the generation of reactive oxigen species (ROS), such as superoxide radicals ($O_2^{\cdot -}$), hydrogen peroxide (H_2O_2) and hydroxil radicals ($OH^{\cdot}$). It was suggested in our previous paper that the auxin autotrophic calli are more resistant to oxidative stress, and the enhanced GST and GPOX activities can play a role in this (Csiszár et al. 2004). We investigated further the tolerance of the two lines using exogenously applied H_2O_2.

The calli were transferred onto fresh MS medium containing 0.1-10 mM H_2O_2. The growth of 2-week-old auxin heterotrophic calli in the presence of 1 mM H_2O_2 decreased by 60% comparing to the control (Fig. 4A); 10 mM H_2O_2 caused the death of the tissues. The fresh weights of auxin autotrophic calli were ca. half of the heterotrophic ones, but their growth was inhibited only by the lethal 10 mM H_2O_2. This proves that the autotrophic calli really do posses a more effective H_2O_2-scavenging mechanism, but the concentration that activated the cell death at the two lines was the same.

Comparison of the GST activities in the heterotrophic and autotrophic calli revealed a considerable induction in the heterotrophic tissues, especially in the presence of 5 mM exogenous H_2O_2. The autotrophic callus had higher GST activity, but with the increasing H_2O_2 concentrations this enzyme did not induced (Fig. 4B). Auxin autotrophic calli exhibited approximately two-fold higher GPOX activities than the heterotrophic cultures, but the activation of this enzyme in the presence of H_2O_2 was not so definite (Fig. 4C). It was established that auxin autotrophic tissues not only produce less ethylene than heterotrophic ones, but high external IAA and 2,4-D concentrations induced differentially their GST activities and the transferred bacterial mannopine synthase *mas1'* promoter which, similarly to several GST genes, also contains stress- and hormone-inducible *cis*-acting element (Marrs 1996; Guevara-Garcia et al. 1998; Csiszár et al. 2001). According to our former results, the crosstalk between the auxin- and ethylene-induced signal transduction pathways may differ in the two types of calli. The present results confirm the involvement of elevated GST and GPOX enzyme activities in oxidative stress resistance and the different induction of their activities in the presence of H_2O_2 suggest an altered signalling mechanism in the auxin autotrophic lines.

Effect of salt stress on AO isoenzyme activities of auxin heterotrophic and autotrophic tissues

To investigate further the role of aldehyde oxidase activities in the abiotic stress tolerance of calli we supplied the media with 100 mM NaCl. Activity staining of samples originated from 2-week-old heterotrophic calli with IAAld substrate revealed that the activity of the AO3 isoenzyme decreased under salt stress, however the appearance of AO1 and even a new isoenzyme band, denoted by AO2, were detectable (Fig. 5). This new isoenzyme was also present in the salt-treated autotrophic tissues and its activity was higher than that in the stress-treated heterotrophic lines. In autotrophic calli the NaCl enhanced the activities both of AO1 and AO2 isoenzymes, indicating the increased IAA biosynthesis in stress conditions (Fig. 5).

Several studies investigated the effect of salinity on AO activities and regulation. NaCl usually increased the AO activity in roots of different plants, in some cases there was no effect in the leaves (Sagi et al. 1998; Omarov et al. 1998; Barabás et al. 2000; Tari et al. 2002). Using an ABA-deficient *Lycopersicon esculentum* mutant (*sitiens*) Dunlap and Binzel (1996) reported that NaCl reduced IAA levels in the roots of tomato plants independent of stress-induced ABA. In our experiments a new isoenzyme was detected in both type of calli and the higher induction was found in auxin autotrophic cultures. Our results suggest that the elevated or maintained IAA level and/or the altered signalling pathway in the auxin autotrophic calli may play a role in their enhanced stress tolerance.

Acknowledgments

This work was supported by National Scientific Foundation (OTKA T 030259 and T 03839) and PHARE CBC HU. 2002/000.627.03-14 grants.

References

Awasthi YC, Beutler E, Srivastava SK (1975) Purification and properties of human erythrocyte glutathione peroxidase. J Biol Chem 250:5144-5149.

Barabás KN, Omarov RT, Erdei L, Lips HS (2000) Distribution of the Mo-enzymes aldehyde oxidase, xanthine dehydrogenase and nitrate reductase in maize (*Zea mays* L.) nodal roots as affected by nitrogen and salinity. Plant Sci 155:49–58.

Basanti M, Srivastava A (2007) Plant glutathione transferases – a decade falls short. Can J Bot 85:443-456.

Bouchet M, Gaspar T, Thorpe TA (1978) Soluble and cell wall peroxidases and auxin destruction in normal and habituated tobacco callus. In Vitro 14:819-823.

Bradford MM (1976) A rapid and sensitive method for the quantitation of microgram quantities of protein utilizing the principle of protein-dye binding. Anal Biochem 72:248-254.

Crozier A, Kamiya Y, Bishop G, Yokota T (2000) Biosynthesis of hormones and elicitor molecules. In Biochemistry and molecular biology of plants. Eds: Buchanan BB, Gruissem W, Jones RL. Printed by American Societies of Plant Physiologists, Rockville, Maryland, USA, Courier Companies, Inc., pp. 850-929.

Csiszár J, Szabó M, Tari I, Erdei L (2001) Control of the glutathione S-transferase and *mas1'* promoter-driven GUS activity in auxin heterotrophic and autotrophic tobacco calli by exogenous 2,4-D-induced ethylene. Physiol Plant 113:100-107.

Csiszár J, Szabó M, Erdei L, Márton L, Horváth F, Tari I (2004) Auxin autotrophic tobacco callus tissue resist oxidative stress: the importance of the glutathione S-transferase and peroxidase activities in auxin heterotrophic and autotrophic calli. J Plant Physiol 161:691-699.

Dunlap JR, Binzel ML (1996) NaCl reduces indole-3- acetic acid levels in the roots of tomato plants independent of stress-induced abscisic acid. Plant Physiol 112:379-384.

Edwards R, Dixon DP, Walbot V (2000) Plant glutathione S-transferases: enzymes with multiple functions in sickness and in health. Trends Plant Sci 5:193-198.

Guevara-Garcia A, Lopez-Ochoa J, Lopez-Bucio J, Simpson J, Herrera-Estrella L (1998) A 42 bp fragment of the pmas1 promoter containing an ocs-like element confers a developmental, wound- and chemically inducible expression pattern. Plant Mol Biol 38:743-753.

Habig WH, Pabst MJ, Jakoby WB (1974) Glutathione S-transferases. The first enzymatic step in mercapturic acid formation. J Biol Chem 246:7130-7139.

Jackson JA, Lyndon RF (1990) Habituation: cultural curiosity or developmental determinant? Physiol Plant 79:579-583.

Koshiba T, Mito N, Miyakado M (1993) L- and D-tryptophan aminotransferases from maize coleoptiles. J Plant Res 106:25-29.

Koshiba T, Saito E, Ono N, Yamamoto N, Sato M (1996) Purification and properties of flavin- and molibdenium-containing aldehyde oxidase from maize coleoptiles. Plant Physiol 110:781-789.

Laemmli UK (1970) Cleavage of structural proteins during the assembly of the head of bacteriophage T4. Nature 227:680-685.

Marrs KA (1996) The functions and regulation of glutathione S-transferases in plants. Annu Rev Plant Physiol Plant Mol Biol 47:127-158.

May MJ, Vernoux T, Leaver C, Van Montague M, Inzé D (1998) Glutathione homeostasis in plants: implications for environmental sensing and plant development. J Exp Bot 49:649-667.

Michalchuk L, Druart P (1999) Indole-3-acetic acid metabolism in hormone-autotrophic, embryogenic callus of Inmil® cherry rootstock (*Prunus insica* x *serrula* 'GM 9') and in hormone-dependent, nonembryogenic calli of *Prunus insica* x *serrula* and *Prunus domestica*. Physiol Plant 107:426-432.

Murashige T, Skoog F (1962) A revised medium for rapid growth and bio assays with tobacco tissue cultures. Physiol Plant 15:473-497.

Nakajima H, Yokota T, Natsumozo T, Noguchi M, Takamasi N (1979) Relationship between hormone content and autonomy in various autonomous tobacco cells cultured in suspension. J Plant Cell Physiol 29:1489-1499.

Omarov RT, Sagi M, Lips SH (1998) Regulation of aldehyde oxidase and nitrate reductase in roots of barley (*Hordeum vulgare* L.) by nitrogen source and salinity. J Exp Bot 49:897-902.

Sagi M, Omarov RT, Lips SH (1998) The Mo-hydroxylases xanthine dehydrogenase and aldehyde oxidase in ryegrass as affected by nitrogen and salinity. Plant Sci 135:125-135.

Seo M, Akaba S, Oritani T, Delarue M, Bellini C, Caboche M, Koshiba T (1998) Higher activity of an aldehyde oxidase in the auxin-overproducing *superroot1* mutant of *Arabidopsis thaliana*. Plant Physiol 116:687-693.

Syono K (1979) Correlation between induction of auxin nonrequiring tobacco calluses and increase in inhibitor of IAA-destruction activity. Plant Cell Physiol 20:29-42.

Szabó M, Köves E, Stefanov I, Molnár J (1994) Auxin autotrophy of *Nicotiana tabacum* tissue cultures originating from protoplasts. Biol Plant 36 (suppl) S40 p 134.

Tari I, Csiszár J, Szalai G, Horváth F, Pécsváradi A, Kiss G, Szepesi Á, Szabó M, Erdei L (2002) Acclimation of tomato plants to salinity stress after a salicylic acid pre-treatment. Acta Biol Szeged 46:55-56.

Wightman F, Forest JC (1978) Properties of plant aminotransferases. Phytochemistry 17:1455-1471.

Zdunek-Zastocka E, Omarov RT, Koshiba T, Lips SH (2004) Activity and protein level of AO isoforms in pea plants (*Pisum sativum* L.) during vegetative development and in response to stress conditions. J Exp Bot 55:1361–1369.

Volume 51(1):53-59, 2007
Acta Biologica Szegediensis
http://www.sci.u-szeged.hu/ABS

ARTICLE

Production of indole acetic acid (bioauxin) from *Azotobacter* sp. isolate and its effect on callus induction of *Dieffenbachia maculata* cv. Marianne

Mohammed Elsayed El-Mahrouk[1]*, E B A Belal[2]

[1]Department of Horticulture, Faculty of Agriculture, Kafr El-sheikh University, Kafr El-sheikh, Egypt, [2]Department of Agriculture Botany, Faculty of Agriculture, Kafr El-sheikh University, Kafr El-sheikh,Egypt

ABSTRACT Indole-3-acetic acid (IAA) in the supernatant of a culture from the strains, *Rhizobium leguminosarum biovar viciae*, *Bradyrhizobium japonicum*, *Pseudomonas* sp. and *Azotobacter* sp was detected. *Azotobacter* sp yielded the highest concentrations of IAA. It was shown that the indole-3-acetic acid (IAA) was induced by the presence of tryptophan, which is used as inducer because the plant provide the bacteria with tryptophan under natural conditions. The highest concentration of IAA was produced by *Azotobacter* sp.(A1) at the end of the logarithmic phase (after 3days). The results obtained in this work provide useful information about the production behavior of IAA under the optimal conditions(temperature 30°C and pH 7) which is of importance for the application in production *Dieffenbachia maculat* cv. Marianne plants by using tissue culture technique. This work was also conducted to study the effect of some growth regulators such as 10 mg/l IAA (synthetic), 5 mg/l BA and 10 mg/l IAA (bioauxin) on callus formation of *Dieffenbachia maculat* cv. Marianne shoot tips and internodal segments were taken from sterilized shoot and cultured on MS medium supplemented with 6 different treatments from growth regulators. Explants cultured on MS medium supplemented with either 10 mg/l IAA +5 mg/l BA or 10 mg/l bioauxin + 5 mg/l BA had the highest callus percentage 97.22 and 93.94%, respectively. MS medium supplemented with 2 mg/l BA + 0.06 mg/l BA was used for callus differentiation.

Acta Biol Szeged 51(1):53-59 (2007)

KEY WORDS

Dieffenbachia
callus formation
indole acetic acid
bezial adenine
Azotobacter sp.

The ability to produce the plant hormone indole-3-acetic acid (IAA) is widespread among soil, epiphytic, and tissue-colonizing bacteria (Costacurta and Vanderleyden 1995; Pat-ten and Glick 1996; Barazani and Friedman 1999). These genera of bacteria comprises *Azospirillum, Azotobacter* sp *Rhizobium, Bradyrhizobium, Enterobacter, Xanthomonas, Klebsiella* sp., *Serratia* sp., *Pseudomonas* spp., cyanobacteria and sulfur oxidizing bacteria. These bacteria have shown to enhance plant growth, by promoting the out-break of secondary roots, acting as protectors against phytopathogenic microorganisms via plant hormones release and siderophores (Tien et al. 1979; Fett et al. 1987; Zimmer and Bothe 1988; Sekine et al. 1989; Minamisawa and Fukai 1991; Gamliel and Katan 1992; Amstroen et al. 1993; Bar and Okon 1993; Glick 1995; Patten and Glick 1996). Other benefits may include suppression of plant defense, which facilitates bacterial invasion (Robinette and Matthysse 1990).

Dieffenbachia maculata cv. Marianne belongs to the family Araceae, it is attractive foliage plant and is generally propagated vegetatively by cuttings. However, the traditional propagation using cutting is sometimes encountered with various difficulties such as fungal, bacterial and viral diseases (Chose 1987). Aroids show a high incidence of aberrant plants when propagated by tissue culture (Debergh and Maene 1981). Cytokinins or auxins are necessary in callus formation and differentiation. Cytokinins are used mostly for induce shoot bud induction, stimulate cell division, both formation and growth axillary and adventitious shoot in tissue culture. On the other hand, auxins are known to affect many process

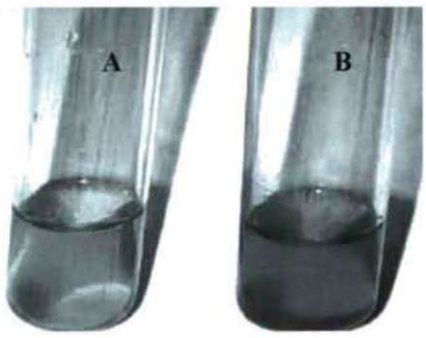

Figure 1. Production of indole-3-acetic acid by *Azotobacter* sp.(A1) , where A without tryptophan, B with tryptophan.

Accepted July 4, 2007
*Corresponding author. E-mail: threemelmahrouk@yahoo.com

Table 1. Indole -3-acetic acid concentration found in liquid medium from the cultures of the most productive strains.

Source of microorganisms	Isolates	Indole-3-acetic acid (mg /ml) Liquid medium without tryptophan	Liquid medium with tryptophan
Soil samples	*Azotobacter* sp. (A1)	-	54
	Azotobacter sp. (A2)	-	52
	Azotobacter sp. (A3)	-	48.1
	Azotobacter sp. (A4)	-	44.1
	Azotobacter sp. (A5)	-	30
	Azotobacter sp. (A6)	-	20
	Azotobacter sp. (A7)	-	16.4
	Azotobacter sp. (A8)	-	16.4
	Azotobacter sp. (A9)	-	14
	Azotobacter sp. (A10)	-	12
	Pseudomonas sp. (P1)	-	15
	Pseudomonas sp. (P2)	-	12
	Pseudomonas sp. (P3)	-	15
Root nodules	*Pseudomonas* sp. (P4)	-	7
	R. leg. biovar viciae (R1)	-	30
	R. leg. biovar viciae (R2)	-	15
	R. leg. biovar viciae (R3)	-	10
	B. japonicum (B1)	-	12
	B. japonicum (B2)	-	30
	B. japonicum (B3)	-	15

in plant including cell elongation and adventitious root formaton (Trigiano and Gray 1996). The presence of either N^6(A-isopentenyl) adenine (2ip) or kinetin in the medium was a prerequisite by Dieffenbachia for shoot formation *in Vitro* (Voyiatazi and Voyiatzis 1989) axillary meristem activation of mammillaria San-angelensis was observed only in the presence of IAA (Rubluo et al. 2002).

The aim of the present study was designed to produce of biouxin (IAA) from *Azotobacter sp.* (A1) and asses its influence on the callus induction of *Dieffenbachia* cv. Marianne

Materials and Methods

Sampling

Microorganisms were collected from rhizosphere of twenty maize plants as well as from active nodules initiated on healthy pea and soybean plants.

Microorganisms isolation and identification

Samples of 10 g of rhizosphere (roots and soil) were shaken with 90 ml of culture king's B medium to isolate *Pseudomonas* sp. Ahmad et al. (2005), Jensen's liquid medium was used for *Azotobacter* sp. (Jensen 1951). The medium was shaked at 30°C and 150 rpm for 30 min, after that dilution series were prepared in glass tube containing 9 ml from each of the used media up to 1: 10^7. One hundred µl from the three later dilution from series were spreaded on plates containing the same medium + tryptophan (0.1g/l) by using drigalisky triangle. The plates were sealed in polyethylene bags and were incubated at 30°C for 4 days monitored for appearance of colonies. Single colonies growing on these dilution plates were picked up and maintained on the same medium to use for further studies. The rhizobial isolates (*Rhizobium leguminosarum* or *Bradyrhizobium japonicum*) were isolated from nodules on Yeast extract mannitol agar (YMA) supplemented with 0.3% calcium carbonate tryptophan (0.1g/l) using the methods described by Vincent (1970), Belal et al. (1996) and El-Nady and Belal (2005). Identification of grown isolated colonies was based on morphological, biochemical and culturing characteristics according to Bergy's manual of systematic bacteriology (1984) and Somasegaran and Hoben (1985).

Indole-3-acetic acid production

IAA was obtained from *R. leguminosarum* and *B. japonicum* in YM lquid medium with 0.1 g/l tryptophan tryptophan and from *Azotobacter* sp. in Jensen's liquid medium supplemented with 0.1g/l tryptophan as well as from *Pseudomonas* sp. in King's B medium with 0.1 g/l tryptophan. All strains were incubated at 30°C and 150 rpm for 3-5 days

Colorimetric analysis

After centrifugation (6000 rpm for 30 min), supernatant was used to determine indole-3-acetic acid (IAA) by the method described by Glickman and Dessaux (1995) and Ahmad et al. (2005). The developed (30 min) color was measured by spectrophotometer at 530 nm. Concentrations were calculated from an adjusted calibration curve.

Cultivation of *Azotobacter* sp. in Jensen's liquid medium for indole-3-acetic acid production

One hundred ml of Jensen's liquid medium supplemented with tryptophan(0.1 g/l) and 1ml of a cell suspension of *Azotobacter* sp. (Jensen's broth medium, 10^7 cfu/ml, incubated at 30°C and 150 rpm for 3 days). The culture was incubated at 30°C and 150 rpm for 3 days. The production of indole-3-acetic acid was determined daily by the described method (Ahmad et al. 2005). The growth representing in intracellular protein content for bacterial isolate was determined in each treatment as intracellular protein content (µg/ml). The bacteria cells were digested as described by Belal (2003) and the protein content was determined according to the method described by Lowry et al. (1951) using bovine serum albumin as standard protein.

Effect of pH and temperature on production of indole-3-acetic acid by *Azotobacter* sp.(A1)

One hundred ml of Jensen's liquid medium supplemented with 0.1 g/l tryptophan was used to determine the effect of

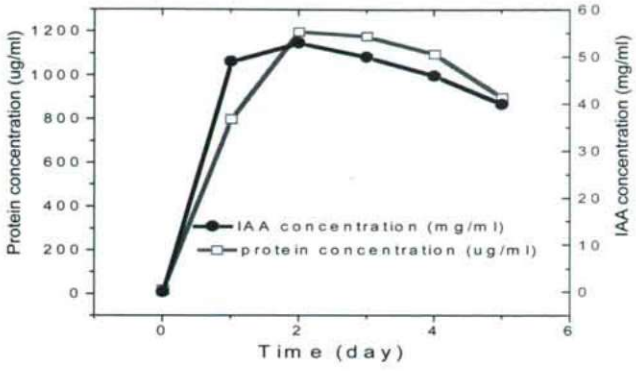

Figure 2. IAA production by *Azotobacter* sp. (A1) isolate in submerged culture with tryptophan.

temperature and pH on production of indole-3-acetic acid by *Azotobacter* sp.(A1).The medium was inoculated by 1ml (10^8 cfu/ml) of culture of *Azotobacter* sp.(A1) strain. The experiments were carried out at pH 6, 7 and 8 and the culture was incubated at 30°C and 150 rpm for 3 days. To determine the optimum temperature Ashby broth medium at pH 7 was incubated at 20, 30 and 40°C and 150 rpm for 3 days.

Callus induction

Shoot tips and internodal segments of Marianne cv. plants were used for callus induction. Surface sterilization was carried out by washing explants thoroughly with mild liquid detergent under a running tap water for 30 min. Then, under cabinet laminar flow, the explants were surface sterilized by dipping in 70% alcohol (ethanol) for two min. and later in 0.1% mercuric chloride with a few drops of wetting agent Tween-20 for 20 min. After sterilization, explants were rinsed four times with a sterilized water, 5 min for each time (Dodds and Roberts 1985; Kyte 1987 and Torres 1989). The sterilized explants were gently held with a fine forceps. Shoot tips and internodal segments of Marianne cv. plants were cultured on MS medium supplemented with 6 different treatments from growth regulators (BA, IAA and bioauxin) as follows:

Control (free growth regulator)
10 mg/l (synthetic) IAA
5 mg/l BA
10 mg/l (bioauxin) IAA
10 mg/l (synthetic) IAA + 5 mg/l BA
10 mg/l (bioauxin) IAA + 5 mg/l BA.

The medium pH was adjusted to 5.7 with 1N NaOH and 1N HC after activated charcoal at 2 g/l was added. Agar (8 g/l) was added before autoclaving. The medium was autoclaved for 15 min. at 121°C and 1.1 kg/cm^2, after that 15 ml medium was dispensed into sterilized Petri-dishes (7 cm). The experiment included 6 different treatments. Each treatment consisted of 8 Petri-dishes in a randomized complete design. The cultures were incubated under dark condition at 26 ± 2°C for two months, where the explants were subcultured after one month. The following data were recorded after two months of culture:

Callus frequency percentage
Callus fresh weight (g)
Callus diameter (cm).

Data were tested by analysis of variance and Dancan's multiple range test was used for the comparison among the treatment means (Duncan 1955).

Callus differentiation

The derived callus from the 6 different treatments of induction medium were cultured on the differentiation medium supposed by (Chamail et al. 1999) which consisted of MS basal nutrient medium supplemented with BA at 2 mg/l and IBA at 0.06 mg/l for one month. The cultures were incubated under light intensity 2000 Lux for 16 hrs photoperiod at 25 ± 2°C. After one month of culture on differentiation medium, callus were transferred to MS hormones free medium for two months. Number of plantlets/callus was recorded.

Analysis of data

Data were tested by analysis of variance and Duncan's multiple range test was used for the comparison among the treatment means (Duncan 1955).

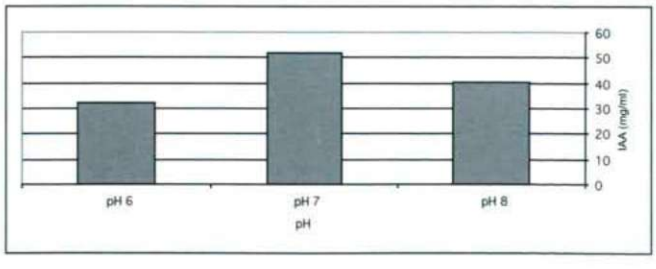

Figure 3. Effect of pH on production IAA by *Azotobacter* sp. (A1).

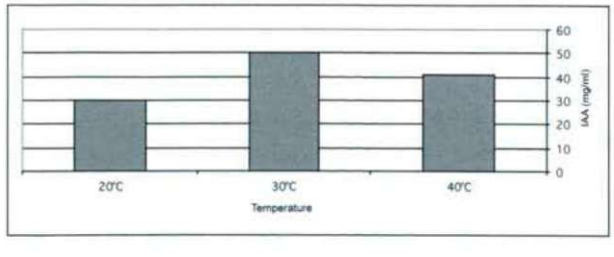

Figure 4. Effect of Temperature on production IAA by *Azotobacter* sp. (A1).

Results and Discussion

Isolation of indole -3-acetic acid producing by bacterial isolates

Two different sources used to isolate the IAA - producing isolates were evaluated in the present work. The first source was soil maize rhizosphere samples which were collected from different locations in Kafr El-Sheikh Governorate, Egypt. The second source was active nodules initiated on healthy pea and soybean plants. By using specific medium supplemented with tryptophan (0.1 g/l) for each isolates, a total of 20 morphologically different microorganisms were isolated from the both described microbial sources. Fourteen of 20 bacterial isolates were isolated from soil samples. Ten of 20 bacterial isolates belong to the genus *Azotobacter* and 4 of 20 belong to genus *Pseudomonas*. Six of 20 were isolated from nodules where 3 isolates belong to *Rhizobium leguminosarum biovar viciae* (isolated from pea plants) and the other third isolates belong to *Bradyrhizobium japonicum* (isolated from soybean plants; Tables 1). All twenty treated strains (10 *Azotobacter* sp., 4 *Pseudomonas* sp., 3 *R. leguminosarum biovar viciae* and 3 *B. japonicum*) in a culture medium containing tryptophan as inducer for IAA, produced IAA, as detected by Glickmann and Dessaux (1995), while the same strains did not produce IAA in the same medium without tryptophan. Most species use tryptophan to produce indole-3-acetic acid (IAA), mainly through the indole-3-pyruvic acid and tryptamine pathways (Bar and Okon 1993). Figure 1 shows samples of the attained solutions of this compound. The highest concentration of IAA was obtained from *Azotobacter* sp. which was designated as (A1).

The strain *Azotobacter* sp. (A1) was selected to characterize the production of IAA and the growth patterns as well as to investigate the effects of the pH and temperature on production of IAA.

Figure 2 illustrates that IAA formation started when the organism grew on the medium supplemented with tryptophan. The highest accumulation of IAA exhibited in the 48th hours of cultivation. The maximum accumulation of IAA occurred at the end of logarithmic phase, and after that the accumulation of IAA decreased at the beginning of the stationary growth phase. IAA accumulation coincided with increase in the specific growth rates of the cultures.

Effect of pH and temperature on production of indole-3-acetic acid by *Azotobacter* sp. (A1) isolate

Normally, the pH and temperature influence the growth of microorganisms and hence, these factors will influence also the production of IAA. The question is now, what are the optimal conditions (pH and temperature) for production of IAA by *Azotobacter* sp. (A1) isolate?

The influence of pH on biomass yield of the selected isolates is shown in Figure 3. As expected that the optimum pH was 7. The maximum of IAA yield production by *Azotobacter* sp. (A1) isolate was recorded at pH7. This bacterial isolate can grow at range from pH6-8.

The effect of different temperatures on production of IAA by *Azotobacter* sp. (A1) is shown in Figure 4. A temperature 30°C appears to be the optimal for production of IAA by the bacterial isolate. Therefore, the produced indole-3-acetic acid by this isolate at the optimum conditions (pH, temperature, at the end of logarithmic phase) was used for callus induction of *Dieffenbachia* cv. Marianne by using tissue culture technique rather than using synthetic IAA.

Our results are in agreement with previous findings reported by (Ernsten et al. 1987; Fukuhara et al. 1994; Glickmann and Dessaux 1995 and Torres-Rubio et al. 2000), who found that an addition of tryptophan in the growth medium led to production of IAA by many bacterial strains. Several different IAA biosynthetic pathways are used by prokaryotes, and a single bacterial strain can contain more than one pathway. Indole –3-acetic acid (IAA) biosynthetic pathways detected in *Erwinia herbicola pv.gypsophilae*. iaaM, iaaH, and ipdC are genes encoding tryptophan-2-monoxygenase, indole-3-acetamide hydrolase, and indole-3-pyruvate decarboxylase, respectively (Manulis et al. 1998).

Callus frequency percentage

Data presented in Table 2 and Figure 5 show that the difference among different growth regulators treatment were highly significant on callus frequency percentages. Explants grown on MS medium supplemented with 10 mg/l IAA + 5 mg/l BA gave the highest callus frequency percentage (97.22%) followed by explants grown on MS medium supplemented with 10mg/l bioauxin + 5 mg/l BA which produced (93.94%), while the control treatment (MS free medium) produced the fewest callus frequency percentage (34.52%). This due to

Table 2. Effect of growth regulators on callus induction and plantlets regeneration from *Dieffenbachia maculate* cv. Marianne.

Treatment	% Callus frequency	Callus fresh weight (g)	Callus diameter (cm)	Number of plantlet/callus
Free MS-medium (Control)	34.52 c	0.045	0.37 b	2.3 d
10 mg/l IAA	80.36 b	0.16	0.47 ab	7.5 c
5 mg/l BA	83.16 b	0.21	0.60 a	8.0 b
10 mg/l bioauxin	80.73 b	0.21	0.52 ab	8.5 b
10 mg/l IAA+ 5mg/l BA	97.22 a	0.14	0.59 a	10.67 a
10 mg/l bioauxin + 5 mg/l BA	93.94 ab	0.11	0.53 a	10.33 a
	**	n.s	**	**

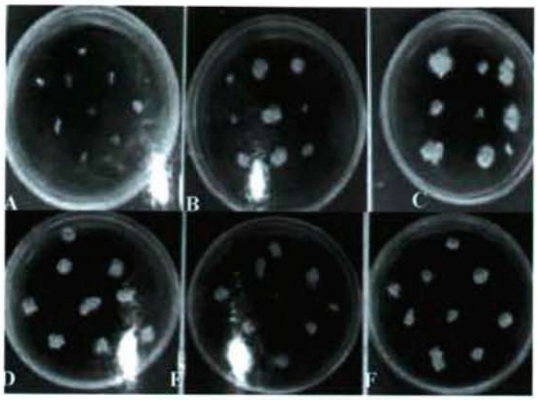

Figure 5. Callus formation of *D. maculata* cv. Marianne as affected by the different treatment after two months. A- control (MS free), B- MS with 10 mg/l IAA, C- MS with 5 mg/l BA, D- MS with10 mg/l bioauxin, E- MS with 10 mg/l IAA + 5 mg/l BA, F- MS with 10 mg/l bioauxin + 5 mg/l BA A.

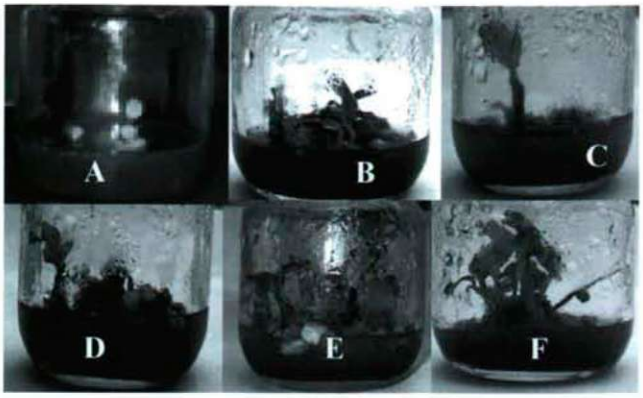

Figure 7. Regeneration plantlets of *D. maculata* cv. Marianne from callus on free -MS medium. A- control (MS free), B- MS with 10 mg/l IAA, C- MS with 5 mg/l BA, D- MS with10 mg/l bioauxin, E- MS with 10 mg/l IAA + 5 mg/l BA, F- MS with 10 mg/l bioauxin + 5 mg/l BA.

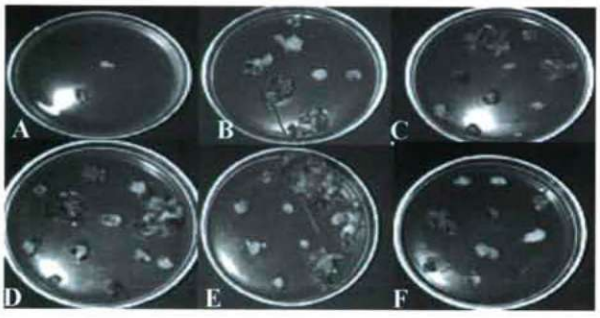

Figure 6. Plantlets formation of *D. maculata* cv. Marianne from callus on the differentiation medium. A- control (MS free), B- MS with 10 mg/l IAA, C- MS with 5mg/l BA, D- MS with10mg/l bioauxin, E- MS with 10 mg/l IAA + 5 mg/l BA, F- MS with 10 mg/l bioauxin + 5 mg/l BA A.

balance between auxin and cytokinin in the medium was nessacery for callus induction. It is evident that exogenous auxin is the most important growth regulator for the induction of embryogenic callus in the majority of angiosperms (Roy and Banerjee 2003). Also, as observed in the present study, *Dieffenbachia maculata* cv. Marianne requires supplementary cytokinin with auxin for optimum response of callus initiation. This requirement for exogenous cytokinin could be related to the maintenance of a proper balance between auxin and cytokinin, which acts synergistically to regulate cell division (Johri and Mitra 2001) a process essential for callus formation.

These results are in harmony with those obtained by Jain et al. (2002) on *Phlox paniculata* Linn., who found that, the intensity of callus proliferation was greater in the medium with BA in combination with IAA. Suthamathi et al. (2002) on papaya obtained the maximum callus induction from shoot tip with 10 mg/l NAA and 4.5 mg/l BA. Chamail et al. (1999) on *Actinidia deliciosa* found that, the best callus induction was obtained when BA (1.5 mg/l) was used in combination 1 mg/l NAA.

Callus fresh weight

Concerning the effect of growth regulators on the average callus fresh weight, there were no significant differences as shown in Table 2, but explants grown on MS medium supplemented with 5 mg/l BA or 10 mg/l bioauxin gave the highest callus fresh weight (0.21 g) followed by explants grown on MS medium supplemented with 10 mg/l IAA which produced 0.16 g for callus fresh weight. The variation might be due to endogenous levels of growth regulator (Kumar et al. 2001). The effect of growth regulator on tissue cultures can vary according to the chemical nature of the compound, plant species, type of the culture and even the developmental state of the explant (Lakshmanan et al. 2002). The obtained results were similar to those of Parthasarathy and Nagaraja (1999) on *Gerbera jamesonii* found that maximum callus weight was observed at 1.0 mg/l BAP.

Callus diameter

Regarding the effect of growth regulators on callus diameter, Data in Table 2 show that highly significant increase in callus diameter was recorded among the used treatments. Explants cultured on MS medium supplemented with 5 mg/l BA, 10 mg/l IAA + 5 mg/l BA and 10 mg/l bioauxin + 5 mg/l BA produced the biggest callus diameter with 0.60, 0.59 and 0.53 cm, respectively, while the control medium produced the smallest callus diameter 0.37 cm. Similar observation that the intensity of callus proliferation was greater in the medium with BA in combination with IAA for *Phlox paniculata* Linn and the response of callus production was more dependent on different concentration of BA and IAA than on the type

of explant source used (Jain et al. 2002). Induction of callus took place in the treatments that included NAA but the frequency was very low and the addition of BA was required for improved response (Roy and Banerjee 2003).

Number and plantlets/callus

Data in Table 2 and Figs (7 and 8) shown that there were highly significant differences in the number of plantlets/callus in differentiation medium (2 mg/l BA + 0.06 mg/l IBA). This may be due to the effect of induction medium. The largest number of plantlets/callus (10.67 and 10.33) resulted from callus was derived from induction medium consist of MS medium supplemented with 10 mg/l IAA + 5 mg/l BA and 10 mg/l bioauxin + 5 mg/l BA, respectively. In the present study, it was also observed that for callus differentiation, both of concentrations BA and IBA were essential to bring out the desirable change in callus differentiation rate. It is well known that for organogenesis, a proper balance between cytokinin and auxin is essential (Chamail et al. 1999). Similar results were reported by Chamail et al. (1999) on *Actinidia deliciosa* who found that 2 mg/l BA + 0.06 mg/l IBA was the best combination for producing maximum average number of shoots per callus.

In conclusion, induction of callus from shoot tips and internodal segments of *Dieffenbachia maculata* cv. Marianne occurred on different media but the presence of BA with auxin was essential for improved response. Also, the effect of bioauxin was similar to that of synthetic IAA on callus induction and regeneration.

References

Ahmad F, Ahmad I, Khan MS (2005) Indole acetic acid production by the indigenous isolates of azotobacter and fluorescent pseudomonas in the presence and absence of tryptophan. Turk J Biol 29:29-34.

Amstroen B, Gustafsson A, Gerhardson B (1993) Characteristics of a plant deleterious rhizosphere pseudomonad and its inhibitory metabolites. J Appl Bacteriol 74:20-28.

Bar T, Okon Y (1993) Tryptophan conversion to indole-3-acetic acid via indole-3-acetamide in *Azospirillum brasilense* Sp7. Can J Microbiol 39:81-86.

Barazani O, Friedman J (1999) Is IAA the major root growth factor secreted from plant-growth-mediating bacteria. J Chem Ecol 25:2406.

Belal EBA (2003) Investigation on the biodegradation of polyesters by isolated mesophilic microbes. Dissertation, Technical University Braunschweig, Germany.

Belal EBA, El-Gremi S, Gabr M, Ibrahim M (1996) Using of peat-based inoculate of selected antagonists against certain soil-borne pathogens of pea in the presence of Rhizobium leguminosarum. J Agric Res Tanta Univ 22 (4):444-450.

Bergys manual of systematic bacteriology (1984) Williams and Wilkins, Baltimore, USA. Vol. 1. Krieg NR (ed). Ordinary gram negative bacteria. Vol. 2. Sneath P h. A (ed.) Ordinary gram positive bacteria.

Chamail A, Kumar S, Sharma DR, Chander S (1999) Regeneration of kiwi fruit (*Actinidia deliciosa*) cv. Hayword from leaf callus. Indian J Hort 56 (4):179-285.

Chose AR (1987) Compendium of ornamental foliage plant disease p.g. The American Phytopathological Society Press, Minnesota USA.

Costacurta A, Vanderleyden J (1995) Synthesis of phytohormones by plant associated bacteria. Crit Rev Microbiol 21:1-18.

Debergh PC, Maene LJ (1981) A scheme for commercial propagation of ornmental plants by tissue culture. Sci Hortic 14:335-245.

Dodds JH , Roberts L W (1985) Experiments in plant tissue culture.2nd ed. Cambridge Univ Press, Cambridge UK.

Duncan DB (1955) Multiple range and multiple F. test. Biometrics 11: 1-42.

El-Nady MF, Belal EBA (2005) Responses of faba bean (*Vicia faba* L.) plants to root nodule bacteria under salinity conditions. J Agric Res Tanta Univ 31(3):362-374.

Ernsten A, Sandberg G, Crozier A, Wheeler CT (1987) Endogenous indoles and the biosynthesis and metaboism of indole-3-acetic acid in cultures of *Rhizobium phaseoli*. Planta 171:42-428.

Fett WF, Osman SF, Dunn MF (1987) Auxin production by plant pathogenic pseudomonads and xanthomonads. Appl Environ Microbiol 53:1839-1845.

Fukuhara H, Minakawa Y, Akao S, Minamisawa K (1994) The involvement of indole-3-acetic acid produced by *Bradyrhizobium elkanii* in nodule formation. Plant Cell Physiol 35:1261-1265.

Gamliel A, Katan J (1992) Influence of seed and root exudates on fluorescent *Pseudomonas* and fungi in solarized soil. Ecol Epidemiol 82:320-327.

Gamliel A, Katan J (1992) Chemotaxis of fluorescent *Pseudomonas* towards seed exudates and germinating seeds in solarized soil. Ecol Epidemiol 82:328-332.

Glick BR (1995) The enhancement of plant growth by free living bacteria. Can J Microbiol 41:109-114.

Glickmann F, Dessaux Y (1995) A critical examination of the specificity of the salkowski Reagent for indolic compounds produced by phytopatogenic bacteria. Appl Environ Microbiol 61(2):793-796.

Jain A, Rout GR, Raina SN (2002) Somatic embryogenesis and plant regeneration from callus cultures of *Phlox paniculata* L. Sci Hortic 94:137-143.

Jensen HL (1951) Notes on the biology of Azotobacter. Proc Soc Appl Bacteriol 14:84-103.

Johri MM, Mitra D (2001) Action of plant hormones. Curr Sci 80:199-202.

Kumar K, Dhatt AS, Gill MIS (2001) In vitro plant regeneration in sweet orange (*Citrus sinenesis L. Osbeck.*) cv. Mosambi and Jaffa. Indian J Hort 58(3):208-211.

Kyte L (1987) In Plants from Test Tubes-An. Introduction to micropropagation (revised edition). Timber Press Oregon USA, Chapter 11:20-35.

Lakshmanan P, Danesh M, Taji A (2002) Production of four commercially cultivated Echinacea species by different methods of in vitro regeneration. J Hort Sci Biotech 77(2):158-163.

Lowry OH, Rsebrough NJ, Farr AL, Rundal RL (1951) Protein measurements with the folin phenol reagent. J Biol Chem 193:265-275.

Manulis S, Haviv-Chesner A, Brandl MT, Lindow SE, Barash I (1998) Differential involvement of indole-3-acetic acid biosynthetic pathways in pathogenicity and epipytic fitness of *Erwinia herbicola pv. Gypsophilae*. Mol Plant-Microbe Interact 11(7):634-642.

Minamisawa K, Fukai K (1991) Production of indole-3-acetic acid by *Bradyrhizobium japonicum*: A correlation with genotype grouping and rhizobitoxine production. Plant Cell Physiol 32(1):1-9.

Patten CL, Glick BR (1996) Bacterial biosynthesis of indole-3-acetic acid. Can J Microbiol 42:207-220.

Robinette D , Matthysse AG (1990) Inhibition of *Agrobacterium tumefaciens* and *Pseudomonas savastanoi* of development of the hypersensitive response elicited by *Pseudomonas syringae* pv. *phaseolicola*. J Bacteriol 172:5742-159.

Rubluo A, Marin-Hernandez T, Duval K, Vargas A, Marquez-Guzman J (2002) Auxin induced morphogenetic responses in long-term *in vitro* subcultured *Mammillaria sanangelensis* Sanchez-Mejorada (Cactaceae). Sci Hortic 95(4):341-349.

Somasegaran P, Hoben MJ (1985) Methods in legume Rhizobium technology. Prepared under USA Agency for international development.

Sekine M, Watanable K, Syono K (1989) Molecular cloning of a gene for indole-3-acetamide hydrolase from *Bradyrhizobium japonicum*. J

Bacteriol 171:1718-1724.

Tien T, Gaskins M, Hubbel D (1979) Plant growth substances produced by *Azospirillum brasilense* and their effect on the growth of Pearl Millet (*Pennisetum americanum* L.). Appl Environ Microbiol 37:1016-1024.

Torres-Rubio MG, Valencia-Plata SA, Bernal-Castillo J, Martinez-Nieto P (2000) Isolation of Enterobacteria, *Azotobacter* sp. and *Pseudomonas* sp., producers of indole-3-acetic acid and siderophores, from Colombian rice rhizosphere. Rev Latinoam Microbiol 42:171-176.

Vincent JM (1970) A manual for the practical study of root-nodule bacteria. IBP handbook No 15 Blackwell Scientific Publications, Oxford and Edinburgh.

Zimmer W, Bothe H (1988) The phytohormonal interaction between *Azospirillum* sp. and wheat. Plant Soil 110:239-247.

Volume 51(1):61-64, 2007
Acta Biologica Szegediensis
http://www.sci.u-szeged.hu/ABS

ARTICLE

RAPD analysis of eleven iranian pomegranate (*Punica granatum* L.) cultivars

Masoud Sheidai[1]*, Z Noormohammadi [2], A Saneghi[1], ZH Shahreiyari[1]

[1]Faculty of Biology Sciences, Shahid Beheshti University, Tehran, Iran, [2]Tarbiat Modarres University, Tehran, Iran

ABSTRACT RAPD markers variations were studied in eleven pomegranate cultivars. Fifteen RAPD primers used out of which 13 primers could produce bands. In total 173 bands were produced out of which 73 bands were common in all the cultivars while 6 bands were specific, which may be used in the cultivars discrimination. Primers OPB12 and OPA13 produced the highest number of polymorphic bands (12 bands out of 16 = 0.75% and 11 bands out of 25 = 0.44), while primers OPR15 and OPA15 produced the least number of polymorphic bands (2 out of 12 = 0.16%). Different similarity coefficients determined among the cultivars studied, showed the highest value of similarity between cultivars Khatooni and Anbari as well as between Khatooni and Atabaki (r = 0.94) while the lowest value of similarity occurred between the cultivars Sefid and Bihaste as well as Sefid and Khatooni (r = 0.62). Different clustering methods showed distinctness of the olive cultivars studied. **Acta Biol Szeged 51(1):61-64 (2007)**

KEY WORDS

clustering
pomegranate
RAPD

The pomegranate (*Punica granatum* L.) is native from Iran to the Himalayas in northern India, cultivated over the whole Mediterranean region since ancient times (Facciola 1990) and is one of the most important endemic horticultural plants of Iran. About 550000 hectare of lands has been devoted to the cultivation of pomegranate in Iran producing about 570000 tones of pomegranate fruit.

In total 764 cultivars of *P. granatum* have been collected during a germplasm collection in Iran and grown in Saveh and Yazd cities, all of which possess their specific fruit characteristic such as size, color, time of ripening, disease resistance, taste, etc. In spite of grate economic importance of pomegranate cultivars in Iran, there have been very limited cytogenetic and genetic studies in them (Gill et al. 1981; Xue et al. 1992; Zhao and Pan 2004; Sheidai and Noormohammadi 2005; Sheidai et al. 2005; Sheidai et al. 2007; Zamani et al. 2007).

Different molecular markers including RAPD (Random Amplified Polymorphic DNA) have been used in the study of genetic diversity as well as cultivar identification in several plant species (Weising et al. 2005). These molecular markers provide an opportunity for direct comparison and identification of different genetic material independent of any influences (Harvey and Botha 1996; Bautista et al. 2003).

Pomegranate cultivars are grown in different parts of Iran and cultivation of the same cultivars for long period of time may lead to the genetic erosion confining the subsequent breeding programs. Therefore it is necessary to study the available diversity and introduce new variability as well. For this reason, the present study considers RAPD molecular analysis of 11 pomegranate cultivars of Iran for the first time.

Materials and Methods

Eleven pomegranate cultivars were used for cytogenetic and molecular studies. For RAPD analysis, fresh leaves were selected (0.1 gr) randomly from 3-5 plants of each cultivar and DNA extraction was done by use of NucleoSpin Plant kit (Macherey-Nagel, Germany). The PCR reaction mixture consisted of 1 ng template DNA, 1 x PCR buffer (10 mM Tris-HCl pH 8.8, 250 mM KCl), 200 µM dNTPs (dineuclotide triphosphosphate), 0.80 µM 10-base random primers (Operon Technology, California, USA) and 1 unit of Taq polymerase (Cinagene Co., Iran), in a total volume of 25 µl. DNA amplification was performed on a palm cycler GP-001 (Corbet, Australia). Template DNA was initially denatured at 92°C for 3 min, followed by 35 cycles of PCR amplification under the following parameters: denaturation for 1 min at 92°C, primer annealing for 1 min at 36°C and primer extension for 2 min at 72°C. A final incubation for 10 min at 72°C was performed to ensure that the primer extension reaction proceeded to completion. The PCR amplified products were separated by electrophoresis on a 2% agarose gels (Merck) using 0.5 X TBE buffer (44.5 mM Tris/Borate, 0.5 mM EDTA, pH 8.0) or 12% polyacrylamide geles. The geles were stained with ethidium bromide and visualized under UV light or silver stained for added sensitivity. RAPD markers were named by primer origin, followed with the primer number and the size

Accepted August 27, 2007
*Corresponding author. E-mail: msheidai@sbu.ac.ir

Table 1. Specific RAPD primers in pomegranate cultivars.

Cultivars	OPB12-12	OPA15-12	OPA18-5	OPA13-8	OPA13-12	OPA13-20
1-Pustsiah Ardestan	0	0	0	0	0	0
2- Pustsefid Shomal	0	0	0	0	1	1
3- Anbari daneghermeze	0	0	1	1	0	0
4- Atabaki Jahrom	0	0	0	0	0	0
5- Meykhosh pustghermez	0	0	0	0	0	0
6- Bihaste Ardestan	1	1	0	0	0	0
7- Shirinnar Pave	0	0	0	0	0	0
8- Goltorsh Taft	0	0	0	0	0	0
9- Khatooni daneghermez	0	0	0	0	0	0
10- Dadashi Ashkezar	0	0	0	0	0	0
11- Pustsiah Ashkezar	0	0	0	0	0	0

of amplified products in base pairs. Fifteen random primers of Operon technology (Alameda, Canada) were used.

RAPD bands were treated as binary characters and coded accordingly (presence =1, absence = 0). Simple matching coefficient and Jaccard coefficients were determined among the cultivars studied and grouping of the genotypes was determined by using different clustering methods and ordination based on principal coordinate analysis (PCO; Ingrouille 1986; Chatfield and Collins 1995). Cophenetic correlation was determined for different clustering methods. NTSYS Ver. 2.02 (1998) was used for clustering and PCO analyses.

Results and Discussion

The RAPD experiment was repeated 3 times and the well reproduced bands were scored for further analysis. The results of RAPD analysis of 11 pomegranate cultivars are presented in Tables 1-3 and Figs 1-3. Fifteen RAPD primers used out of

Table 2. The RAPD bands missing only in one pomegranate cultivars.

Cultivars	OPB12-11	OPB12-13	OPB07-3	OPA15-8	OPA18-2	OPA04-1	OPA04-3	OPA04-4	OPA04-5
1-Pustsiah Ardestan	1	1	1	1	1	1	1	1	1
2- Pustsefid Shomal	0	0	1	0	0	0	0	0	0
3- Anbari daneghermeze	1	1	1	1	1	1	1	1	1
4- Atabaki Jahrom	1	1	1	1	1	1	1	1	1
5- Meykhosh pustghermez	1	1	1	1	1	1	1	1	1
6- Bihaste Ardestan	1	1	1	1	1	1	1	1	1
7- Shirinnar Pave	1	1	1	1	1	1	1	1	1
8- Goltorsh Taft	1	1	1	1	1	1	1	1	1
9- Khatooni daneghermez	1	1	1	1	1	1	1	1	1
10- Dadashi Ashkezar	1	1	0	1	1	1	1	1	1
11- Pustsiah Ashkezar	1	1	1	1	1	1	1	1	1

Cultivars	OPA04-11	OPB05-6	OPB05-9	OPB05-1	OPB12-12	OPA15-12	OPA18-5	OPA13-8	OPA13-12	OPA13-20
1	1	1	1	1	0	0	0	0	0	0
2	0	1	1	1	0	0	0	0	1	1
3	1	1	1	1	0	0	1	1	0	0
4	1	1	1	1	0	0	0	0	0	0
5	1	0	0	0	0	0	0	0	0	0
6	1	1	1	1	1	1	0	0	0	0
7	1	1	1	1	0	0	0	0	0	0
8	1	1	1	1	0	0	0	0	0	0
9	1	1	1	1	0	0	0	0	0	0
10	1	1	1	1	0	0	0	0	0	0
11	1	1	1	1	0	0	0	0	0	0

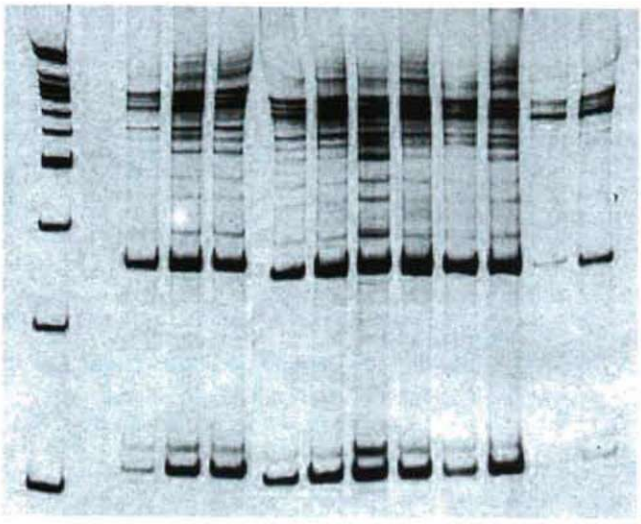

Figure 1. RAPD profile of pomegranate cultivars by primer OPR12. (Columns from right to left: pomegranate cultivars as in Table 1, No DNA and Molecular marker.

which 13 primers produced 173 bands in total. All 13 primers produced polymorphic bands. Seventy-three bands (loci) were present in all the cultivars studied and may be considered as the common bands in pomegranate cultivars. Six RAPD loci were specific in some of the cultivars which may be used in the cultivars discrimination. For example, OPA05-12 and OPB12-12 loci were present only in the cultivar Bihaste, while OPA13-8 and OPA18-5 loci were present only in the cultivar Anbari. The OPA-13-12 and OPA-13-20 loci were present only in the cultivar Sefid. The presence of specific loci indicates the genetic distinctness of the pomegranate cultivars studied.

Table 3. Jaccard similarity among pomegranate cultivars. (Cultivars number as in Table 1).

Cultivars	1	2	3	4	5	6	7	8	9	10	11
1	1.00										
2	0.75	1.00									
3	0.75	0.64	1.00								
4	0.76	0.66	0.94	1.00							
5	0.73	0.65	0.85	0.85	1.00						
6	0.72	0.62	0.87	0.89	0.84	1.00					
7	0.77	0.64	0.87	0.90	0.82	0.85	1.00				
8	0.72	0.67	0.88	0.89	0.82	0.84	0.91	1.00			
9	0.72	0.62	0.91	0.91	0.82	0.87	0.89	0.90	1.00		
10	0.70	0.66	0.82	0.83	0.78	0.80	0.80	0.86	0.84	1.00	
11	0.74	0.63	0.85	0.84	0.75	0.81	0.83	0.85	0.87	0.80	1.00

The primers OPB12 and OPA13 produced the highest number of polymorphic bands (12 bands out of 16 = 0.75% and 11 bands out of 25 = 0.44), while the primers OPR15 and OPA15 produced the least number of polymorphic bands (2 out of 12 = 0.16%).

There were 16 loci which were missing only in one cultivar; such loci may also be of use in the pomegranate cultivar differentiation. For example OPB07-3 loci was present in all pomegranate cultivars except the cultivar Bihaste, while the bands OPB05-1, 6 and 9 were absent only in the cultivar Meykhosh. The other 12 loci were absent only in the cultivar Sefid.

Different similarity coefficients determined among the cultivars studied, showed the highest value of similarity between cultivars Khatooni and Anbari as well as between Anbari and Atabaki (for example r = 0.94 in Jaccard similarity) while the lowest value of similarity occurred between the cultivars Pustsefid and Bihaste as well as Pustsefid and Khatooni (for example r = 0.62 in Jaccard similarity).

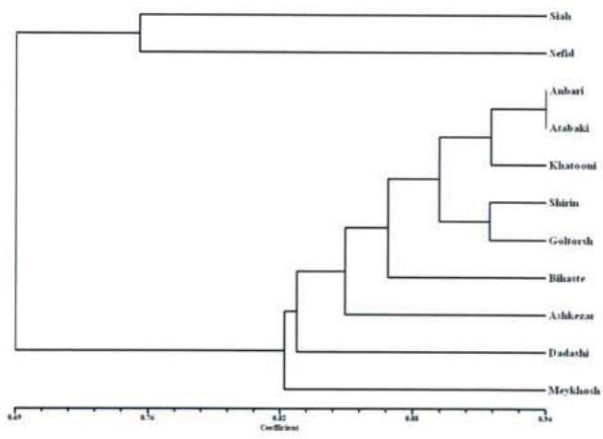

Figure 2. UPGMA clustering of pomegranate cultivars based on RAPD markers.

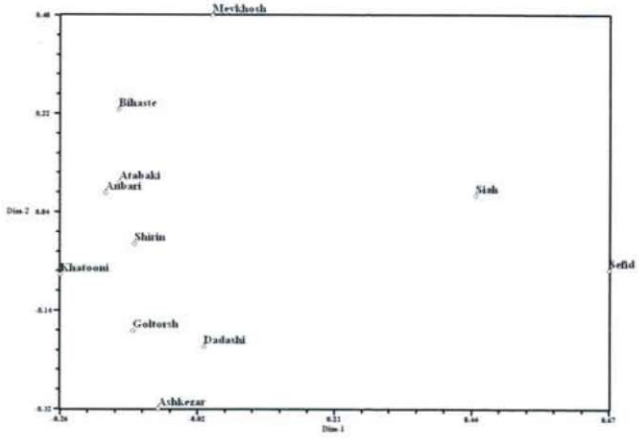

Figure 3. PCO ordination of pomegranate cultivars based on RAPD markers.

Different clustering methods showed distinctness of the olive cultivars studied, for example, UPGMA (unweighted paired group with arithmetic average), single linkage and complete linkage methods using the Jaccard similarity and Nei and Li coefficients produced similar results, supported by PCO ordination of the cultivars (Figs. 2 and 3). The cophenetic correlation determined showed the highest value for UPGMA method (r = 0.92), indicating a good fit of clustering to the original similarity of the cultivars. Therefore the result of UPGMA clustering along with PCO ordination is discussed bellow.

In general two major clusters or groups are formed (Figs. 2 and 3). The first major cluster is comprised of the cultivars Pustsiah and Pustsefid which are placed far from the other pomegranate cultivars. The second major cluster or group is comprised of the other cultivars joined each other with grate distances. Among these the cultivars Anbari and Atabaki show more similarity and along with Khatooni form the first subcluster, while Shirinnar and Goltorsh cultivars form the second sub-cluster, joined to the members of the first sub-cluster with some distance. The other cultivars join this cluster step by step, out of which the cultivar Meykhosh differs the most and join with a grater distance to the other cultivars.

In general, the present study shows the usefulness of RAPD analysis in distinguishing the pomegranate cultivars, particularly identification of the specific bands may be considered important in the pomegranate cultivar identification. If RAPD diversity is combined with fruit and other important agronomic characteristics, performing the similar studies on the other pomegranate genotypes may lead to planning of a better breeding program in the country.

References

Bautista R, C´anovas FM, Claros MG (2003) Genomic evidence for a repetitive nature of the RAPD polymorphisms in *Olea europaea* (olive-tree). Euphytica 130:185–190.

Chatfield C, Collins AJ (1995) Introduction to Multivariate Analysis. Chapman & Hall, London.

Facciola S (1990) Cornucopia: a source book of edible plants. Kampong Publications 166-167.

Gill B, Bir SS, Bediy S (1981) Cytological studies on woody Euphorbiaceae from North and Central India. New Botanist 8:35-44.

Harvey M, Botha FC (1996) Use of PCR-based methodologies for the determination of DNA diversity between *Saccharum* varieties. Euphytica 89:257-265.

Raman VS, Manimekaliai G, Sreerangaswamy SR (1971) Chromosome behavior at meiosis in *Punica granatum* L. Cytologia 36:400-404.

Sheidai M, Noormohammadi Z (2005) Chromosome pairing and unreduced gamete formation in nineteen pomegranate (*Punica granatum* L.) cultivars. Cytologia 70(3):257-265.

Sheidai M, Khandan M, Nasre-Esfahani Sh (2005) Cytogenetical study of some Iranian pomegranate (*Punica granatum* L.) cultivars. Caryologia 58(2):132-139.

Sheidai M, Khandan M, Nasre-Esfahani Sh (2007) B-chromosomes in Iranian pomegranate (*Punica granatum* L.) cultivars. Caryologia (in press).

Ingrouille MJ (1986) The construction of cluster webs in numerical taxonomic investigations. Taxon 35:541-545

Weising K, Nybom H, Wolf K, Kahl G (2005) DNA fingerprinting in plants. Principles, Methods, and Applications. Second Edit., Taylor and Francis, New York.

Xue BS, Weng RF, Z-Zhang M (1992) Chromosome numbers of Shanghai plants I. Investigatio et Studium Naturae 12:48-65.

Zamani Z, Sarkhosh A, Fatahi R, Ebadi A 2007. Genetic relationships among pomegranate genotypes studied by fruit characteristics and RAPD markers. J Hort Sci Biotech 82(1):11-18.

Zhao W, Pan Y (2004) Genetic diversity of genus morus revealed by RAPD Markers. Int J Agri Biol 6(6):950-956.

Volume 51(1):65-80, 2007
Acta Biologica Szegediensis
http://www.sci.u-szeged.hu/ABS

ARTICLE

Floristic analysis and biogeography of Tubiflorae in Egypt

Nahed El-Husseini[1], Monier M Abd El-Ghani[1]*, Salah I El-Naggar[2]

[1]The Herbarium, Faculty of Science, Cairo University, Giza, Egypt, [2]Botany Department, Faculty of Science, Assiut University, Egypt

ABSTRACT The species distribution and biogeography of the Egyptian Tubiflorae were examined in detail. We found 284 species of vascular plants belonging to 96 genera and 12 families, making the Egyptian Tubiflorae richer in species than that of other arid region floras: Libya and Saudi Arabia. The most species rich families were Scrophulariaceae, Boraginaceae, Labiatae, Convolvulaceae and Solanaceae, constituting more than 85% of the total species in the order. The generic spectrum dominated by a suite of species-rich genera (*Convolvulus, Heliotropium, Veronica, Solanum, Salvia, Cuscuta, Echium, Ipomoea* and *Orobanche*). Therophytes were the most dominant life forms among the families, followed by chamaephytes and hemicryptophytes. Boraginaceae and Scrophulariaceae had the highest share of annuals. Remarkable distribution patterns of the life forms in the seven studied biogeographic zones were noticed. Trees were dominant in the Mediterranean zone, while shrubs, perennial herbs and therophytes were dominant in the Sinai. Altogether 8 endemic species and 14 near-endemics were included in the Tubiflorae of Egypt; mostly from southern Sinai. We found that Labiatae and Scrophulariaceae were the families with higher concentration of endemics. Notably, *Teucrium* was among the genera of the Mediterranean Africa with highest endemism. Gamma diversity varied from 171 in the Sinai Peninsula to 43 and 39 in the Oases of the western Desert and along the Red Sea, respectively. Interestingly, highest significant values of similarity and species turnover (beta diversity) were observed between the Oases and the Nile lands. It is worthy noting the combined effect of both temperature and precipitation on gamma diversity of Tubiflorae in the 7 biogeographic zones. Our results indicated that almost one-half of the species showed a certain degree of consistency, *i.e.*, with narrow geographic expansion. On the basis of UPGMA clustering and PCoA analysis, 4 floristic groups were recognized, each include one or more biogeographic zone. The occurrence of the species of Tubiflorae in the adjacent regional arid floras and their phytochorological affinities, were discussed.

Acta Biol Szeged 51(1):65-80 (2007)

KEY WORDS

geographical distribution
gamma diversity
desert ecosystems
flora
endemism
chorology

Tubiflorae is by far the largest order of the Egyptian vascular flora. Generally, Engler and Diels (1936) recognised the order Tubiflorae to be composed of 8 suborders and 23 families of the flowering plants. On the other hand, Hutchinson (1959) organized the families in 5 orders: Verbenales, Solanales, Personales, Boraginales and Lamiales. In Egypt, it is represented by 5 suborders (Convolvulineae, Boragineae, Verbenineae, Solanineae, and Acanthineae), 96 genera, 12 families (Convolvulaceae, Boraginaceae, Verbenaceae, Avicenniaceae, Labiatae, Solanaceae, Scrophulariaceae, Orobanchaceae, Globulariaceae, Acanthaceae, Pedaliaceae, and Lentibulariaceae) and 284 species comprising 13.7% of the total flora. It is a group of great importance, not only for its species diversity, but also for the capacity of their species to colonize a great variety of environments, wide range of life forms, habitats and distribution patterns (Täckholm 1974; Boulos 2000, 2002). Interestingly, one third of its total number of species was considered endangered and vulnerable (El Hadidi 1979). However, Boulos (1989) enumerated 14 desert plant species belonging to Boraginaceae, Convolvulaceae, Labiatae, Orobanchaceae and Solanaceae of promising economic potentialities. It also includes shrubs that present clear adaptation syndromes to the arid and semi-arid environs (e.g. pubescence and spinescence), which have given them a great diversification not only in Egypt, but also in the entire Middle East and Mediterranean North Africa. Furthermore, the order constitutes a model system for the study of arid biogeographical patterns, and could generate useful information for the conservation of certain vegetation enclaves inside the country and the whole region as well. In fact, the Convention on International Trade in Endangered Species of wild Fauna and Flora (CITES 1990) includes most of the families of Tubiflorae in its Appendix 2 and a considerable number of its species are listed in Appendix 1.

Biological diversity, or biodiversity, refers to the variety of distinct ecosystems or habitats, the number and variety of species within them, and the range of genetic diversity within the populations of these species. Two attributes of biodiversity have attracted particular attention from the

Accepted Sept 5, 2007
*Corresponding author. E-mail: elghani@yahoo.com

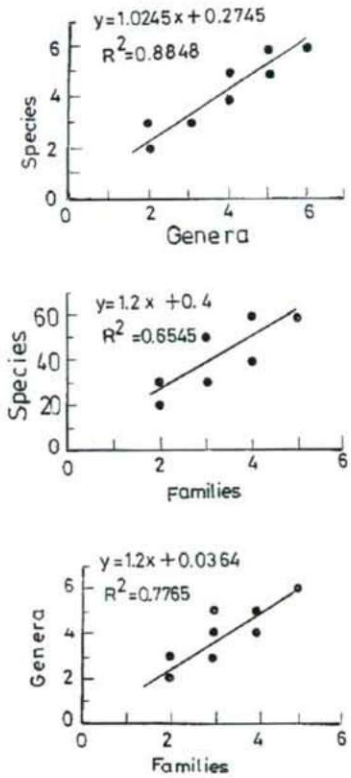

Figure 1. Relationships between taxic richness of Egyptian Tubiflorae at different levels.

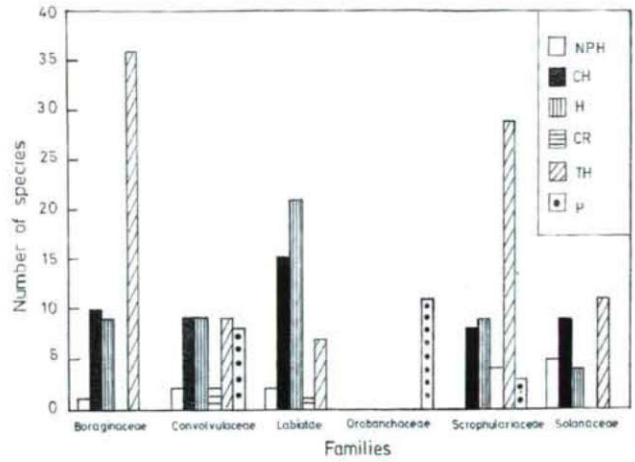

Figure 2. Life form spectrum within the species-rich families of Tubiflorae.

international conservation community: gamma diversity (the total number of species in an area), and endemism (the number of species in that area that occur nowhere else). Because these two attributes reflect the complexity, uniqueness and intactness of natural ecosystems, they are believed to indicate overall patterns of biodiversity in a useful manner. Phylogenetic diversity is in part a function of the size of a flora, and partly of the pattern of distribution of the species into higher taxa (Fenner et al. 1997). Recently the pattern of species distribution among higher taxa has been shown to be an effective indicator of phylogenetic diversity (Williams and Humphries 1994).

The biogeography of the flora of Egypt is still poorly documented, and with few notable exceptions (El Hadidi et al. 1996; Abd El-Ghani and El-Sawaf 2004), there has been little attempt to analyze the biogeographical implications of most species distribution patterns. Khedr et al. (2002) reported that the flora of Egypt contains many families and genera relative to the number of species (120 families, 742 genera, 2088 species) and a relatively large number of oligotypic families, each represented by only one or a few species. They suggested that a flora, in which the species are distributed among numerous genera or families, or other higher-order ranks, should contain greater phylogenetic diversity and genomic information than one in which the same number of species is concentrated into fewer higher-order taxa. The high fraction (97%) of native species in the Egyptian flora may reflect fewer opportunities to acquire more species per genus or per family, due to fewer successful biotic invasions as well as lower speciation rates.

Despite the fact that some families of Egyptian Tubiflorae have been taxonomically revised (Boulos 2000, 2002), our basic knowledge on the diversity and biogeography of this order is still fragmentary and far from complete. This paper attempts to analyse and interpret the diversity in relation to relative family and genus sizes, spatial distribution patterns and phytogeography of the members of Tubiflorae particularly in Egypt, compared to another North African arid country (Libya), and Saudi Arabia as well. It also stresses the need to combine taxonomic, floristic, life form differentiations and biogeographical parameters to understand the relationship between plant habit and the speciation propensity of the Tubiflorae.

Materials and Methods

The provisional account presented here was based on the authors' own data from field work carried out during several years (1999-2005) in all seasons from different parts of Egypt; especially those from the Oases of the western Desert, Sinai and Gebel Elba. In addition, an inventory of all available herbarium collections from Egypt was compiled, and taxonomic determinations were revisited. The plant materials assembled by MM Abd El-Ghani and S El-Naggar during their field work in western Saudi Arabia for the former and Gebel Akhdar of Libya for the latter were also used. Specimens were examined from the herbarium of Cairo University (CAI), the herbarium of the Agriculture Museum (CAIM) and the Herbarium of Assiut University (AST). Taxonomic revisions for some families and genera of Egyptian Tubiflorae were

Table 1. A summary of systematic diversity of the families of Tubiflorae in Egypt. S/G= species per genera.

Family	Number of species (S)	% of species	Number of genera (G)	S/G
Scrophulariaceae	60	21.1	17	3.5
Boraginaceae	58	20.4	19	3.0
Labiatae	54	19	22	2.8
Convolvulaceae	46	16.2	10	4.6
Solanaceae	31	11	8	3.8
Orobanchaceae	11	3.9	2	5.5
Verbenaceae	8	2.8	6	1.3
Acanthaceae	8	2.8	6	1.3
Pedaliaceae	3	1.1	3	1
Lentibulariaceae	2	0.7	1	2
Avicenniaceae	1	0.3	1	1
Globulariaceae	2	0.7	1	2
Total	284	100	96	3.0

also consulted (El-Husseini 1986; El-Husseini and Zareh 1989; Hepper 1998; El Hadidi et al. 1999). Nomenclature and species distribution was based mainly on Täckholm (1974), Boulos (2000, 2002) for Egypt, Collenette (1985), Chaudhary and Al-Jowaid (1999) for Saudi Arabia, and Jafri and El-Gadi (1977-1984) for Libya. The system of phyogeographical territories of Egypt that proposed by El Hadidi (2000) was adopted in this study. Each territory will be here referred to as "biogeographic zone". Thus seven major biogeographic zones were included in this study: the Mediterranean (M), the Nile region (N), the Eastern Desert (De), Sinai Peninsula (S), the Red Sea coastal land (R), Gebel Elba (Ge) and the Oases of the Western Desert (O).

The biogeographical analysis was done down to species level. A species list that formed the base of the analysis was prepared using the authors' plant collections and field notes, all relevant references and floras of Egypt and adjacent countries. Two levels of biogeographic analysis were considered: genera and species. For the analysis, the number of species each genus possesses weighted the importance of genera. For each species, the following attributes were also recorded: life span (annual or perennial), and life-form categories were identified according to Raunkiaer's system of classification (Raunkiaer 1937). When several life forms were given for a species, the most representative species was chosen. The phytogeographical affinity of each taxon was also included. The latter information was determined largely from sources such as Wickens (1976), Zohary (1972) and Feinbrun-Dothan (1978). When these resources for a single taxon gave more than one phytogeographical element, the most appropriate was chosen.

Based on the presence-absence matrix of the 284 species in the seven major bigeographic zones of Egypt, a cluster analysis was performed using the agglomerative algorithm UPGMA that included in the Multivariate Statistical Package MVSP for Windows, version 3.1 (Kovach 1999). The obtained groups were represented in a dendrogram. A Principal Coordinate Analysis (PCoA) was preferred using the product-moment correlation as a coefficient. We preferred PCoA than a PCA (Principal Components Analysis) because the former performs better on data sets with missing data (Rohlf 1972). Gamma diversity was calculated as the total number of species in each biogeographic zone. Species turnover (beta diversity) was calculated using I-Jaccard's index of similarity since it provides a way to measure species turnover between different areas (Whittaker 1960; Magurran 1998). The calculation of the index has been designed to equal 1 in case of complete similarity. Fifty percent turnover of species composition, termed half change, has been used as the unit of beta diversity. All the statistical analyses were carried out using SPSS for Windows version 10.0.

Results and Discussion

Taxonomic composition

The Egyptian flora falls into the category of a widespread mid-continental flora having low mean genus size and a very low level of endemism (Fenner et al. 1997). It has a low level of speciation and a high level of monotypism, with very few genera having more than 30 species. The continuous nature of geographic distribution of habitats and relative lack of reproductive isolation are perhaps the most important factors influencing the rate of speciation in this country. However, Kedr et al. (2002) found that the number of species per family in Egypt was higher in cosmopolitan families and families whose dominant mode of dispersal is abiotic and which possess a herbaceous growth habit. Yet, the actual family speciation rate (*i.e.*, the number of varieties per species) did not differ among the traits. Our results proved that the species diversity was unevenly distributed among taxonomic groups (Table 1). The family size in the Egyptian Tubiflorae was relatively high: 5 dominant cosmopolitan families (Scrophulariaceae, Boraginaceae, Labiatae, Convolvulaceae and Solanaceae) had more than 30 species comprising 87.7% (249 species of the total species in the order) and 6 families had less than 10 species each (table 1). There were a suite of species-rich genera, but the majority (50) of the 96 genera was represented by a single species. The most species-rich genera were *Convolvulus* (23), *Heliotropium* (17), *Veronica* (13), *Solanum* (11), *Salvia* (9), *Cuscuta* and *Echium* (8 each) and *Ipomoea* and *Orobanche* (7 each). Altogether, they constitute 36.3% of the total number of the order (284), while monospecific genera (40) accounted for 14.1%.

The overall lower ratio of species/genus (3.0) for the whole order may explain its higher diversity. Interestingly, lower ratios of S/G (1-2) were estimated in Lentibulariaceae, Globulariaceae, Verbenaceae, Acanthaceae, Pedaliaceae and Avicenniaceae indicated higher diversity among families. The

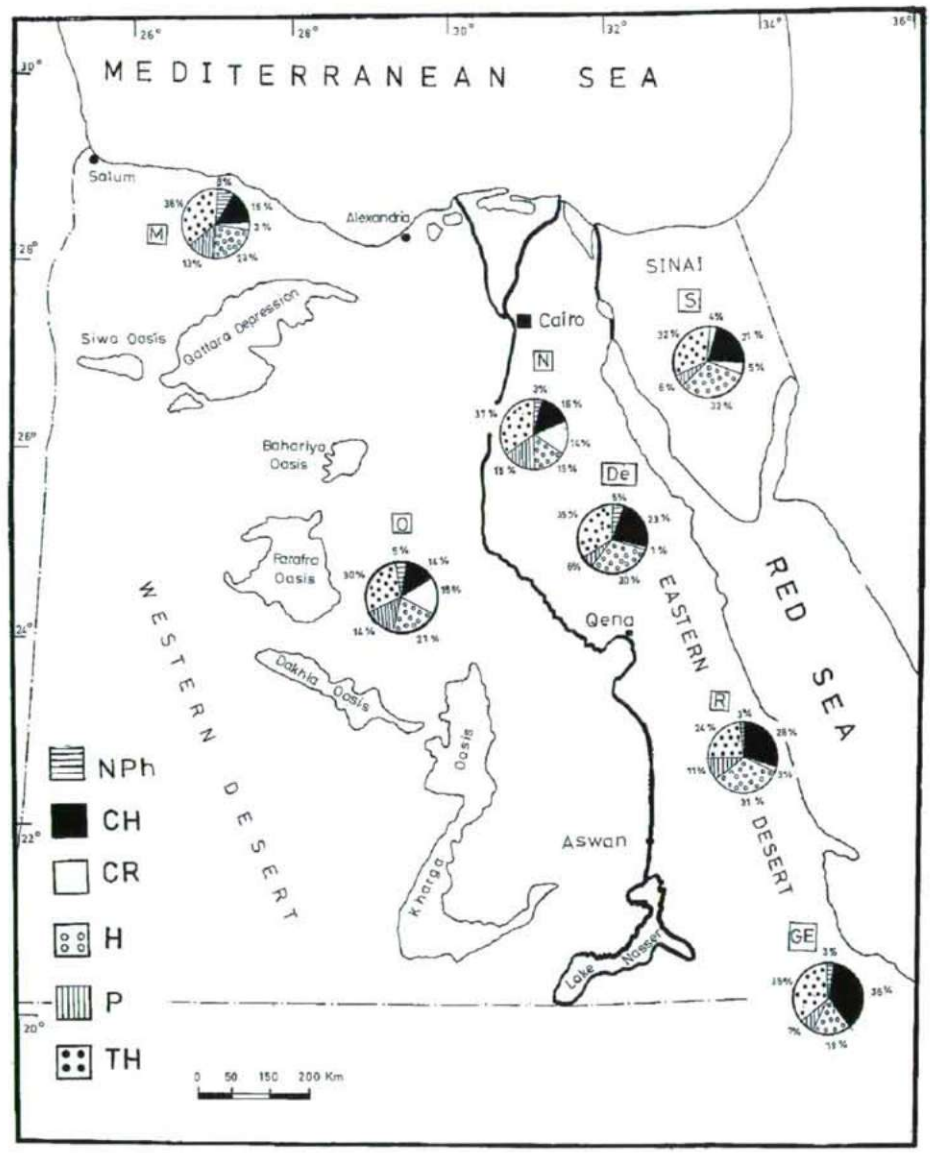

Figure 3. Distribution of life forms in different biogeographic zones of Egypt. For abbreviations, see text.

relationships among taxonomic ranks of species, largest genera and the species-rich families with respect to their gamma diversity along with fitted regression equations (models) were shown in Figure 1. There was significantly positive correlation ($p<0.005$) between species, genera and family level. Thus, the higher taxonomic units such as genera or the families may be employed as surrogates for predicting species diversity of the Egyptian Tubiflorae.

Life-strategies of species

The life form spectrum within the families of the order showed the dominance of therophytes (annuals), followed by chamaephytes and hemicryptophytes (Fig. 2). Non-succulent trees, parasites and perennial herbs (terrestrial or aquatic) were all represented by few species, compared to other categories. The overall comparison of frequencies for the different categories of life forms showed significant variation among families ($p<0.001$). Boraginaceae and Scrophulariaceae had the highest share of annuals. The uncontested leader for shrubs and shrublets was Labiatae, whereas Orobachaceae was strictly for parasites. Notably, Convolvulaceae was the only family in which all life form categories were represented. It is to be mentioned here that, most genera of the Egyptian Tubiflorae had a single characteristic life form. However, some genera exhibited diversity. *Convolvulus* had several different growth forms, particularly annual erect herbs, dwarf shrubs and

Table 2. Endemic and near-endemic species in the species-rich families of Tubiflorae of Egypt, Libya and Saudi Arabia. += present.

Taxa	Endemics			Near-Endemics		
	Libya	Egypt	Saudi Arabia	Libya	Egypt	Saudi Arabia
Boraginaceae						
Heliotropium longiflorum (A.DC.) Hochst et St. ex Bunge						+
Nonea viviani A.DC.				+	+	
Onosma cyrenaica Durand & Barratte	+					
Convolvulaceae						
Convolvulus maireanus Pamp.	+					
C. shimperi Boiss.					+	+
C. spicatus Hallier.f.					+	
Labiatae						
Ballota andrenzziana Pamp.	+					
Marrubium deserti Noe ex Coss.				+		
Micromeria guichardii (Quézel & Zaffran) Brullo & Furnari	+					
M. serbaliana Danin & Hedge		+				
Nepeta cyrenaica Quézel & Zaffran						
N. septemcrenata Benth.					+	+
N. vivianii (Coss.) Bég. & Vacc.	+					
Origanum cyrenaicum Bég. & Vacc.	+					
O. isthmicum Danin		+				
O. syriacum L. subsp. *sinaicum* (Boiss.) Greuter & Burdet		+				
Phlomis aurea Decan.		+				
Stachys tournefortii Poiret				+		
Teucrium apollinis Maire & Weiller	+					
T. barbeyanum Ascher. & Taubert	+					
T. davaeanum Cosson	+					
T. lini-vaccarii Pamp.	+					
T. zanonii Pamp.	+					
T. decussatus Benth.					+	+
Orobanchaceae						
Orobanche cyrenaica Beck	+					
Scrophulariaceae						
Anarrhinum forsskalii (J.E. Gmel.) Cufod. subsp. *pubescens* (Fresen.) D.A. Sutton		+				
Kickxia floribunda (Boiss.) Täckh. & Boulos					+	+
K. macilenta (Decne.) Danin					+	
K. pseudoscoparia V.W. Smith & D.A. Sutton					+	+
Linaria joppensis Bornm.					+	
Parentucellia floribunda Viv.	+					
Verbascum fruticulosum Post					+	+
V. letourneuxii Asch.				+	+	
V. schimperianum Boiss.					+	+
Veronica anagallis-aquatica L. var. *nilotica* R. Uechtr.					+	
V. kaiseri V. Täckh.		+				
V. musa V. Täckh. & Hadidi		+				
Solanaceae						
Hyoscyamus boveanus (Dunall) Asch. & Schweinf.		+				
Solanum sinaicum Boiss.					+	

shrublets, and twiners or climbers. *Heliotropium* had both annuals and shrubs, while *Nicotiana* was represented by two species, one a tree and the other an erect annual herb. The wide range of tolerance of the members of this order enabled the genera to occupy wide range of habitats. For example, *Limosella* and *Bacopa* (Scrophulariaceae) were subaquatic in water courses, *Stachys* and *Thymus* (Labiatae) an indicator of stony ground (Girgis 1972), *Lamium, Convolvulus, Mentha, Veronica* and *Datura* were alien weeds of the agro-ecosystem, *Trichodesma, Salvia, Hyoscyamus, Scrophularia, Lavandula* and *Lycium* were dominants of the Egyptian desert ecosystem. Though few in number, parasitic genera were of special interest. Beside *Orobanche* and *Cistanche* (Orobanchaceae), *Cuscuta* (Convolvulaceae), *Striga* (Scrophulariaceae) were encountered in this study.

The distribution of the life-form categories within the seven biogeographic zones was demonstrated in Figure 3. The composition of life forms reflects the response of vegetation to variations in certain environmental factors. In this study, preponderance of therophytes, chamaephytes and hemicryptophytes over other life forms is a response to the hot dry climate, topographic variations and human and animal interference (Abd El-Ghani 1998; Abd El-Ghani and Amer 2003; Salama et al. 2003). The abundance of cryptophytes along the

Table 3. Gamma diversity of the families of Tubiflorae recorded in the studied biogeographic zones of Egypt, with their total numbers and percentages (see text for biogeographic zones abbreviations).

Family	Biogeographic zone						
	N	M	O	S	R	GE	De
Scrophulariaceae	18	13	9	36	10	12	13
Boraginaceae	27	28	7	39	9	13	19
Labiatae	3	15	3	42	4	8	17
Convolvulaceae	17	17	11	22	5	19	12
Solanaceae	15	10	7	21	4	8	13
Orobanchaceae	6	10	2	6	3	2	4
Verbenaceae	4	3	3	2	1	3	0
Acanthaceae	0	0	0	1	1	8	2
Pedaliaceae	0	0	0	0	0	2	1
Lentibulariaceae	1	0	1	0	0	0	0
Avicenniaceae	0	0	0	1	1	1	0
Globulariaceae	0	2	0	1	1	0	1
Total number of species	91	98	43	171	39	76	82
% of the total	32	34.5	15.1	60.2	13.7	26.7	28.9

Table 5. Annual means of climatic data of representative meteorological stations in each of the studied biogeographic zone (after Zahran & Willis, 1992; Abd El-Ghani, 1998 & 2000). Max= Maximum, Min= Minimum.

Biogeographic zone	Temperature (°C)		Rainfall (mm year^{-1})	Relative Humidity (%)
	Max	Min		
The Mediterranean				
Sallum	24	14	90	65
Mersa Matruh	24	14	144	66
Alexandria	25	16	192	68
El-Arish	26	12	180	70
The Nile land				
Menofiya	28	14	3	65
Faiyum	29	14	11	51
Luxor	33	16	<1	35
Oases of the Western Desert				
Siwa	30	13	10	41
Bahariya	30	14	4	39
Kharga	32	16	<1	31
Sinai proper (south Sinai)				
Saint Catherine	25	5	45	38
Red Sea coastal lands				
Suez	31	17	16	53
Hurghada	28	19	4	46
Quseir	28	19	3	50

Nile banks may be related to their rhizomatous growth habit, which was believed to be more resistant to decomposition under water submergence. This detected distribution pattern conforms to previous studies at this zone, especially those of Shaltout and Sharaf El-Din (1988). It is of interest to note that

Table 4. Sørensen coefficients of floristic similarity (lower half), and the beta diversity (upper half) between the 7 studied biogeographic zones of Egypt. * = p<0.05, ** = p< 0.01.

Biogeographic zones	N	M	O	S	GE	De	R
N		0.5	0.6	0.4	0.2	0.4	0.1
M	0.3		0.3	0.5	0.1	0.3	0.2
O	0.4**	0.2		0.2	0.2	0.2	0.1
S	0.2	0.3	0.1		0.2	0.5	0.2
GE	0.1	0.07	0.1	0.2		0.3	0.4
De	0.2	0.2	0.1	0.3*	0.2		0.3
R	0.1	0.02	0.04	0.2*	0.3*	0.3*	
Gamma diversity	91	98	43	171	76	82	39

the trees of Tubiflorae grow well in the Mediterranean zone, while shrubs, perennial herbs and therophytes occurred in Sinai. High percentages of therophytes and hemicryptophytes were coincides with the floristic characters of the arid zones in the Mediterranean Basin, and in general for the floras of arid and semi-arid zones (Bornkamm and Kehl 1985; Pignatti and Pignatti 1989).

Endemism

Studies have focused predominantly on determining patterns of endemism at global and regional scales (Major 1988; Cowling 1983). Endemics are usually rare and restricted to rather small geographical region, so they deserve special attention for their conservation. No endemic families are known from the Middle East and North Africa (Boulos 1997). Zohary (1973) suggested that the source of this poverty is doubtless in the huge stretches of open and almost plantless desert that provide no isolating barrier against connection with adjacent countries, themselves part of the extremely barren Sahara. The major families with highest endemic species in the tropical areas are Asclepiadaceae, Acanthaceae, Liliaceae (*sensu lato*) and Euphorbiaceae, whereas Labiatae, Compositae, Scrophulariaceae and Cruciferae in temperate areas. Endemic taxa to Egypt are very few: 61 species or 2.9% of the total flora. However, 60.7% of the endemics are known from Sinai (Boulos 1995; Ayyad et al. 2000). Highest endemics within families of the Egyptian vascular flora are in Labiatae, followed by Liliaceae and Scrophulariaceae constituting 10.9, 10.4 and 6.5% of the total flora, respectively.

It has been estimated that 8 endemic and 14 near endemic species were included in the taxa of the Egyptian Tubiflorae. This study showed also that the majority of the endemic species in Tubiflorae of Egypt was recorded from southern Sinai (Sinai proper *sensu* El Hadidi 2000) in the rugged mountainous areas that support the highest peaks in Egypt (Zohary 1973; Moustafa and Klopatek 1995). Labiatae (4 species) and Scrophulariaceae (3 species) were the families of higher concentration of endemics. *Teucrium* and *Veronica* were the

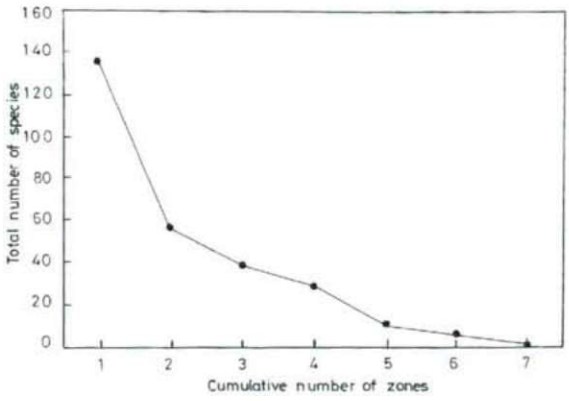

Figure 4. Species distribution in the biogeographic zones (cumulative numbers).

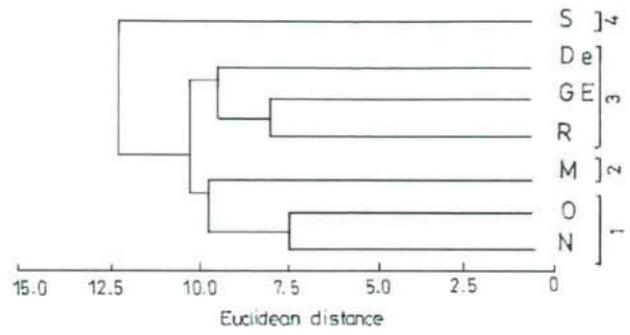

Figure 5. Dendrogram of similarity among the analysed biogeographic zones.

endemic-rich genera. Similarly, Libya and Saudi Arabia have most of their endemics in the mountainous regions: Gebel Akhdar in the former (Boulos 1975), and the highlands of southwestern Saudi Arabia of the latter (Chaudhary 1999-2001). Both are considered among the endemic-rich areas for vascular plants in the region of the Middle East (Boulos 1997).

Comparing the level of endemism among the species of Tubiflorae in the regional floras of Egypt, Libya and Saudi Arabia, we found that the endemic species (*sensu lato*) were not very numerous and can be currently estimated at 39 taxa (Table 2). The highest number of endemics was recorded in Libya (13 or 7.5% of the total flora), followed by Egypt (8 or 11.0% of the total flora), but none in the flora of Saudi Arabia. At the generic level, six genera were totally, or almost, restricted to Libya (*Onosma, Convolvulus, Ballota, Teucrium, Parentucellia* and *Orobanche*), three to Egypt (*Phlomis, Anarrhinum* and *Hyoscyamus*). It can here be noted that *Teucrium* is among genera of the Mediterranean Africa with highest endemism. It is represented by 67 species of which 44 or 65.7% are endemic (Greuter et al. 1986). Despite the importance of the endemic species in their regional floras, these species have been poorly studied. More research is required on the management requirements of the endemic taxa in the Middle East and Mediterranean North Africa.

Variations in beta and gamma diversities

Gamma diversity differed considerably among the studies biogeographic zones of Egypt (Table 3). Sinai Peninsula was the richest in species (171), while the lowest number of species was found in the Oases of the Western Desert and along the Red Sea coastal lands (43 and 39, respectively). Interestingly, highest significant values of Sørensen's coefficient of floristic similarities (0.4, p=0.01) and species turnover (0.6) were noticed between the Oases and the Nile land (Table 4). Clearly, the floristic composition of these two zones was closely related and characterised by the occurrence of many species in common. Fakhry (1973, 1974) reported the existence of an old relation between the two biogeographic zones. All travellers and government officials used an important ancient caravan route linking the Oases with the Nile Valley (near Minya on the Nile) until 1968 for the oases' commerce. The low gamma diversity and species turnover of the Gebel Elba may be related to the fact that most of its species were highly specific to the prevailing environmental conditions and geographic situation. This means that the species replacement or biotic change is low in this area (Wilson and Shmida 1984). Through the combined effect of climate (temperature and rainfall) and human activities (grazing, building new settlements and establishment of summer resorts) along the coasts of the Mediterranean and the Red Sea substantially altered the vegetation structure and the floristic composition of these biogeographic zones to include new habitats that were not found earlier (Ayyad and Fakhry 1996), with reduced gamma and beta-diversities.

Climatic zonation is probably the most important factor influencing plant distribution, particularly summer heat, winter cold and precipitation (Zahran and Willis 1990). On the other hand, as minimal precipitation and frequent droughts characterize arid zones, availability of water may be one of the primary factors controlling the distribution of species (Yair and Danin 1980; Abd El-Ghani 2000). Table 5 gives some climatic characteristics of selected meteorological stations to represent each of the studied biogeoraphic zones. The most striking climatic feature is the precipitation gradient. Temperatures below zero can be reached in the more continental parts of the Western Desert, and soil surface frost is a regular phenomenon in the mid-winter months. The gamma diversity gradient was decreased from Sinai Peninsula where a less arid climate prevails, to the Oases and the Red Sea coastal lands where more arid climate prevails. It is worthy noting the combined effect of temperature and precipitation on the gamma diversity of Tubiflorae in the seven studied

Table 6. Distribution patterns of species of the Egyptian Tubiflorae confined to a certain biogeographic zone. For zone abbreviations, see text. += recorded.

Species	Biogeographic zone						
	N	M	O	S	R	GE	De
Ipomoea carnea Jacq.	+						
I. eriocarpa R.Br.	+						
Dichondra micrantha Urb.	+						
Cuscuta monogyna Vahl	+						
C. epilinum Weihe	+						
Heliotropium curassavicum L.	+						
H. amplexicaule Vahl	+						
Clerodendrum acerbianum (Vis.) Benth. & Hook.f.	+						
Physalis angulata L.	+						
Salpichroa origanifolia (Lam.) Baill.	+						
Nicotiana plumbaginifolia Viv.	+						
Sutera glandulosa Roth	+						
Limosella aquatica L.	+						
Striga hermonthica (Delile) Benth.	+						
S. asiatica (L.) Kuntze	+						
Parentucellia viscosa (L.) Caruel	+						
Lindernia parviflora (Roxb.) Haines	+						
Utricularia inflexa Forssk.	+						
Convolvulus lineatus L.		+					
C. stachydifolius Choisy		+					
C. humilis Jacq.		+					
Calystegia silvatica (Kit.) Griseb.		+					
Heliotropium hirsutissimum Grauer		+					
Buglossoides incrassata (Guss.) I.M. Johnst.		+					
Nonea melanocarpa Boiss.		+					
Echium plantagineum L.		+					
E. sabulicola Pomel		+					
E. glomeratum Poir.		+					
Thymus capitatus (L.) Link		+					
Prasium majus L.		+					
Teucrium brevifolium Schreb.		+					
Linaria micrantha (Cav.) Hoffmanns. & Link		+					
Scrophularia canina L.		+					
Veronica persica Poir.		+					
V. syriaca Roem. & Schult.		+					
V. anagalloides Guss. subsp. *taeckholmiorum* Chrtek & Osb.-Kos.		+					
Globularia alypum L.		+					
Orobanche lavandulacea Rchb.		+					
O. schultzii Mutel		+					
Cistanche violacea (Desf.) Beck		+					
Striga gesnerioides (Willd.) Vatke			+				
Utricularia gibba L.			+				
Convolvulus spicatus Hallier f.				+			
C. schimperi Boiss.				+			
C. scammonia L.				+			
C. palaestinus Boiss.				+			
Heliotropium bovei Boiss.				+			
H. makallense O. Schwartz				+			
Paracaryum rugulosum (DC.) Boiss.				+			
P. bungei (Boiss.) Brand				+			
P. calathicarpum (Stocks) Boiss.				+			
Lappula sinaica (DC.) Asch. & Schweinf.				+			
Asperugo procumbens L.				+			
Alkanna orientalis (L.) Boiss.				+			
A. strigosa Boiss. & Hohen.				+			
Nonea ventricosa (Sm.) Griseb.				+			
Mentha spicata L.				+			
Origanum syriacum L. subsp. *sinaicum* (Boiss.) Greuter & Burdet				+			

Table 6. Continued

Species	Biogeographic zone						
	N	M	O	S	R	GE	De
O. isthmicum Danin				+			
Thymus decussatus Benth.				+			
Satureja serbaliana (Danin & Hedge) Greuter & Burdet				+			
S. myrtifolia (Boiss. & Hohen.) Greuter & Burdet				+			
Ziziphora capitata L.				+			
Z. tenuior L.				+			
Salvia multicaulis Vahl				+			
S. dominica L.				+			
S. sclarea L.				+			
Nepeta septemcrenata Benth.				+			
Stachys nivea Labill.				+			
Ballota saxatilis C. Presl				+			
B. kaiseri Täckh.				+			
Phlomis aurea Decne.				+			
Eremostachys laciniata (L.) Bunge				+			
Ajuga chamaepitys (L.) Schreb. subsp. tridactylites (Benth.) P.H. Davis				+			
Solanum sinaicum Boiss.				+			
S. villosum (L.) Mill.				+			
Nicotiana rustica L.				+			
Hyoscyamus reticulatus L.				+			
Verbascum fruticulosum Post				+			
V. schimperianum Boiss.				+			
V. sinaiticum Benth.				+			
V. eremobium Murb.				+			
V. decaisneanum Kuntze				+			
Anarrhinum pubescens Fresen.				+			
Linaria joppensis Bornm.				+			
*L. simplex*Desf.				+			
Kickxia macilenta (Decne.) Danin				+			
K. scariosepala Täckh. & Boulos				+			
Scrophularia libanotica Boiss.				+			
Veronica kaiseri Täckh.				+			
V. macropoda Boiss.				+			
V. biloba Schreb.				+			
V. campylopoda Boiss.				+			
V. rubrifolia Boiss. subsp. *respectatissima* M.A. Fisch.				+			
Cistanche salsa (C.A. Mey.) Beck				+			
Kickxia nubica (Skan) Dandy					+		
Convolvulus rhyniospermus Choisy						+	
Jacquemontia tamnifolia (L.) Griseb.						+	
Merremia aegyptia (L.) Urb.						+	
M. semisagitata (Peter) Dandy						+	
Ipomoea obscura (L.) Ker Gawl.						+	
Evolvulus alsinoides (L.) L.						+	
E. nummularius (L.) L.						+	
Seddera arabica (Forssk.) Choisy						+	
Cuscuta chinensis Lam.						+	
Heliotropium zeylanicum (Burm. f.) Lam.						+	
H. strigosum Willd.						+	
Brandella erythraea (Brand) R.R. Mill						+	
Lantana viburnoides (Forssk.) Vahl						+	
L. rugosa Thunb.						+	
Priva cordifolia (L.) Greene						+	
Plectranthus hadiensis (Forssk.) Spreng.						+	
Orthosiphon pallidus Royle ex Benth.						+	
Satureja biflora (D. Don) Briq.						+	
Leucas neuflizeana Courbai						+	
L. urticifolia (Vahl) R. Br.						+	
Solanum aethiopicum L.						+	

Table 6. Continued

Species	Biogeographic zone						
	N	M	O	S	R	GE	De
S. carense Dunal						+	
S. forsskaolii Kotschy ex Dunal						+	
Kickxia hastata (R. Br. ex Benth.) Dandy						+	
Scrophularia arguta Sol.						+	
Schweinfurthia pedicellata (T. Anderson) Balf. F.						+	
Barleria hochstetteri Nees						+	
Ruellia patula Jacq.						+	
Ecbolium viride (Forssk.) Alston						+	
Justicia heterocarpa T. Anderson						+	
J. schimperi (Hochst.) Dandy						+	
Peristrophe paniculata (Forssk.) Brummitt						+	
Pedalium murex L.						+	
Rogeria adenophylla J. Gay ex Delile						+	
Ipomoea pes-caprae (L.) R. Br.							+
Podonosma galalensis Schweinf. ex Boiss.							+
Lavandula atriplicifolia Benth.							+
L. multifida L.							+
Sesamum alatum Thonn.							+
Cressa cretica L.	+	+	+	+	+	+	
Cuscuta planiflora Ten.	+	+	+	+	+	+	
Hyoscyamus muticus L.	+	+	+	+	+	+	
Orobanche ramosa L.	+	+	+	+	+	+	
Trichodesma africanum (L.) var. *africanum*	+	+	+	+	+	+	+
Solanum nigrum L.	+	+	+	+	+	+	+

biogeographic zones. When the correlation analyses were performed independently for each of temperature and rainfall at each zone with gamma diversity, the results showed weak correlations (Spearman rank correlation coefficient $r= 0.175$, $p=0.43$ for the former and $r=0.23$, $p=0.27$ for the latter). Yet, gamma diversity showed high significant positive correlations with both temperature and rainfall in Sinai ($r=0.39$, $p=0.01$), but neither in the Mediterranean zone ($r=0.17$, $p= 0.50$) nor in the Oases ($r=0.67$, $r=0.01$). Therefore, colder temperature and relatively high precipitation rate may play a major role in decreasing gamma diversity. The relationship between the climate and species distribution has long been studied in other parts of the world; amongst others, Freitag (1986) in Iran and Afghanistan, Rahman and Wilcok (1991) in south-west Asia and the Indian subcontinent, Cowling et al. (1994) in arid and semi-arid southern Africa, and Gómez-Gonzáles et al. (2004) in the Iberian Peninsula and Balearic Islands.

Geographical expansion and distribution pattern

Our results demonstrated a very strong geographical pattern in the distribution of the Egyptian species of Tubiflorae. There were few highly-frequent species and very many that were infrequent. The majority of species were narrowly distributed. Almost one-half (48%) of the species showed a certain degree of consistency, where they exclusively recorded in or confined to a single biogeographic zone and do not penetrate elsewhere (Table 6). These species were distributed as follows: 18 in the Nile land (e.g., *Ipomoea carnea, Heliotropium amplexicaule, Limosella aquatica, Striga hermonthica* and *Utricularia inflexa*), 22 in the Mediterranean (e.g., *Echium plantagineum, Thymus capitatus, Veronica persica, Globularia olypum* and *Cistanche violacea*), 2 in the Oases (*Striga gesnerioides* and *Utricularia gibba*), 54 in the Sinai Peninsula (e.g., *Paracaryum calathicarpum, Alkanna orientalis, Thymus decussatus, Nepeta septemcrenata, Solanum sinaicum, Verbascum schimperianum, Kickxia macilenta* and *Veronica kaiseri*), one in the Red Sea (*Kickxia nubica*), 34 in the Gebel Elba (e.g., *Seddera arabica, Heliotropium zeylanicum, Lantana rugosa, Leucas urticifolia, Barleria hochstetteri* and *Peristrophe paniculata*) and 5 in the Eastern Desert (e.g., *Ipomoea pes-carpae, Podonosma galalensis*, and *Lavandula multifida*). Only 2 species (*Trichodesma africanum* and *Solanum nigrum*) of the 284 species; that have wide ecological and sociological range of distribution; occur at all the 7 studied biogeographic zones, yet 29 species (about 10% of the total) had a frequency more than 50% (*i.e.*, recorded in 4 zones; see Fig. 4).

Figure 5 shows the dendrogram obtained with the UPGMA clustering species according to their geographical similarity. Four floristic groups (1-4) of Tubiflorae can be detected for Egypt. Results of the Principal Coordinate Analysis (PCoA) support this classification (Fig. 6). Floristic

Table 7. Occurrence of species (excluding endemics) within the major six families of the Tubiflorae in Egypt, Libya and Saudi Arabia. += recorded. Chorotype abbreviations: ES= Euro-Siberian, M= Mediterranean, IT=Irano-Turanian, SA=Saharo-Arabian, SZ= Sudano-Zambezian, COSM= Cosmopolita, Nat= Naturalized, PAL= Palaeotropical, PAN= Pantropical. Sources: 1 = S. El-Naggar; unpublished data, 2= M. Abd El-Ghani; unpublished data.

Taxa	Libya[1]	Egypt	Saudi Arabia[2]	Chorotype
Borago officinalis L.	+			M
Cynoglossum cheirifolium L.	+			M
Echium arenarium Guss.	+			M
E. humile Desf.	+			M
E. italicum L.	+			M
E. parviflorum Moench	+			M
E. tuberculatum Hoffmanns & Link	+			M
Elizaldia calycina (Roem. & Schultes) Maire	+			M
Nonea micrantha Boiss. & Reuter	+			M
N. vesicaria (L.) Reichenb.	+			M
C. supinus Cosson & Kralik	+			M
C. tricolor L.	+			M
Ballota hirsute Benth.	+			M
Micomeria Juliana (L.) Reichenb.	+			M
Nepeta scordotis L.	+			M
Phlomis floccosa D. Don	+			M
Teucrium campanulatum L.	+			M
Thymus algeriensis Boiss. & Reut.	+			M
Anarrhinum fruticosum Desf.	+			M
Antirrhinum siculum Mill.	+			M
Bellardia trixago (L.) All.	+			M
L. laxiflora Desf.	+			M
Parentucellia latifolia (L.) Caruel	+			M
Verbascum balli (Batt.) Qaiser	+			M
V. blatteria Boiss.	+			M
V. tripolitanum Boiss.	+			M
V. cymbalaria Bod.	+			M
Neatostema apulum (L.) I.M. Johns.	+			M + SA
Cuscuta epithymum (L.) Murray	+			M + SA
C. europaea L.	+			M + SA
Mentha aquatica L.	+			M + SA
Veronica hederifolia L.	+			M + SA
Convolvulus cantabaricus L.	+			M + IT
Sideritis curvidens Stapf	+			M + IT
Scrophularia peregrina L.	+			M + IT
Linaria arvensis (L.) Desf.	+			M + ES
Veronica agrestis L.	+			M + ES
Sideritis romana L.	+			IT + Libya
Veronica peregrine L.	+			ES (Nat.)
Ipomoea cairica (L.) Sweet		+		PAL
Ipomoea eriocarpa R. Br.		+		PAL
Ipomoea purpurea (L.) Roth.		+		PAL
Jacquemontia tamnifolia Choisy		+		PAL
Lindernia parviflora (Roxb.) Haines		+		PAL
Ipomoea carnea Jacq.		+		PAN
Ipomoea obscura (L.) Ker Gawl.		+		PAN
Marremeia aegyptiaca (L.) Urb.		+		PAN
Solanum elaeagnifolium Cav.		+		PAN
Ballota damascene Boiss.		+		M
Micromeria sinaica Benth.		+		M
Salvia dominica L.		+		M
Veronica scardica Griseb.		+		M
Podonosma galalensis Schweinf. & Boiss.		+		SA
Convolvulus hystrix Vahl		+		SA
Verbascum eremobium Murb.		+		SA
Veronica rubrifolia Boiss. subsp. *respectatissima* M.A. Fisch.		+		SA
Nogalia drepanophylla (Baker) Verdc.		+		SZ

Table 7. Continued

Taxa	Libya[1]	Egypt	Saudi Arabia[2]	Chorotype
Evolvulus nummularis (L.) L.		+		SZ
Kickxia nubica (Skan) Dandy		+		SZ
Paracaryum calathicarpum (Stacks) Boiss.		+		IT
Convolvulus palaestinus Boiss.		+		IT
Kickxia gracilis (Benth.) D.A. Sutton		+		IT
Echium glomeratum Poiret		+		M + SA
Alkanna strigosa Boiss. & Hohen.		+		M + IT
A. orientalis (L.) Boiss.		+		M + IT
Heliotropium bovei Boiss.		+		M + IT
H. rotundifolium Lehm.		+		M + IT
Nonea melanocarpa Boiss.		+		M + IT
Convolvulus scammonia L.		+		M + IT
Convolvulus stachydifolius Choisy		+		M + IT
Cuscuta monogyna Vahl		+		M + IT
Cuscuta palaestina Boiss.		+		M + IT
Ballota saxatilis C. Presl		+		M + IT
Eremostachys laciniata (L.) Bunge		+		M + IT
Salvia multicaulis Vahl		+		M + IT
Salvia palaestina Benth.		+		M + IT
Salvia sclarea L.		+		M + IT
Hyoscyamus reticulatus L.		+		M + IT
Nonea ventricosa (Sm.) Griseb.		+		M + ES
Kickxia elatine (L.) Dumort.		+		M + ES
Veronica catenata Pennell		+		M + ES
Lappula sinaica (A.DC.) Asch. & Scweinf.		+		SA + IT
Cistanche salsa (C.A. Mey.) C. Beck		+		SA + IT
Anticharis linearis (Benth.) Hochst. & Asch.		+		SA + IT
Veronica campylopoda Boiss.		+		SA + IT
Striga asiatica (L.) Kuntze		+		SA + SZ
Paracaryum intermedium (Fresen.) Lipsky		+		M + SA + IT
Cuscuta approximate Bab.		+		M + SA + IT
Scrophularia sinaica Benth.		+		M + SA + IT
Calystegia silvatica (Kit.) Griseb.		+		M + IT + ES
Cuscuta epilinum Weihe		+		M + IT + ES
Ziziphora capitata L.		+		M + IT + ES
Ziziphora tenuior L.		+		SA + IT + ES
Dicandra micrantha Urb.		+		Nat.
Ipomoea hederacea Jacq.		+		Nat.
Ipomoea pes-caprea (L.) R. Br.		+		Nat.
Nicotiana plumbaginifolia Viv.		+		Nat.
Nicotiana rustica L.		+		Nat.
Physalis angulata L.		+		Nat.
Physalis ixocarpa Hornem.		+		Nat.
Cordia abyssinica R. Br.			+	SZ
Ocimum hadinese Forssk.			+	SZ
Cressa cretica L.	+	+	+	COSM
Convolvulus arvensis L.	+	+	+	COSM
Lamium amplexicaule L.	+	+	+	COSM
Mentha pulegium L.	+	+	+	COSM
Teucrium polium L.	+	+	+	COSM
Datura sramonium L.	+	+	+	COSM
Solanum schimperianum Hochst. & A. Rich	+	+	+	COSM
Ajuva iva (L.) Schreber	+	+	+	M
Salvia verbenaca L.	+	+	+	M
Arnebia tinctoria Forssk.	+	+	+	SA
Echium longifolium Delile	+	+	+	SA
Ogastema pusillum (Bonett & Barratte) Brummitt	+	+	+	SA
Convolvulus prostrates Forssk.	+	+	+	SA
Teucrium decaisne C. Presl	+	+	+	SA
Misopates orontium (L.) Rafin.	+	+	+	SA

Table 7. Continued

Taxa	Libya[1]	Egypt	Saudi Arabia[2]	Chorotype
Scrophularia canina L.	+	+	+	SA
Scrophularia hypericifolia Wydl.	+	+	+	SA
Scrophularia libanotica Boiss.	+	+	+	SA
Echiochilon fruticosum Desf.	+	+	+	M + SA
Echium horridum Batt.	+	+	+	M + SA
Echium rauwolfii Delile	+	+	+	M + SA
Trichodesma africanum (L.) R. Br.	+	+	+	M + SA
Heliotropium hirsutissimum Grauer	+	+	+	M + SA
Linaria albifrons (Sm.) Spreng.	+	+	+	M + SA
Linaria haelava (Forssk.) F. Dietr.	+	+	+	M + SA
Linaria simplex Desf.	+	+	+	M + SA
Linaria tenuis (Viv.) Spreng.	+	+	+	M + SA
Kickxia aegyptiaca Nàbelek	+	+	+	M + SA
Scrophularia arguta Sol.	+	+	+	M + SA
Cistanche phelypaea (L.) Cout.	+	+	+	M + SA
Orobanche cernua Loefl.	+	+	+	M + SA
Hyoscyamus albus L.	+	+	+	M + SA
Lycium europaeum L.	+	+	+	M + SA
Anarrhium forsskahlii (J.E. Gmel.) Cufod. subsp. *forsskahli*	+	+	+	M + SZ
Moltkiopsis ciliata (Forssk.) I.M. Johns.	+	+	+	M + IT
Convolvulus siculus L.	+	+	+	M + IT
Mentha longifolia (L.) Huds. subsp *typhoides* (Briq) Harley	+	+	+	M + IT
Salvia lanigera Poiret	+	+	+	M + IT
Cistanche tubulosa (Schenk) Wight	+	+	+	M + IT
Orobanche mutelii F.W. Schultz	+	+	+	M + IT
Veronica polita Fr.	+	+	+	M + IT
Heliotropium ovalifolium Forssk.	+	+	+	SA + SZ
Salvia aegyptiaca L.	+	+	+	SA + SZ
Kickxia acerbiana (Boiss.) Täckh.& Boulos	+	+	+	SA + SZ
Lycium shawii Roem. & Shult.	+	+	+	SA + SZ
Heliotropium lasiocarpum Fisch. & C.A. Mey.	+	+	+	SA + IT
Heliotropium ramosissimum (Lehm.) Sieb. ex A. DC.	+	+	+	SA + IT
Convolvulus fatmensis Kunze	+	+	+	SA + IT
Verbascum sinuatum L.	+	+	+	SA + IT
Hyoscyamus muticus L.	+	+	+	SA + IT
Heliotropium bacciferum Forssk. var. *bacciferum*	+	+	+	M + SA + SZ
Heliotropium supinum L.	+	+	+	M + SA + SZ
Anchusa aegyptiaca (L.) A. DC.	+	+	+	M + SA + IT
Anchusa hispida Forssk.	+	+	+	M + SA + IT
Arnebia linearifolia A. DC.	+	+	+	M + SA + IT
Cuscuta planiflora Ten.	+	+	+	M + SA + IT
Veronica persica Poir.	+	+	+	M + SA + IT
Withania somnifera (L.) Dunal	+	+	+	M + SA + IT
Orobanche ramosa L.	+	+	+	M + SA + ES
Asperugo procumbens L.	+	+	+	M + IT + ES
Marrubium vulgare L.	+	+	+	M + IT + ES
Datura innoxia Mill.	+	+	+	Nat.
Total number of species	152	260	141	

group (1) includes the species of Tubiflorae in both the Nile lands and the Oases, as these two regions were closely related either commercially or through the introduction of field crops. Consequently, several common alien weed species of arable lands may grow in both agro-ecosystems. This is consistent with the findings of Abd El-Ghani and El-Sawaf (2004) in their account on the diversity and distribution of plant species in the agro-ecosystems of Egypt, who reported a clear segregation of the species composition in both the Nile lands and the Oases biogeographic zones than the others.

Floristic group (2) characterizes the Mediterranean region, in which 34.5% of the species of Tubiflorae were recorded. Certain families showed higher presence in this zone, e.g., Orobanchaceae and Globulariaceae. Despite its long shores on the Mediterranean Sea, the gamma diversity of Tubiflorae ranked second. The primary cause of the decline of biodiver-

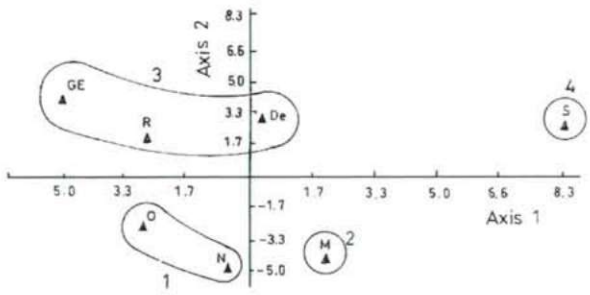

Figure 6. Scatterplot of the studied biogeographic zones against the first principal coordinate by the second principal coordinate.

sity is not direct human exploitation or malevolence, but the habitat destruction that inevitably results from the expansion of human populations and human activities (Wilson 1988). It is to be mentioned here that the western Mediterranean coastal strip has been subjected to ecosystem degradation and species impoverishment due to the way in which man has used and misused the natural resources of the zone. A variety of human-induced stresses have already taken their toll on ecosystems. With so much habitats being lost, the populations of many species were being dramatically reduced. The continued uncontrolled wood-cutting, overgrazing and rain-fed farming for cultivation of annual crops have dominated the Mediterranean zone for centuries. More recent land use activities have been even more devastating, e.g., intensive irrigated agriculture, obliteration of limestone ridges for bricks making which is endangering many chasmophytic species, and the occupation of large areas of the coastal sand dunes by summer resorts is endangering many psammophytic species. Ayyad and Fakhry (1996) overviewed the plant biodiversity in the western Mediterranean desert of Egypt in terms of habitat, community and species diversity. They concluded that the nature of human impact on biodiversity may be either sudden and/or radical (e.g., establishment of new settlements, and summer resorts) or may be gradual (e.g., grazing of wild vegetation). Generally, loss of species is the ultimate result.

The third floristic group (Group 3) includes three closely related biogeographic zones; the Eastern Desert, the Gebel Elba and the Red Sea coastal lands. It is noteworthy, but not surprising, that these three zone form one entity, and can be known as the "Eastern Desert complex" group. Forty-nine species of the order were distributed among this complex, and manifests either very narrowly or widely distributed species (Table 6). *Podonosma galalensis, Sesamum alatum, Satureja biflora* and *Leucas neufliziana* were recorded in the three zones. Geographical areas containing high gamma diversity, a high level of endemism, and/or harbouring a high number of rare or threatened species have been defined as biodiversity hotspots, and have been considered to set priorities for conservation planning (Myers 1990; Reid 1998). In spite of the interesting biogeographical and botanical features of the Gebel Elba mountain range, it has been overlooked in most global biodiversity assessments (Heywood and Watson 1995). Of the 142 woody perennial threatened plant species that are included in the Plant Red Data Book of Egypt (El Hadidi et al. 1992), 56 or 39.4% were known from the Gebel Elba district. Endangered and rare species include *Seddera arabica* (Forssk.) Choisy (Convolvulaceae); *Cordia sinensis* Lam. (Boraginaceae); *Lantana viburnoides* (Forssk.) Vahl (Verbenaceae) and *Solanum albicaule* Ky. ex Dun (Solanaceae). Its ecological features, together with its particular geographic position, seem to have promoted plant diversity, singularity and endemism in this biogeographic zone. It comprises elements of the Sahelian regional transition zone (*sensu* White and Léonard 1991) and represents the northern limit of this geoelement in Africa. The phytogeographical analysis of some arboreal species in Egypt revealed that the Red Sea coast represents the main pathway for the penetration of the arboreal species to Egypt together with the southern border of both Western and Eastern Deserts (Hassan and Abd El-Ghani 1992).

The Sinai group (Group 4) represents the most diversified and species-rich zone in the Egyptian Tubiflorae. The natural conditions and geographical position of the Sinai Peninsula make it a very distinctive region. The Sinai Desert is a desert of the 'Saharan type' (McGinnies et al. 1968) linking Asia with Africa, and constitutes a transition between the Egyptian Deserts and those of the Middle East. The great diversity of climate (mean annual precipitation decreases from about 100 mm in the north, near the Mediterranean, to 5-30 mm in the south; Danin 1978), rock and soil types make the existence of some 900 species and 200-300 associations possible (Danin 1986). Besides, it is an interesting phytogeographic area as it borders the Mediterranean, Irano-Turanian, Saharo-Arabian and Sudanian regions (Zohary 1973). Recent studies on plant diversity in southern Sinai (Moustafa and Klopatek 1995; Moustafa et al. 2001) reported that many species were now under threat due to the severe human impacts such as over-cutting for fuel, over-collection, overgrazing, tourism activities and urbanization. High contribution of these species was from Labiatae, Compositae and Gramineae. It is to be also noted that the threatened endemic species of St. Catherine area (southern Sinai) were either facing grazing stresses due to their high palatability for domestic animals (e.g., *Anarrhinum pubescens, Veronica islensis* and *V. kaiseri*) or were used frequently in the folk medicine and gradually reduced its coverage and number (e.g., *Nepeta septemcrenata* and *Ballota kaiseri*).

Distribution of the Tubiflorae in adjacent countries

The highlands of western Saudi Arabia and Gebel Akhdar at the north-eastern part of Libya are among the major spe-

cies-rich and endemic-rich areas in the Middle East region (Boulos 1997). Distribution of the species within the major six families (Boraginaceae, Convolvulaceae, Labiatae, Orobanchaceae, Scrophulariaceae and Solanaceae) of the Tubiflorae in Egypt, Gebel Akhdar (Libya) and western Saudi Arabia, together with their chorology was demonstrated in Table 7. The total number of species varied from 260 in Egypt to 152 in Libya and 141 in Saudi Arabia. Interestingly, Boraginaceae, Labiatae and Scrophulariaceae were the species-rich families, while Orobanchaceae was the poorest. Thirty-nine species were confined to Libya, 61 to Egypt and 2 to Saudi Arabia. Prevalence of the Mediterranean geoelement in the Libyan Tubiflorae was noticeable, where 73 species representing different Mediterranean chorotypes (mono, bi- and pluriregional) were recognised. The pure Mediterranean geoelement was best represented in Libya (29), and decreasing eastwards in Egypt (6) and Saudi Arabia (2). In general, a remarkable decrease in the number of Mediterranean taxa was recorded in the west-east direction: 65 in Egypt and 38 in Saudi Arabia. Although the fact that the presence of a Mediterranean territory in Egypt was well documented since Engler (1882), several authors (Zohary 1973; Boulos 1975; Ayyad and Ghabbour 1986) stressed the absence of such territory due to the lack of any arboreal Mediterranean species in Egypt. The annual rainfall (*c* 200 mm) can hardly support the growth of such species characteristic to the Mediterranean biome. Wickens (1977) reported that there was ample evidence to suggest that the apparent increase in the desert conditions since the Roman time is due to activities of Man. The Saharo-Arabian geoelement, in the contrary, attained its highest number of species in Egypt (28), decreased in Libya and Saudi Arabia (18 for both). Recently, Salama et al. (2003) reviewed the chorological analysis of the Sallum area (at the Egyptian-Libyan border) on the western Mediterranean coast of Egypt. They concluded that despite its occurrence within the Mediterranean phytogeographic territory of Egypt, yet the monoregional Saharo-Arabian chorotype overrode the pure Mediterranean. This may be attributed to the fact that plants of the Saharo-Arabian geoelement are good indicators for harsh desert environmental conditions, while Mediterranean species stand for more mesic conditions.

References

Abd El-Ghani MM (1998) Environmental correlates of species distribution in arid desert ecosystems of eastern Egypt. J Arid Environ 38: 297-313.

Abd El-Ghani MM (2000) Floristics and environmental relations in two extreme desert zones of western Egypt. Global Ecol Biogeogr 9:499-516.

Abd El-Ghani MM, Amer WM (2003) Soil-vegetation relationships in a coastal desert plain of southern Sinai. J Arid Environ 55:607-628.

Abd El-Ghani MM, El-Sawaf N (2004) Diversity and distribution of plant species in the agro-ecosystem of Egypt. Syst Geogr Pl 74:319-336.

Ayyad MA, Fakhry A (1996) Plant biodiversity in the Western Mediterranean Desert of Egypt. Verh Ges Ökol 25:65-76.

Ayyad M, Fakhry AM, Abdel-Raouf A (2000) Plant biodiversity in the Saint Catherine area of the Sinai peninsula. Egypt Biodiv & Conserv 9:265-281.

Bornkamm R, Kehl H (1985) Pflanzengeographische zonen in der Marmarika (Nordwest-Ägypten). Flora 176:141-151.

Bornkamm R, Kehl H (1989) Landscape ecology of the Western Desert of Egypt. J Arid Environ 17:271-277.

Boulos L (1975) The mediterranean element in the flora of Egypt and Libya. La flore du Basin Mediterraneen, Colleques Internationaux du CNRS, 235:119-24.

Boulos L (1989) Egyptian desert plants with promising economic potentialities. Arab Gulf J Scient Res 7(2):91-108.

Boulos L (1995) Flora of Egypt Check list. Al-Hadara Publishing, Cairo.

Boulos L (1997) Endemic flora of the Middle East and North Africa. In Barakat HN, Hegazy AK (Eds.), Reviews in Ecology: Desert Conservation and Development. Metropole, Cairo, pp. 229-260.

Boulos L (2000) Flora of Egypt. Vol. 2. Geraniaceae- Boraginaceae. Al-Hadara Publishing, Cairo.

Boulos L (2002) Flora of Egypt. Vol. 3. Verbenaceae-Compositae. Al-Hadara Publishing, Cairo.

Chaudhary SA (1999-2001) Flora of the Kingdom of Saudi Arabia. Vols 1-3. Ministry of Agriculture and Water, Riyadh.

Chaudhary SA, Al-Jowaid AA (1999) Vegetation of the Kingdom of Saudi Arabia. Ministry of Agriculture and Water, Riyadh.

CITES (1990) Appendices I, II and III to the convention. US Fish and Wildlife Service, Washington DC.

Collenette S (1985) An illustrated guide to the flowers of Saudi Arabia. Scorpion Publishing Ltd, London.

Cowling RM (1983) Phytochorology and vegetation history in the south-eastern Cape. SAJ Biogeogr 10:393-419.

Cowling RM, Esler KJ, Midgley GF, Honig MA (1994) Plant functional diversity, species diversity and climate in arid and semi-arid southern Africa. J Arid Environ 27:141-158.

Danin A (1986) Flora and vegetation of Sinai. Proc Roy Soc Edinb 89B: 159-168.

El Hadidi MN (1979) List of threatened plants in the Flora of Egypt. TPU-IUCN, Royal Botanic Gardens, Kew, London.

El Hadidi MN (2000) The main features of the natural vegetation. In El Hadidi MN, Hosni HA (Eds.), Flora Aegyptiaca, Vol. 1, part 1. The Palm Press, Cairo, pp. 27-105.

El Hadidi MN, Abd El-Ghani MM, Fahmy AG (1992) The Plant Red Data Book of Egypt. I. Woody perennials. The Palm Press, Cairo.

El Hadidi MN, Hosny AI, El-Husseini N (1996) Some aspects of the biodiversity of the weed flora in the farmlands of Egypt. In Van der Maesen LJG, Van der Burgt XM, Van Madenbach de Rovy JM (Eds.), The biodiversity of African plants. The Netherlands, pp. 788-794.

El Hadidi MN, Hosny AI, El-Husseini NM, Shamso E (1999) Scrophulariaceae in the flora of Egypt, 1. Systematic revision of the indigenous taxa. Taeckholmia 19(2):227-259.

El-Husseini NM (1986) Flora of Egypt, taxonomic revision of Labiatae. Ph. D. Thesis, Cairo University, Cairo.

El-Husseini NM, Zareh MM (1989) Annotated list of the flora of Sinai (Egypt). 7. Angiospermae: Primulaceae-Plantaginaceae. Taeckholmia 12:79-85.

Engler A (1882) Versuch einer Entwicklungsgeschichte der Pflanzenwelt, insbesondere der Florengebiete seit der Tertiärperiode. 2. Teil. Die extratropischen Giebete der südlischen Hemisphre und die tropischen Gebiete. Wilhelm Engelmann, Leipzig.

Engler A, Diel L (1936) Syllabus der Pflanzenfamilien. Ed. 11. Borntroeger, Berlin.

Fakhry A (1973) The Oases of Egypt. Volume I. Siwa Oasis. The American University in Cairo Press, Cairo.

Fakhry A (1974) The Oases of Egypt. Volume II. Bahariyah and Farafra Oases. The American University in Cairo Press, Cairo.

Feinbrun-Dothan N (1978) Flora Palestina. Vol. 3. Israel Academy of Sciences and Humanities, Jerusalem.

Fenner M, Lee WG, Wilson JB (1997) A comparative study of the distribution of genus size in twenty angiosperm floras. Biol J Linn Soc 62:225-237.

Freitag H (1986) Notes on the distribution, climate and flora of the sand deserts of Iran and Afghanistan. Proc Roy Soc Edinb 89B:153-146.
Girgis WA (1972) Plant indicators in the Egyptian deserts. Bull Des Inst Arab Rep Egypt 21:511-515.
Gómez-Gonzáles S, Cavieres LA, Teneb EA, Arroya J (2004) Biogeographical analysis of species of the tribe Cytiseae (Fabaceae) in the Iberian Peninsula and Balearic Islands. J Biogeogr 31:1659-1671.
Greuter W, Burdet HM, Long G (1986) Med-Checklist. A Critical Inventory of Vascular Plants of the Circummediterranean Countries. 3. Dicotyledones (Convolvulaceoe - Laniatae). Genéve and Berlin.
Hassan LM, Abd El-Ghani MM (1992) Phytogeographical analysis of some arboreal species in Egypt. Bull Fac Agric Univ Cairo 43(3):841-852.
Hepper FN (1998) Solanaceae. In El Hadidi MN (Ed.), Flora of Egypt, Taechholmia Add. Ser. 6. Cairo.
Heywood VH, Watson RT (1995) Global biodiversity assessment. Cambridge University Press, Cambridge.
Huchinson J (1959) The families of the flowering plants. 2nd ed., Clarendon Press, Oxford.
Jafri SMH, El-Gadi A (1977-84) Flora of Libya. Al Fateh University, Tripoli.
Khedr A, Cadotte MW, El-Keblawy A, Lovett-Doust J (2002) Phylogenetic diversity and ecological features in the Egyptian flora. Biodiv & Conserv 11:1809-1824.
Kovach WL (1999) MVSP - A multivariate statistical package for Windows, version 3.1. UK.
Magurran AE (1988) Ecological diversity and its measurements. Princeton University Press, New Jersey.
Major J (1988) Endemism: a botanical perspective. In Myers AA, Giller PS (Eds.), Analytical biogeography: an integrated approach in the study of animal and plant distributions. Chapman and Hall, London/New York, pp. 117-146.
McGinnies WG, Goldman BJ, Paylore P (1968) Deserts of the World. An appraisal of research into their physical and biological environments. University of Arizona Press, Tucson, Arizona.
Moustafa AA, Klopatek JM (1995) Vegetation and landforms of the Saint Catherine area, southern Sinai, Egypt. J Arid Environ 30:385-395.
Moustafa AA, Zaghloul MS, Abd El-Wahab RH, Shaker M (2001) Evaluation of plant diversity in Saint Catherine protectorate, south Sinai, Egypt. Egypt J Bot 41:121-139.
Myres N (1990) The biodiversity challenge: expanded hot-spot analysis. The Environmentalist 10:243-256.
Pignatti E, Pignatti S (1989) Life forms and phytogeographical affinities of the Canarian flora. Flora 183:87-95.
Rahman MA, Wilcok CC (1991) Diversity of life-form and distribution of the Asclepiadaceae in south-west Asia and the Indian subcontinent. J Biogeogr 18:51-58.
Raunkiaer C (1937) The plant life forms and statistical plant geography. Clarendon Press, Oxford, UK.
Reid WV (1998) Biodiversity hotspots. Trends Ecol Evol 13:275-280.
Rohlf FJ (1972) An empirical comparison of three ordination techniques in numerical taxonomy. Syst Zool 21:271-280.
Salama FM, Abd El-Ghani MM, El-Naggar SM, Baayo KA (2003) Floristic composition and chorological analysis of the Sallum area, west Mediterranean, Egypt. J Union Arab Biol Cairo 13(B):27-47.
Shaltout KH, Sharaf El-Din A (1988) Habitat types and plant communities along a transect in the Nile Delta region. Feddes Repert 99(3-4):153-162.
Täckholm V (1974) Students' Flora of Egypt. 2nd ed., Cairo University Press, Cairo.
White F, Léonard J (1991) Phytogeographical links between Africa and southwest Asia. Fl Veg Mundi 9:229-246.
Whittaker RH (1960) Vegetation of the Siskiyon Mountains, Oregon and California. Ecol Monogr 30:279-338.
Wickens GE (1976) The flora of Jebel Marra (Sudan Republic) and its geographical affinities. Kew Bull Add Ser V. HMSO Books, London
Wickens G (1977) Some of the phytogeographical problems associated with Egypt. Pub Cairo Univ Herb 7&8:223-230.
Williams PH, Humphries CJ (1994) Biodiversity, taxonomy relatedness and endemism in conservation. In Forty PL, Humphries CJ, Vane-Wright RI (Eds.), Systematics and conservation evaluation. Clarendon Press, Oxford, UK. pp. 269-287.
Wilson EO (1988) Biodiversity. National Academy Press, Washington DC.
Wilson MV, Shmida A (1984) Measuring beta diversity with presence-absence data. J Ecol 72:1055-1064.
Yair A, Danin A (1980) Spatial variation as related to the soil moisture regime over an arid limestone hillside, northern Negev, Israel. Oecologia 47:83-88.
Zahran MA, Willis AJ (1992) The vegetation of Egypt. Chapman and Hall, London.
Zohary M (1972) Flora Palestina. Vol. 2. Israel Academy of Sciences and Humanities, Jerusalem.
Zohary M (1973) Geobotanical foundations of the Middle East. Gustav Fischer Verlag, Stuttgart.

Instructions to Authors

Submission of manuscripts

Submission of a manuscript to Acta Biologica Szegediensis automatically involves the assurance that it has not been published and will not be published elsewhere in the same form. Manuscripts should be written in English. Since poorly-written material will not be considered for publication, authors are encouraged to have their manuscripts corrected for language and usage by a trusted expert.

There are no explicit length limitations: a normal research article will occupy 4-6 printed pages; reviews might be considerably longer. Authors should submit three sets of the complete manuscript and illustrations, together with a computer disk containing an electronic version of their manuscript. The elctronic file is considered the final material. Both Macintosh and PC versions will be accepted. The disk should be labeled with the date, the first author's name, the file name of the manuscript and the software, disk format and hardware used. Acta Biologica Szegediensis will not return copies of submitted manuscripts and figures. Requests to return original figures will be honored as a courtesy, but cannot be guaranteed. If instructions are not followed, authors will be asked to retype their manuscripts.

Manuscript format

Only good-quality laser printouts will be accepted. All pages should be printed with full double spacing, 2.5 cm margins, and a nonjustified right margin. A standard 12 point typeface (e.g. Times, Helvetica or Courier) should be used throughout the manuscript, with symbol font for Greek letters. Boldface, italics or underlined text should not be used anywhere in the manuscript. Footnotes are not permitted. Each page should be numbered at the bottom as follows:

Page 1. Title page: Complete title, first name, middle initial, last name of each author; where the work was done (authors' initials in parentheses if necessary); mailing address, phone, fax, and e-mail of the corresponding author; a running title of no more than 48 characters and spaces.

Page 2. Abstract: no more than 200 words, followed by 4-6 key words.

Beginning on page 3: Introduction, Materials and Methods, Results, Discussion, Acknowledgments, References, Figure Legends, Tables. Each section should be begun on a new page.

The manufacturer's name and location should be given in parentheses for reagents and instruments. Sources for all antibodies and nucleotide sequences should be indicated. Customary abbreviations in common use need not be defined in the text (e.g. DNA or ATP). Other abbreviations should be defined the first time that they are used. Quantitative results must be presented as graphs or tables and supported by appropriate experimental design and statistical tests. Only SI units may be used. For studies that involve animals or human subjects, the institutional, national or international guidelines that were followed should be indicated.

References

Only work that has been published or is in the press may be referred to. Personal communications should be acknowledged in the text and accompanied by written permission. In the text, references should be cited by name and year, e.g. Bloom (1983) or (Schwarz-Sommer et al. 1990) or (Maxam and Gilbert 1977). In the References, references should be listed alphabetically by first authors (including all co-authors) and chronologically for a given author (beginning with the most recent date of publication). Where the same author has more than one publication in a year, lower case letters should be used (e.g. 1999a, 1999b, etc.). Periods should not be used after authors' initials or abbreviated journal titles (e.g. Acta Biologica Szegediensis should be cited as Acta Biol Szeged). Inclusive page numbers should be used. Examples:

Bloom FE (1983) The endorphins: a growing family of pharmacologically pertinent peptides. Annu Rev Pharmacol Toxicol 23:151-170.

Coons AH (1978) Fluorescent antibody methods. In Danielli JF, ed., General Cytochemical Methods. Academic Press, New York, 399-422.

Maxam AM, Gilbert WA (1977) A new method for sequencing DNA. Proc Natl Acad Sci USA 74:560-564.

Monod J, Changeux J-P, Jacob F (1963) Allosteric proteins and cellular control systems. J Mol Biol 6:306-329.

Schwarz-Sommer Z, Huijser P, Nacken W, Saedler H, Sommer H (1990) Genetic control of flower development by homeotic genes in Antirrhinum majus. Science 250:931-936.

Illustrations

Three complete sets, including a high-quality "original" for publication, must be submitted with the manuscript. The back of each figure or composite plate should be labeled in soft lead pencil, indicating the orientation, the figure number, and the first author's name. The back of the best set should be marked "use for reproduction" or "original". Authors are encouraged to submit digital images of photographs, line drawings or graphs for printing. Most major image editing and drawing/illustrator computer software files (both Macintosh and PC) in TIFF or EPS formats are acceptable. It is particularly important that adequate resolution (at least 300 dpi, preferably 600 dpi) is used in making the original image.

Figure legends

Figures should be numbered consecutively with Arabic numerals. Material in the text should not be duplicated and methods should not be described. The size of scale bars should be indicated when appropriate. The first figure in the text should be referred to as Fig. 1, and so on.

Tables

Tables should be numbered consecutively with Arabic numerals. A brief title should be included above the table. Each table should be printed double spaced, without vertical or horizontal lines, and on a separate sheet. Material in text should not be duplicated and methods should not be described. The first table in the text should be referred to as Table 1, and so on.